SELECTED ASPECTS OF RAFT AGENTS

The Use of Thiophene as an Activating Group in the RAFT Mediated Polymerization of Styrene

and

The Stereo-Controlled Polymerization of MMA via RAFT

by

Osama Bshena

Thesis presented in partial fulfillment of the requirements for the degree of

Master of Science (Polymer Science)

at the University of Stellenbosch

Promoter: Prof. R.D Sanderson

Co-promoters: Dr W. Weber and Dr M. Tonge

December 2007

DECLARATION

I, the undersigned, hereby declare that the work contained in this thesis is my own original work and that I have not previously, in its entirety or in part, submitted it at any university for a degree.

Ek, die ondergetekende verklaar hiermee dat die werk gedoen in hierdie tesis my eie oorspronklike werk is wat nog nie voorheen gedeeltelik of volledig by enige universiteit vir 'n graad aangebied is nie.

December 2007

Osama Bshena

ABSTRACT

In this study six Reversible Addition-Fragmentation chain Transfer (RAFT) agents with different leaving groups and different activating moieties were prepared. Three are novel thiophene-based RAFT agents having a thiophene substituent as the activating moiety, namely: (2-thienyl thiocarbonyl)disulfide (BTD), 1-cyano-1-methylethyl 2-thiophene dithiocarboxylate (CPDT), and benzyl thiophene-2-dithiocarboxylate (BDTT). The other three are model RAFT agents bearing a phenyl group as the activating moiety, namely: bis(thiobenzoyl) disulfide (BBD), benzyl dithiobenzoate (BDTB), 2-cyano-2-yl dithiobenzoate (CPDB). These agents were characterized by Nuclear Magnetic Resonance spectroscopy (NMR), Fourier-Transform Infrared spectroscopy (FT-IR) and Ultraviolet - visible spectroscopy (UV/vis).

These compounds were studied as RAFT agents, and used as mediators in the bulk polymerization of styrene, self-initiated thermally at 100 °C. The novel thiophene-based mediated systems were compared with the phenyl-based ones in terms of polymerization kinetics, molecular weight and polydispersity index (PDI).

The polymerization results showed that the novel CPDT and BDTT thiophene-based compounds were effective RAFT agents for the RAFT polymerization of styrene with the characteristics of "living"/controlled free radical polymerization. The BTD mediated system showed the poorest control, as the PDI progressively broadened with monomer to polymer conversion, and it had the lowest reaction rate. In general, the thiophene-based mediated systems had slower reaction rates (higher retardation) when compared to the analogous phenyl-based mediated systems.

The RAFT technique was then used to synthesize stereo-controlled poly (methyl methacrylates) in the presence of CPDB (since the thiophene-based RAFT agents showed unfavorable rate retardation) in different solvents, namely: toluene, 2-propanol and 1,1,1,3,3,3-hexafluoro-2-propanol (HFIP) at different temperatures, namely: 60, 30, 4, and –18 °C. The prepared polymers were characterized by ^{1}H-NMR spectroscopy in order to monitor the tacticity and SEC for the determination of the controlled/living behavior of the polymerization system. Results showed that the simultaneous control of the molecular weight and stereochemistry of PMMA was accomplished via RAFT-mediated polymerization, especially in HFIP at –18 °C, where the syndiotactic content of the polymer was the highest and low PDI values (< 1.4) were achieved.

OPSOMMING

Hierdie navorsing behels die studie van ses omkeerbare addisie fragmentasie kettingoordrag (OAFO) (Eng. reversible addition fragmentation chain transfer, RAFT) verbindings met verskillende verlatende groepe en verskillende aktiverende groepe. Drie van die verbindings is nuwe tiofeenbevattende RAFT-verbindings met 'n tiofeen groep as die aktiverende gedeelte (moiety), naamlik (2-tieniel tiokarboniel)disulfied (BTD), 1-siano-1-metieletiel 2-tiofeen ditiokarboksilaat (CPDT), en bensiel tiofeen-2-ditiokarboksilaat (BDTT). Die ander drie verbindings is 'model' RAFT-verbindings met fenielgroepe as die aktiverende groepe, naamlik bis(tiobensoiel) disulfied (BBD), bensiel ditiobensoaat (BDTB), en 2-siano-2-iel ditiobensoaat (CPDB). Hierdie verbindings is met behulp van kernmagnetieseresonansiespektroskopie (KMR), Fourier-Transforminfrarooispektroskopie (FT-IR) en ultraviolet-sigbare lig spektroskopie (UV-vis) gekarakteriseer.

Die gebruik van bogenoemde verbindings as RAFT-verbindings in die massapolimerisasie van stireen, self-afsettend by 100°C, is bestudeer. Die nuwe tiofeenbevattende RAFT-verbindings is met die fenielbevattende RAFT-verbindings in terme van polimerisasiekinetika, molekulêre massa en die poliverspreiding (PDI) vergelyk.

Die nuwe tiofeen-bemiddelde (Eng. mediated) verbindings was goeie RAFT-verbindings vir gebruik in die RAFT-polimerisasie van stireen. Die reaksie het kenmerke van "lewende"/gekontroleerde vryeradikaalpolimerisasie getoon. Die BTD-bemiddelde sisteem het die swakste kontrole gelewer. Die PDI-waarde het toegeneem namate die monomeer na polimeer omgeskakel is. Dit het boonop die laagste reaksietempo gehad. In die algemeen het die tiofeenbevattende sisteme die laagste reaksietempos gehad (hoër vertraging) in vergelyking met die fenielbevattende sisteme.

Daarna is die RAFT tegniek gebruik om stereogereguleerde poli(metielmetakrilate) in die teenwoordigheid van CPDB te berei (aangesien die tiofeenbevattende OAFO verbindings swak tempovertraging getoon het). Verskillende reaksiekondisies is gebruik: die oplosmiddels was tolueen, 2-propanol en 1,1,1,3,3,3-heksafluoro-2-propanol (HFIP) en die temperature was 60, 30, 4, en –18 °C. Die polimere wat berei is is met behulp van ^{1}H-KMR geanaliseer om die taktisiteit te bepaal. Gelpermeasiechromatografie is gebruik om die gekontrolleerde/"lewende" aard van die polimerisasiesisteem te bepaal. Sukses is behaal met die gelyktydige beheer van die molekulêre massa en stereochemie van die PMMA, veral in HFIP by –18 °C. Onder hierdie reaksiekondisies was die sindiotaktiese inhoud van die polimeer die hoogste en die PDI-waardes die laagste (< 1.4).

Dedications

This thesis is dedicated to my beloved parents who supported me all the way since the beginning of my studies. They taught me that even the largest task can be accomplished if it is done one step at a time.

This thesis is also dedicated to my beloved wife and my sweet daughter Lujane.

TABLE OF CONTENTS

LIST OF FIGURES

LIST OF SCHEMES

TABLES

LIST OF SYMBOLS

A	frequency factor
C_T	chain transfer constant
$DP_{n.}$	average degree of polymerization
E_a	activation energy
f	radical efficiency
$h\nu$	energy
I	initiator
$[I]$	initiator concentration
$[I]_o$	initial concentration of initiator
k_{add}	addition rate coefficient
k_{-add}	fragmentation rate coefficient
k_d	initiator decomposition rate coefficient
K_{eq}	equilibrium constant
k_i	initiation rate coefficient
k_p	propagation rate coefficient
$<k_t>$	average termination rate coefficient
k_{trT}	rate coefficient for the transfer agent
k_{tr}	chain transfer rate coefficient
k_{tc}	termination rate constant
k_{td}	termination by disproportionation rate coefficient
λ	wavelength
M	monomer
$M_{n,theory}$	calculated number average molar mass
$[M]_o$	initial concentration of monomer
$[M]_t$	monomer concentration at time (t)
[Monomer]	monomer concentration
$\bar{M}_n$	number average molar mass
M_{RAFT}	molecular weight of RAFT agent
$\bar{M}_w$	weight average molar mass
M^n_t/L	transition metal complex for atom transfer reaction
$P^{\bullet}$	propagating chain radical

$R^{\bullet}$	primary radical
R	RAFT agent leaving group
[RAFT]	RAFT agent concentration
$[RAFT]_o$	initial concentration of RAFT agent
S	solvent
[S]	concentration of the chain transfer agent in form of solvent
T	temperature
t	time
$t_{1/2}$	initiator half-life
ν_i	rate of initiation
ν_p	rate of polymerization
ν_p	rate of propagation
ν_t	rate of termination
x	fractional conversion
Z	RAFT agent stabilizing group

LIST OF ACRONYMS

AH	Diels-Alder styrene dimer
AIBN	2,2'-azobis(isobutyronitrile)
AGET	activator generated by electron transfer
ATRP	atom transfer radical polymerization
BA	butyl acrylate
BBD	bis(thiobenzoyl) disulfide
BDTB	benzyl dithiobenzoate
BDTT	benzyl thiophene-2-dithiocarboxylate
BPO	dibenzoyl peroxide
BTD	bis(2-thienyl thiocarbonyl)disulfide
Bpy	2,2'-bipyidine
CDB	cumyl dithiobenzoate
^{13}C-NMR	carbon nuclear magnetic resonance spectroscopy
CPDB	2-cyano-2-propyl dithiobenzoate
CPDT	1-cyano-1-methylethyl2-thiophene dithiocar
CSIRO	commonwealth Scientific, Industrial Research Organization
CS_2	carbon disulfide
DCB	1,2-diphenylcyclobutane
DSC	differential scanning calorimetry
DMSO	dimethyl sulfoxide
ESR	electron spin resonance
FT-IR	fourier-transform infrared
HCl	hydrochloric acid
HMTETA	1,1,4,7,10,10-hexamethyltriethylenetetramine
HFIP	1,1,1,3,3,3 hexafluoro-2-propanol
^{1}H-NMR	proton nuclear magnetic resonance spectroscopy
IBN	isobutyronitrile
KCN	potassium cyanide
KI	ketenimine
LFRP	living free radical polymerization
MA	methyl acrylate
MADIX	macromolecular design via interchange of xanthates

MAN	methacrylonitrile
Me_6TREN)	tris[2-(dimethylamino)ethyl]amine
Mg	magnesium
MMA	methyl methacrylate
NMP	nitroxide mediated polymerization
NMR	nuclear magnetic resonance spectroscopy
PAS	photoacoustic
PDI	polydispersity index
PMMA	poly methyl methacrylate
PFTB	perfluoro-*tert*-butyl alcohol
Ph	phenyl
ppm	parts per million
PSt	polystyrene
RAFT	reversible addition-fragmentation chain transfer
RI	refractive index
SEC	size exclusion chromatography
SFRP	stable free radical polymerization
St	styrene
TEMPO	2,2,6,6-tetramethyl-piperidinyl-1-oxy free radical
TMSN	(tetramethyl)succinonitrile
TPO	trimethylbenzoyl diphenylphosphine oxide
UV	ultraviolet
$Yb(OTf)_3$	ytterbium trifluoromethanesulfonate
$Y(OTf)_3$	yttrium trifluoromethanesulfonate

Acknowledgments

I would like to acknowledge the enthusiastic supervision of Prof. R. Sanderson during this study, and Dr. J.B. McLeary for his kind guidance and support right from the initial stages of this work.

From the formative stages of this thesis to the final draft I owe immense debt of gratitude to Dr. Matthew Tonge, for his invaluable advice and guidance throughout this study.

Very special thanks also go to Dr. Wolfgang Weber, for his assistance, especially with the experimental work.

Thanks go to Nadine Pretorius and Gareth Bayley for running the GPC samples. I also would like to thank Elsa Malherbe and Jean McKenzie for running the NMR samples.

I would like to express my sincere gratitude to Dr. Margie Hurndall, for her patience and editing the manuscript to its present form.

Many thanks go to Dr. Jenna and Trudy their assistance in using the incubator facility in the department if microbiology.

Thanks go to my friends and colleagues who played important roles during my study.

In conclusion, I recognize the fact that this research would not have been possible without the financial support of the Center for Macromolecular Chemistry and Technology; Tripoli/Libya. Therefore my gratitude goes to the center.

Chapter 1: Introduction and Objectives

1.1 Introduction

The use of synthetic polymeric materials has increased significantly over the past few decades, which has resulted in a huge impact in industry. At present, synthetic polymers are so well integrated into the fabric of society that we take little notice of our dependence on them. Examples of some extensively used polymers are polystyrene (PSt), poly methyl methacrylate (PMMA) and polyethylene (PE), amongst others.

Polymers are synthesized by different polymerization techniques, including free radical polymerization (FRP), cationic and anionic polymerizations, ring opening polymerization, polycondensation,[1] and biological polymerization.[2]

The FRP technique is one of the most widely used and (relatively) convenient techniques to prepare polymers on a large industrial scale. Today more than 50% of plastics are prepared by FRP.[3,4] The versatility of the technique arises from its tolerance towards different types of impurities (e.g. stabilizers and traces of oxygen), its suitability for use under various reaction conditions, and the fact that polymerization can be performed in water and because this technique accommodates a wide range of monomers.

It is however difficult to achieve control over the polymer architecture, particularly the control over the polymer molecular weight distribution and the chain end groups. This constitutes a disadvantage of the conventional FRP technique.

Since a focus of modern polymer technology is the creation of new materials with suitable properties for specific applications, the preparation of new materials and the enhancement of the macroscopic behavior of the existing polymers usually require modifications to the existing materials. Modifications of polymers can be successfully accomplished by using controlled / living polymerization techniques.

Over the past two decades numerous studies have focused on developing FRP techniques that display the fundamental characteristics of living polymerizations.[5] A lot of effort has

gone into the study and the development of synthetic techniques to design and control complex macromolecular architectures, which in turn influence the properties and behavior of the materials.

Living free radical polymerization (LFRP) techniques have been found to be suitable for the preparation of polymers with specific structures. The types of LFRP techniques that have received attention are: stable free radical mediated polymerization (SFRP) techniques which include nitroxyl radical mediated polymerization (NMP),[6] atom transfer radical polymerization (ATRP)[7] and reversible addition fragmentation chain transfer polymerization (RAFT).[8]

The RAFT technique is a relatively new radical polymerization technique, and currently one of the most versatile for preparing complex polymer architectures.[9] It is based on the use of chain transfer agents (RAFT agents), e.g. dithioesters or dithiocarbamates having a general formula [S=C (Z) S (R)], and a high transfer constant. Consequently, the types of R groups (leaving groups) and Z groups (activating groups) are responsible for providing a living mechanism for the system through their performance in the polymerization reaction. A detailed discussion of the roles of the R and Z groups is presented in Section 2.3.3.1. For example, recent studies have shown that using a phenyl moiety as the activating group (Z) enhances the reactivity of the RAFT agent, and leaving groups such as isobutyronitrile and cumyl are suitable R groups, providing good control in the polymerization system.[10-12]

In free radical polymerization the end functionalities of the polymer chains originate from the selected initiators or transfer agents.[13] When the polymerization is conducted in the presence of a RAFT agent, ideally (according to the RAFT mechanism), all polymer chains should possess the RAFT moiety at one of the chain ends in the form of [S=C (Z) S], thus the chain end functionality can, in principle, be easily introduced to the polymer by adjusting the structure of the RAFT agent used during the polymerization reaction. This provides the advantage of exploiting the potential reactivity of the end groups in various ways, including chain extension to form copolymers, and functionalities that are chemically labile for a specific reaction (e.g. crosslinking, grafting, interacting/bonding with metal ions).

Numerous studies have focused on the RAFT process with a wide range of monomers and a considerable number of different synthesized RAFT agents.[9] The challenge remains

however to design suitable RAFT agents with which to obtain desired products, and thus, investigations into the use of new R and Z groups remains an area of significant interest.

The phenyl group has been shown to be an efficient activating group. Hence, an aromatic compound chemically similar to benzene, namely thiophene, can be expected to perform in a similar fashion to the phenyl group in the RAFT process.[14] This has not yet been investigated. Thiophene interacts with various metals to form reasonably strong bonds, where the mode of interaction depends on the type of metal; for example, thiophene bonds strongly to Cu(?) by S-Cu interaction, which is not affected by substituents on the actual thiophene ring. It was therefore considered to be of interest to investigate the effect of thiophene as an activating group, and also the role of the thiophene functionality at the end of the polymer chain which may add interesting characteristics to the polymer produced. e.g. improve adhesion properties with metal surfaces and improve the compatibility between organic and inorganic materials.

Hence, the first part of this study involves looking at the role of the thiophene ring as the activating group (Z) in the RAFT process and comparing it with its analogous phenyl ring in different RAFT agents. Attention was also to be given to determining any advantages that it offers.

Styrene was initially selected for use in the RAFT polymerization reactions since it is widely used in polymer chemistry and considerable information, with respect to its kinetics and polymerization mechanism, is available in literature.

The study area was then extended from styrene to MMA as MMA is more susceptible to the medium used. Various solvents were used and their effects on the polymer microstructure were determined. The reason for this is that; it is not only the macromolecular structure of polymers that is important, but also (more recently), the production of well-defined stereocontrolled polymers and copolymers has attracted considerable attention.[15-19] This is largely because polymers of various stereoselectivity possess different properties; for example, the glass-transition temperature (T_g) of methacrylic polymers is known to change as a function of tacticity.[2,20-23] The simultaneous control of the molecular weight and tacticity using LFRP techniques is still a relatively new research area. It was initially limited to meth(acrylamide) monomers in the presence of Lewis acids via the RAFT process. The ATRP technique has been used for the simultaneous control of molecular weight and tacticity of MMA in the presence of

fluoroalcohols.[24,25] However, no attempt has been made to utilize the RAFT technique for producing stereocontrolled PMMA. Hence, in the second part of the study, an investigation was carried out into the stereocontrolled polymerization of MMA by utilizing the RAFT technique, under different reaction conditions.

1.2 Objectives

This study included consideration of two aspects of the RAFT process namely:

(1) The role of thiophene as an activation group in a new RAFT agent for the mediated polymerization of styrene (as a standard).

(2) The stereo-controlled polymerization of MAA via RAFT.

The specific objectives of part (1) of this study were:

1. To synthesize six different chain transfer agents: three novel thiophene-based RAFT agents and three standard phenyl-based RAFT agents.
2. To use the above RAFT agents in the self-initiation homo-polymerization of styrene in bulk.
3. To investigate the chain transfer performance of the novel thiophene-based compounds by their molecular weight control and kinetic behavior in the bulk polymerization of styrene.
4. To compare the molecular weight control of the thiophene-based polymer systems and the phenyl-based analogues, by means of SEC analysis of the polymers obtained.

The specific objectives of part (2) of the study were:

1. To prepare a series of PMMA homopolymers mediated by CPDB in different solvents, namely: 2-propanol, HFIP, and toluene, at four different temperatures (60, 30, 4, and -18 °C).
2. To characterize the polymers obtained by various techniques: NMR spectroscopy for monitoring the tacticity, and SEC for determining the molecular weight and molecular weight distributions and the control of the living polymerization behaviour.

3. To investigate the simultaneous control of molecular weight and tacticity of the obtained PMMA homopolymers, and to compare the roles of solvent and temperature on the stereoregularity and the living behavior of the polymers.

1.3 Layout of the thesis

This thesis comprises six chapters:

Chapter 1: Introduction and Objectives

A general introduction is given to the major areas of this study, including the versatility of free radical polymerization techniques, their development, and their role in producing various complex polymeric materials. The specific objectives of the study are stated.

Chapter 2: Theoretical and Historical Background

This chapter presents a review of the historical, theoretical and empirical aspects that relate to this study. It includes some results achieved by other research groups to date.

Chapter 3: RAFT Agent Synthesis and Characterization

The synthesis and characterization of RAFT agents that were used in this research are presented.

Chapter 4: Evaluation of Thiophene as the Activating Group in the RAFT Mediated Polymerization of Styrene

The performance of living polymerization was investigated using styrne and each of six different RAFT agents. A general comparison between thiophene-based RAFT-mediated systems and phenyl-based analogues are discussed with respect to the kinetic profiles, molecular weight control and molecular weight distribution of the products.

Chapter 5: Stereo-controlled Polymerization of MMA via RAFT

This chapter focuses on the effect of different solvents used in the stereo-controlled polymerization of MMA at different temperatures, utilizing the RAFT technique. The suitability of the RAFT process to produce well-defined polymers with chain end functionality is discussed.

Chapter 6: Conclusions and Recommendations.

Conclusions are drawn and recommendations for future work are made.

1.4 References

1. Matyjaszewski, K.; Gnanou, Y.; Leibler, L., *Macromolecular Engineering: Precise Synthesis, Materials Properties, Applications*. Wiley-VCH: Weinheim, 2007; Vol. 1; Synthetic techniques pp 7-345.

2. Elias, H.-G., Biological polymerization, In *Macromolecules*. Wiley-VCH: Weinheim, 2005; Vol. 1; Chemical structures and synthesis; pp 511-569.

3. Otsu, T. *J. Polym. Sci. Part A: Polym. Chem.* 2000, 38, 2121-2136.

4. Hong, K.; Zhang, H.; Mays, J. W.; Visser, A. E.; Brazel, S.; Holbrey, D.; Reichert, W. M.; Rogers, R. D. *Chem. Comm.* 2002, 1368-1369.

5. Moad, G.; Solomon, D. H., *The Chemistry of Free Radical Polymerization*, Second ed.; Elsevier: Amsterdam, 2006.

6. Hawker, C. J.; Bosman, A. W.; Harth, E. *Chem. Rev.* 2001, 101, 3661-3688.

7. Matyjaszewski, K.; Xia, J. *Chem. Rev.* 2001, 101, 2921-2990.

8. Le, T. P.; Moad, G.; Rizzardo, E.; Thang, S. H. PCT. Int. Appl. wo98/01478; 1998.

9. Moad, G.; Rizzardo, E.; Thang, S. H. *Aust. J. Chem.* 2005, 58, 379-410.

10. Chiefari, J.; Mayadunne, R. T. A.; Moad, C. L.; Moad, G.; Rizzardo, E.; Postma, A.; Skidmore, M. A.; Thang, S. H. *Macromolecules* 2003, 36, (7), 2273-2282.

11. Chong, Y. K. B.; Krstina, J.; Le, T. P. T.; Moad, G.; Postma, A.; Rizzardo, E.; Thang, S. H. *Macromolecules* 2003, 36, 2256-2272.

12. Benaglia, M.; Rizzardo, E.; Alberti, A.; Guerra, M. *Macromolecules* 2005, 38, 3129-3140.

13. Lai, J. T.; Filla, D.; Shea, R. *Macromolecules* 2002, 35, 6754-6756.

14. Dyreborg, S.; Arvin, E.; Broholm, K. *Environ. Toxicol. Chem.* 1998, 17, 851-858.

15. Wan, D.; Satoh, K.; Kamigaito, M.; Okamoto, Y. *Macromolecules* 2005, 38, 10397-10405.

16. Ray, B.; Isobe, Y.; Matsumoto, A.; Habaue, S.; Okamoto, Y.; Kamigaito, M.; Sawamoto, M. *Macromolecules* 2004, 37, 1702-1710.

17. Ray, B.; Isobe, Y.; Morioka, K.; Habaue, S.; Okamoto, Y.; Kamigaito, M.; Sawamoto, M. *Macromolecules* 2003, 36, 543-545.

18. Lutz, J.-F.; Neugebauer, D.; Matyjaszewski, K. *J. Am. Chem. Soc.* 2003, 125, 6986-6993.

19. Habaue, S.; Isobe, Y.; Okamoto, Y. *Tetrahedron* 2002, 58, 8205-8209.

20. Sauer, B. B.; Kim, Y. H. *Macromolecules* 1997, 30, 3323-3328.

21. Denny, L. R.; Boyer, R. F.; Elias, H. G. *J. Macromol. Sci., Part B: Polym. Phys.* 1986, B25, 227-65.

22. Biros, J.; Larina, T.; Trekoval, J.; Pouchlý, J. *Colloid. Polym. Sci.* 1982, 260, 27-30.

23. Wittmann, J. C.; Kovacs, A. J. *J. Polym. Sci.: Polym. Symp.* 1969, 16, 4443-4452.

24. Karasz, F. E.; MacKnight, W. J. *Macromolecules* 1968, 1, 537-540.

25. Miura, Y.; Satoh, T.; Narumi, A.; Nishizawa, O.; Okamoto, Y.; Kakuchi, T. *Macromolecules* 2005, 38, 1041-1043.

26. Miura, Y.; Satoh, T.; Narumi, A.; Nishizawa, O.; Okamoto, Y. *J. Polym. Sci., Part A: Polym. Chem.* 2006, 44, 1436-1446.

Chapter 2:

Theoretical and Historical Background

2.1 Introduction

Free radical polymerization is one of the most widely used polymerization techniques for the synthesis of various high molecular weight polymers. A polymer can be defined as a large molecule (or macromolecule) consisting of a number of repeating units, referred to as monomers. The word polymer is derived from the Greek: (poly) meaning "many" and (meros) meaning "part".[1] A polymer structure depends on the monomer or monomers used in its preparation. If only a few monomers are joined together, then the low molecular weight polymer is called an oligomer, which originated from Greek word oligos meaning "few".[2]

When n monomer units are joined, the resulting materials can be classified as follows:[3]

- $n = 2$ (dimer)
- $2 < n < 100$ (oligomer)
- $n > 100$ (polymer)

The reason why free radical polymerization is a widely used process arises from its applicability to a wide variety of monomers, including styrenic, vinylic, acrylic, and methacrylic derivatives, its tolerance to many solvents and traces of impurities, and its tolerance to different functional groups present in the monomer (e.g. OH, NR_2, COOH, $CONR_2$).[4,5] Free radical polymerization can also be performed under different conditions, including bulk, solution, emulsion, miniemulsion and suspension polymerization.[5,6]

2.2 The free radical polymerization process

All synthetic polymers are prepared by linking the monomers together to form a polymer chain. Free radical polymerizations are chain reactions in which the propagating species is a long-chain free radical, and grows via the addition of the monomer molecules to each other very rapidly through a chain reaction.[5,7] The product has almost the same elemental composition as that of the monomer. The growth of each polymer chain involves the addition of a monomer to the terminal free radical reactive site or active center, which transfers to a newly created chain end, each time a monomer is added to the active site by a chain type kinetic mechanism.[7]

The main reactions in the mechanism of free radical polymerization can be classified into three steps, initiation, propagation and termination.[5-10]

2.2.1 Initiation

To initiate a radical polymerization reaction, there must be free radicals available. In this step, there are two reactions:

a) The free radical active center is created, which usually requires an initiator. The initiator is normally an organic compound that possesses weak dissociation energy bonds such as (O–O or R-N=N-R) which can be broken thermally or by irradiation to produce free radicals.[10,11] If one considers (I) as the initiator, the homolytic decomposition of (I) forms two fragments $R^{\bullet}$ each carrying one unpaired electron with it, i.e. each one is a free radical.

$$I \xrightarrow{k_d} 2R^{\bullet}$$

$$?_d = 2k_d[I] \qquad (2.1)$$

Where k_d is the initiator decomposition rate coefficient, ν_d is the rate of decomposition of the initiator. The factor of 2 in Equation 2.1 refers to a pair of radicals produced per initiator molecule.

The rate of decomposition of an initiator is temperature dependent[3] and often categorized purely according to its half-life ($t_{½}$), at a given temperature. For initiators that undergo Unimolecular decomposition, the half-life is expressed by:

$$t_{1/2} = \frac{\ln 2}{k_d} \tag{2.2}$$

From the relevant Arrhenius equation:

$$k_d = A\, e^{-E_a/RT} \tag{2.3}$$

A is a constant designated as the frequency factor, E_a is the activation energy, R is the gas constant and T is the absolute temperature. By substituting k_d into equation 2.1:

$$\nu_d = 2A\, e^{\left(\frac{-E_a}{RT}\right)}[I] \tag{2.4}$$

From equation 2.4, it can be concluded that the rate of decomposition of an initiator increases with temperature and initiator concentration.

b) The second reaction involved in the initiation step is the addition of the radical formed to a monomer, M to produce the initial propagating species $P_1^{\bullet}$

$$R^{\bullet} + M \xrightarrow{k_i} P_1^{\bullet}$$

The initiation rate can be expressed as:

$$\frac{-d[R^{\bullet}]}{dt} = \nu_i = k_i[M][R^{\bullet}] \tag{2.5}$$

where k_i is the initiation rate coefficient. Free radicals are extremely reactive and as soon as they are formed they will add to or abstract species that are vulnerable. In the case of a polymerization reaction, the main reaction is addition to the double bond of a vinyl monomer, starting the initiation process. If one assumes that the rate of formation of free initiator radicals equals the rate of disappearance of the free initiator radicals (a steady state assumption), $\nu_i = \nu_d$, then the rate expression is written as:

$$\frac{-d[I]}{dt} = \nu_d = 2k_d[I] \tag{2.6}$$

However, equation 2.6 is valid only if all of the radicals produced are effective in initiating the growth of a polymer chain. Practically speaking, not all of the radicals contribute to the actual polymer growth, as they can be lost in side reactions and/or in the recombination reactions including the cage effect, which can have a dramatic effect on the initiation mechanism.[7-10,12] Examples of some initiators will be illustrated later in this section.

This leads to the consideration of the efficiency of the initiator; a factor (*f*), the efficiency factor, must be introduced in equation 2.5. This factor refers to the fraction of effective radical fragments that contribute in initiating chain growth. Taking this factor into account, equation 2.6 can be modified to give:

$$\frac{-d[I]}{dt} = v_i = 2f k_d [I] \qquad (2.7)$$

Initiator systems are commonly considered efficient if the *f* value is between 0.5 and 1,[8,9] for example azobis isobutyronitrile (AIBN) has an initiation efficiency of between 0.6 – 1 when it is used for the polymerization of methyl methacrylate, vinyl acetate, styrene, vinyl chloride and acrylonitrile.[8]

There are several initiation systems that are used in FRP reactions. Selecting the most suitable initiator depends on several factors, including the conditions and the environment of the polymerization reaction. Apart from the thermal system discussed in detail in this section, there are a number of different ways of generating radicals these include chemically (redox), photochemically or, less commonly, by high-energy radiation (electron beam, gamma-radiation, plasma and ultrasonic initiation).[5,10]

2.2.1.1 Azo-compounds and peroxides

The azo compounds and peroxides are among the most common initiators that are decomposed to form radicals through the application of heat, light or redox processes.[2-12] Initiators such as hydrogen peroxide, potassium persulfate, and sodium perborate are popular in aqueous systems.[6] Scheme 2.1 presents the general formula of different types of peroxides.

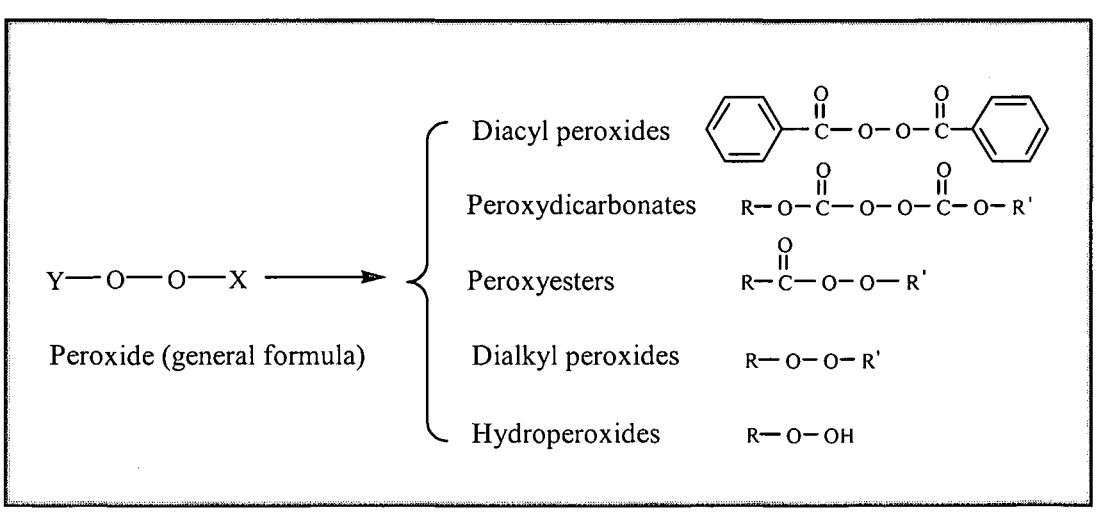

Scheme 2.1: General description of various peroxides[10]

Benzoyl peroxide (BPO) thermally decomposes to form both benzoyloxy and phenyl radicals that can initiate a polymerization reaction. Scheme 2.2 illustrates the proposed decomposition reaction.

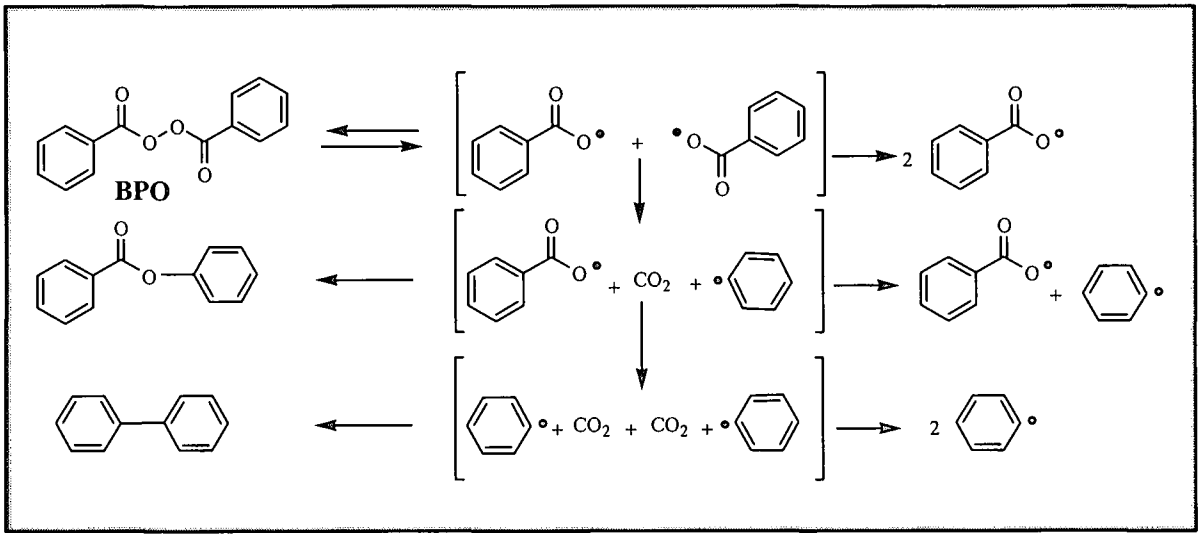

Scheme 2.2: The proposed decomposition of dibenzoyl peroxide.[10]

The azo-compounds are a class of initiators that are obtainable in different categories; such as symmetrical, multifunctional initiators with azo-linkages and polymeric azo-compounds. A comprehensive study on the thermal and photochemical decomposition of dialkyldiazenes has been compiled by Engel.[13] Symmetrical azo-compounds include two general classes: dialkyldiazenes such as (AIBN), and dialkyl hyponitrites. Scheme 2.3 presents the general structure of the azo-compounds.

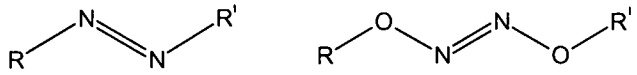

Dialkyldiazenes Hyponitriles

Scheme 2.3: General structure of azo-compounds.

As discussed in Section 2.2.1, one should consider that the decomposition of an initiator rarely produces a quantitative yield of initiating radicals. Since the majority of initiators produce radicals in pairs, side reactions, including self-reactions (cage reaction) can and do occur. This can lead to the formation of byproducts that are not initiating species; and moreover, the incorporation of byproducts into the polymer produced could affect its final properties (e.g. toxicity and thermal stability).[5,7,10,14]

Scheme 2.4 illustrates the decomposition of AIBN and the potential cage reactions involved. AIBN undergoes thermal or photochemical homolysis to yield a nitrogen molecule and a pair of isobutyronitrile radicals. The disproportionation of isobutyronitrile radicals give abnormally high yields of isobutyronitrile (IBN) and methacrylonitrile (MAN), the latter being susceptible to polymerization and can be incorporated in the final product. Low yields of tetramethylsuccinodinitrile (TMSN), which is a toxic material,[10] and the unsymmetrical coupling product, dimethyl-*N*-(2-cyano-2-propyl) ketenimine (KI), also occur.[14]

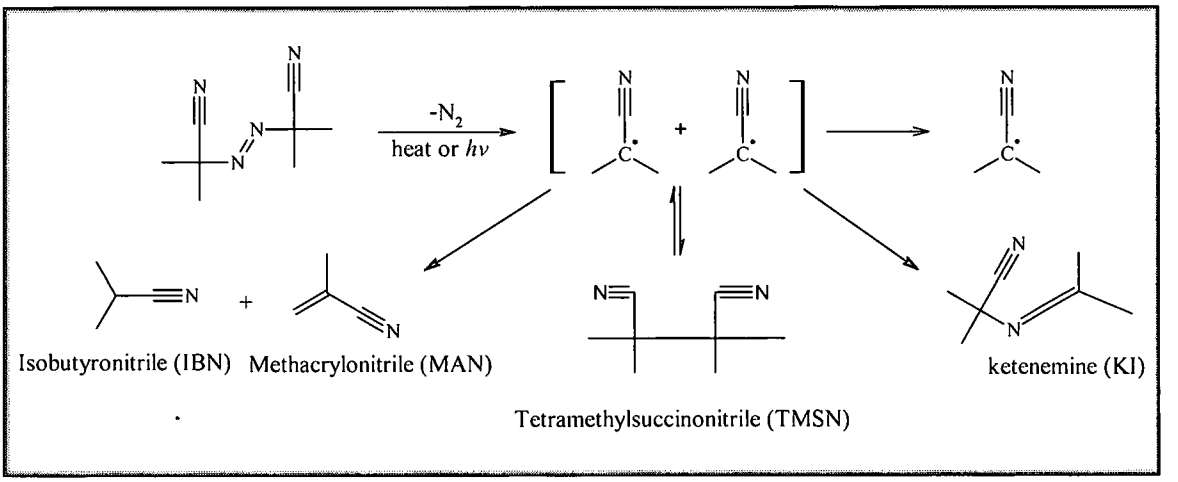

Scheme 2.4: AIBN decomposition, including self-reaction pathways.

Consideration of the cage recombination reaction is rather important, as it is a significant factor in determining the efficiency of the initiator, the reaction conditions including the temperature, solvent system used and the viscosity medium play significant roles in increasing the cage reactions and vice versa.[10,13,14] The effect of structural isomers of an initiator such as AIBN will be discussed in Section 5.3, as it has a dramatic effect when it is exposed to UV radiation at low temperature.[10,11,14]

2.2.1.2 Redox initiators

Radical generation via a redox process primarily involves electron transfer between a reducing agent and an oxidizing agent. Common redox systems are peroxides and transition metal ion complexes.[5] A typical example of a redox reaction is presented in **Scheme 2.5**.

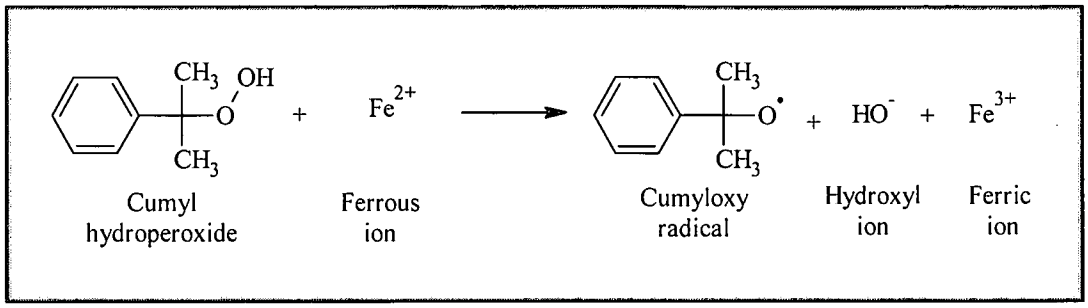

Scheme 2.5: A typical redox reaction.

2.2.1.3 Photochemical initiation

A photoinitiator is a compound specifically added to a reaction to convert absorbed energy (UV or visible light) into chemical energy, resulting in the formation of an initiating species. In general, energy is stored in the molecule in the form of kinetic (translational, rotational and vibrational) and electronic energy, and the processes that are important in photochemistry are those in which light absorption leads to changes in the electronic states.[15]

Light at a given frequency can only be absorbed or emitted in units of energy given by the following relation:[15]

$$E = h\nu \qquad (2.8)$$

where ? is the frequency and h is the Planck's constant. The principle of photoinitiation involves the absorption of a photon from the incident radiation by the photoinitiator molecule in its ground electronic state. The absorption is simply an energy uptake process, where the absorbing molecule is lifted from its normal state of lowest energy (highest stability) to an excited (higher energy) state via electronic transitions in the molecule. It must be noted that light of a given frequency can only be absorbed by a molecule if the difference between energy levels in an allowed transition is equal to h? .[15]

A detailed presentation on this topic is far beyond the scope of this study; for further reading on elementary quantum mechanics and atomic energy levels, texts by Crivello and Dietliker,[16] Guillet,[17] Solomons,[18] and Morrison and Boyd,[19,20] contain valuable information. Only a brief description of electronic transitions will be discussed here.

In most molecules, there are electrons in different kinds of orbitals including s, p and nonbonding (n) orbitals, with different energies in the ground state that might be excited to higher levels, giving many excited states (Figure 2.1). Thus, many transitions from the

ground state to different excited states are possible. Electronic transitions, which can occur from bonding or nonbonding orbitals, include:[21]

i. $\sigma \rightarrow \sigma^*$

ii. $\pi \rightarrow \pi^*$

iii. $\pi \rightarrow \sigma^*$

iv. $n \rightarrow \pi^*$

In particular, transitions involving π orbitals and lone pairs of electrons (n = nonbonding) are of most interest. It is known from both theoretical calculations and experimental evidence that in simple carbonyl systems, the highest energy occupied molecular orbital is a non-bonding n orbital and the lowest unoccupied molecular orbital is a π^* anti-bonding orbital that is delocalized across the C–O bond.[22]

The unit of the molecule that is responsible for the absorption is called the chromophore, of which the most common are C=C double bonds ($\pi \rightarrow \pi^*$) and C=O ($n \rightarrow \pi^*$). The $\pi \rightarrow \pi^*$ is the transition in which an electron goes from a stable (bonding) π orbital to an unstable (anti-bonding) p orbital. The $n \rightarrow \pi^*$ transition is that in which the electron of an unshared pair goes to an unstable p orbital.

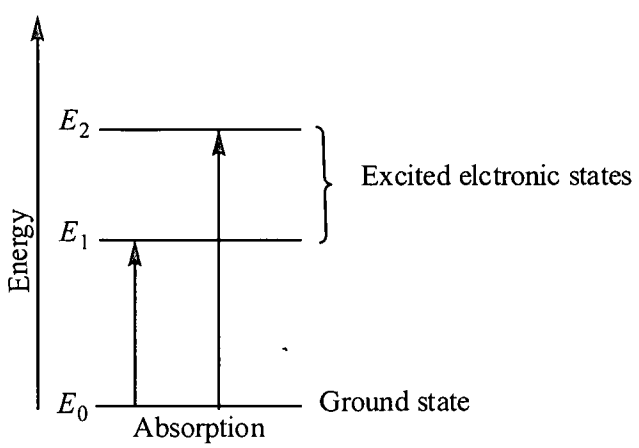

Figure 2.1: Schematic representation of electronic transitions by UV absorption.

For free radical photoinitiators, a conjugated system, including a carbonyl group, is the photoactive moiety that is most often involved in the absorption of photons. When the carbonyl group is in its ground state the number of occupied bonding orbitals exceeds the number of anti-bonding orbitals and hence the bond remains intact. If, however, the number of occupied anti-bonding orbitals are equal to or exceeds the number of occupied

bonding orbitals, the bond is susceptible to breakage and dissociates. Figure 2.2 is a schematic diagram of the possible electronic transitions in the carbonyl moiety.

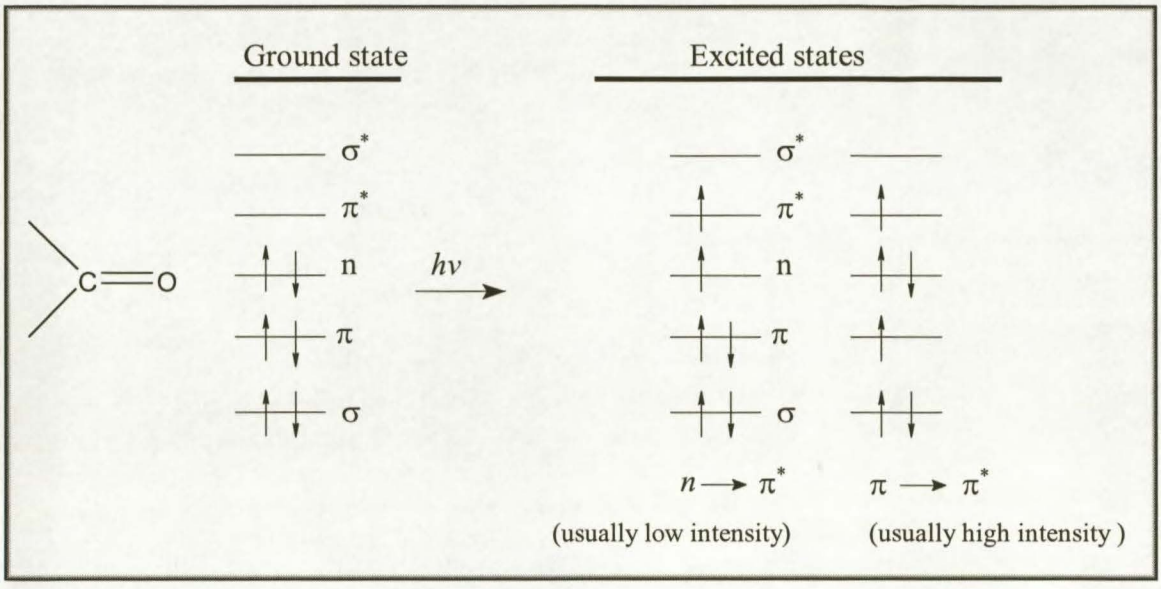

Figure 2.2: Possible electronic transitions in the carbonyl group.

However, it must be noted that the absorption can be affected by the type of groups attached to the carbonyl group or any other chromophore, as they may shift the absorption spectrum of the chromophore, especially if the moieties contain delocalized orbitals which can interact with those of the chromophore.[23]

There are two general types of photochemical initiation; one is the direct photolytic fragmentation of the initiator, such as alkyl halides and ketones. The second type involves a bimolecular reaction, where the excited state of the photoinitiator interacts with a second molecule (a co-initiator) to generate free radicals.[24,25] Examples of various photoinitiators and photopolymerization via UV can be found in reviews by Kaur and Srivastava,[26] Decker[27] and Allen.[28]

Most of the compounds, including the peroxides and azocompounds.[13,15] that dissociate thermally into radicals can also dissociate under the absorption of UV radiation, However, peroxides suffer a drawback in that they show appreciable absorption even below a wavelength of 320 nm, and the radicals produced are often involved in side reactions, such as hydrogen abstraction.[29] In contrast, azo compounds such as AIBN show an absorption peak at a wavelength of 345 nm and considerable absorption all the way to a wavelength of 400 nm.[15]

Photopolymerization provides several advantages over other forms of polymerization methods such as redox couple and thermally initiated polymerization.[30] The most prominent feature of photopolymerization is that the activation energy is lower than in redox and thermally initiated polymerizations. Photopolymerization can proceed over a wide temperature range with an extremely rapid reaction rate, which is especially useful at lower temperatures. Photopolymerization uniquely offers both spatial and temporal control of the initiation reaction through illumination control, and the production rate of active centers is often independent of temperature.[26]

In industry photoinitiators are commonly used for different applications, including curing of coatings on various materials, adhesives, printing inks, photoresists, or printing plates.[25,28,31,32] A typical example of a photoinitiation reaction is given in Scheme 2.6.

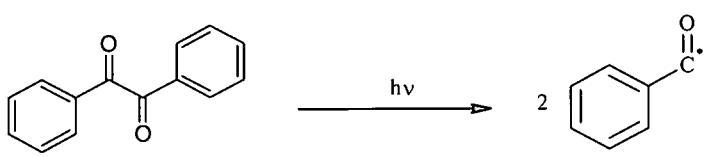

Scheme 2.6: Benzil photolysis.

2.2.1.4 Thermal self-initiation

Apart from the initiation systems that were illustrated earlier, certain monomers can undergo thermal polymerization by self-initiation processes. This involves a thermal reaction of the monomer molecules, which are capable of producing initiating species that start the polymerization reaction upon heating, normally above ambient temperature. Monomers such as MMA, styrene and its derivatives can be polymerized thermally by self-initiating reactions.[33] The focus of this discussion, will be on the thermal polymerization of styrene, which was the monomer most used in this study.

The mechanism of self-initiated polymerization of styrene in bulk liquid or solution has been a challenging subject of debate.[33-36] A valuable review by Pryor and Lasswell[35] describes the history of the thermal initiation of styrene and the extensive mechanistic studies of styrene polymerization in bulk liquid and solution since the early days of polymer chemistry.

The mechanisms that were proposed by Flory[37] and Mayo[38] for the spontaneous generation of radicals from styrene are widely accorded in literature.[33-36] According to

Mayo's mechanism, presented in Scheme 2.7, the initiation proceeds by a Diels-Alder dimerization of styrene to generate the adduct **1** (AH) dimer, which donates a hydrogen atom to a third styrene molecule to give two monoradicals (2 and 3), through molecular-assisted homolysis, that can initiate polymerization. Flory proposed his mechanism illustrating that styrene dimerizes to form a diradical adduct **5**, which is converted to monoradical initiators via hydrogen transfer to a third styrene molecule. In contrast, the diradical itself is capable of starting polymerization or it might undergo a cyclization reaction to give the byproduct 1,2-diphenylcyclobutane (**DCB**), a species that is inactive in polymerization. The proposed mechanisms are summarized in Scheme 2.7.

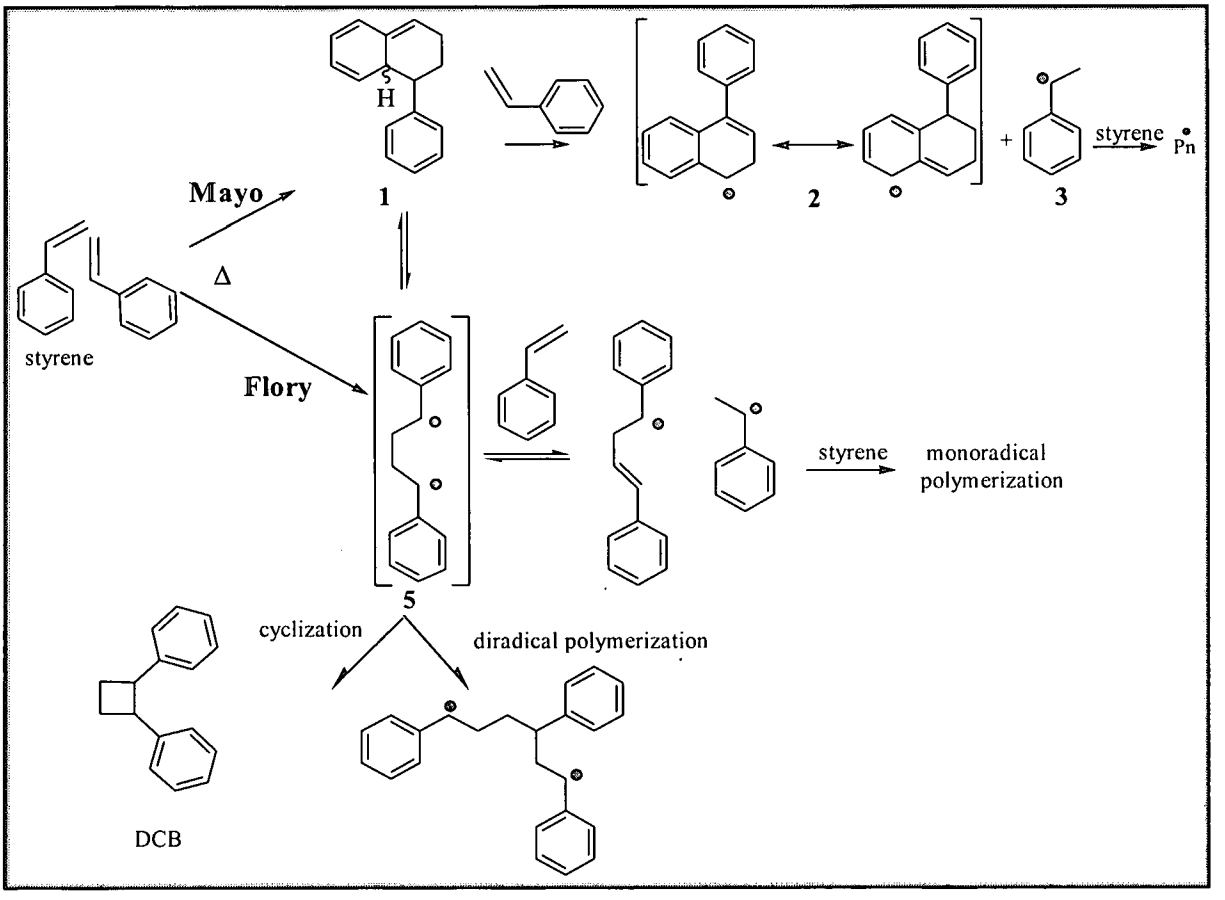

Scheme 2.7: Mayo's and Flory's mechanisms of styrene thermal initiation.[37,38]

Recently Khuong and coworkers[34] investigated Mayo and Flory's mechanisms using modern computational correlations, where they focused mainly on the process of initiation, although the propagation, termination and chain transfer reactions were also studied. The authors confirmed that the Diels-Alder styrene dimer (AH) is the key intermediate for the self-initiation of styrene polymerization, and therefore postulated a

mechanism claimed to include the necessary steps in the actual thermal polymerization. This is illustrated in Scheme 2.8.

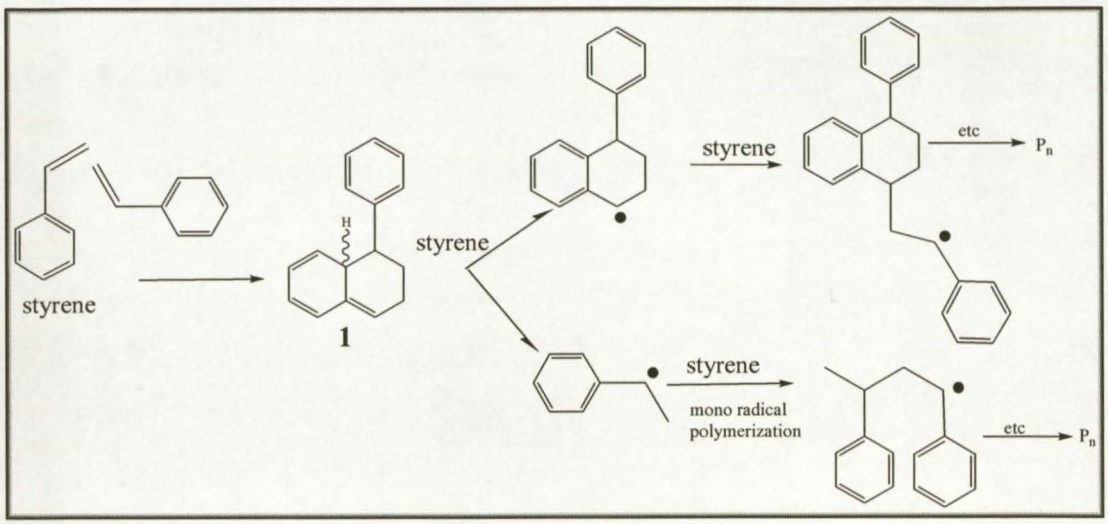

Scheme 2.8: Important reaction steps in thermal polymerization of styrene as proposed by Khuong *et al.*[34]

2.2.2 Propagation

The propagation step takes place with the availability of reactive radicals provided from the initiation step. After the initial propagating species of chain length ($P_1^{\bullet}$), (number of monomer units incorporated) is available, a rapid and successive addition of a large number of monomer units occurs, which can take place within a few seconds.[39] Each sequential addition of a monomer molecule (normally through carbon–carbon double bonds) creates a new propagating radical identical to the previous one, but larger by one monomer unit, ($P_{n+1}^{\bullet}$). The propagation steps are presented as follows:

$$P_1^{\bullet} + M \xrightarrow{k_p} P_n^{\bullet} \qquad\qquad P_n^{\bullet} + M \xrightarrow{k_p} P_{n+1}^{\bullet}$$

Where k_p is the propagation rate coefficient that is chain length dependent especially for the first few steps.[40] Thus, the rate of propagation is represented by:

$$\frac{-d[M]}{dt} = v_p = k_p [M] [P^{\bullet}] \qquad (2.9)$$

From equation 2.9, the rate of propagation is proportional to the concentration of the growing chains (active radical sites) and the monomer concentration.

2.2.3 Termination

In this step the active propagating chains are terminated by means of radical consumption through different pathways. In a typical free radical polymerization the initiation is continuous while the source of radicals is still available. However, termination leading to radical consumption is also continuous. The termination of growing polymer chains occurs irreversibly, usually involving bimolecular reactions that can occur by combination, disproportionation, or chain transfer reactions. In the case of chain transfer reactions, the process primarily stops the growing chains, yet free radicals still remain available and are been transferred via an active species that can reinitiate a new polymer chain and/or be involved in side reactions.

Generally, the termination rate coefficient is dependent on several factors, including the system viscosity, the chain lengths of the terminating chain radicals, reaction temperature, pressure, and the monomer conversion.[41]

Termination by combination occurs when the free radical ends of two propagating radical chains of arbitrary degrees of polymerization meet as follows:

$$P_n^{\bullet} + P_m^{\bullet} \xrightarrow{k_{tc,n,m}} P_{n+m} \qquad n, m = 0, 1, 2,\ldots$$

Where $k_{tc,n,m}$ is the termination rate coefficient by combination involving two macroradicals with chain lengths n and m and thus the average chain length dependent termination rate coefficient is expressed as $\langle k_{tc} \rangle$. Hence, the rate of termination ν_{tc} is given by:

$$\nu_{tc} = \langle k_{tc} \rangle [P^{\bullet}]_n [P^{\bullet}]_m \qquad (2.10)$$

Termination by disproportionation gives two terminated chains. The reaction involves a hydrogen abstraction from a growing chain, and transfer to another growing chain. In this case, the products are one chain with an unsaturated carbon-carbon terminated end bond, and the other a saturated terminated end.

$$P_n^{\bullet} + P_m^{\bullet} \xrightarrow{k_{td,n,m}} P_n + P_m$$

The above reaction represents termination by disproportionation, where $<k_{td}>$ is the rate coefficient, and the rate of termination by disproportionation, ν_{td} is given by:

$$\nu_{td} = <k_{td}> [P^{\bullet}]_n [P^{\bullet}]_m \qquad (2.11)$$

Thus, the overall rate of termination with respect to chain length effects is given by the equation 2.12:

$$\frac{-d[P^{\bullet}]}{dt} = \nu_t = \sum_n \sum_m k_t^{n,m} [P^{\bullet}]_n [P^{\bullet}]_m \qquad (2.12)$$

If the chain length effects are ignored then:

$$\frac{-d[P^{\bullet}]}{dt} = \nu_t = 2<k_t> [P^{\bullet}]^2 \qquad (2.13)$$

Where $k_t^{n,m}$ corresponds to the average termination rate coefficient $<k_t> = (<k_{tc}> + <k_{td}>)$.

The chain stoppage, via chain transfer can be achieved by hydrogen abstraction from an initiator, monomer, polymer, solvent molecule, or by deliberate addition of a compound with a labile proton or any other readily abstractable group, such as a halogen. The chain transfer reaction is a reaction in which the radical site is transferred from a growing chain to another molecule to terminate the growing chain while obtaining a new radical being capable of starting a new chain. In this case, the transfer reaction is not formally a termination reaction but it does have a significant effect on the kinetics of the polymerization process; since it depends on the particular propagating radicals involved, the polymerization medium and conditions.[42,43] Consequently, the number average degree of polymerization decreases and the reaction may yield a low molecular weight polymer, even though the concentration of free radicals is still relatively high.

A molecule which takes part in a chain transfer reaction is termed a chain transfer agent (CTA). Transfer reactions are simply described by the general schematic equations proposed by Flory:[37,42]

Transfer to solvent or a transfer agent

$$P_n^{\bullet} + T \xrightarrow{k_{trT}} P_n + T^{\bullet} \longrightarrow \textit{Reinitiating a new chain}\ T^{\bullet} + M \longrightarrow P_1^{\bullet}$$

Transfer to monomer

A growing chain is terminated, and a new initiating species is formed:

$$P_n^{\bullet} + M \xrightarrow{k_{trM}} P_n + M^{\bullet} \longrightarrow M^{\bullet} + M \longrightarrow P_1^{\bullet}$$

In some cases, the free radicals produced by chain transfer reaction may or may not initiate another polymer chain; they may be converted to an unreactive species. This is observed in reactions that are performed in the presence of various chemical substances containing functional groups with atoms of oxygen, nitrogen or sulfur, known as inhibitors. Inhibitors such as hydroquinone are normally added to prevent or at least retard the premature free radical polymerization of readily polymerizable monomers.

The agents are generally described in terms of a chain transfer constant, as defined by the general equation:

$$C_T = \frac{k_{tr,T}}{k_p} \tag{2.14}$$

Where $k_{tr,T}$ is the rate coefficient for the chain transfer agent. The subscript is changed according to the type of the transfer agent, i.e. if T is subscribed as M then it refers to transfer to monomer, and if it subscribed as S, it refers the transfer to solvent.

Taking all of the reactions that can occur during a polymerization into account and assuming that the effect of transfer is limited when the polymerization reaches steady state conditions, in which the rate of termination equals the rate of initiation, combining equations 2.7 and 2.13, then:

$$[P^{\bullet}] = \left(\frac{fk_d[I]}{\langle k_t \rangle}\right)^{1/2} \tag{2.15}$$

Combining equations 2.15 and 2.9 gives:

$$v_p = \frac{-d[M]}{dt} = k_p[M]\left(\frac{fk_d[I]}{\langle k_t \rangle}\right)^{1/2} \tag{2.16}$$

The above general equation describes the rate of thermally initiated free radical polymerization in the presence of a Unimolecular decomposing initiator, where the rate is proportional to the monomer concentration and to the square root of initiator concentration. If the propagation rate is much faster than the initiation rate, it can be assumed that $d[I]/dt$ is very small, thus equation 2.16 is modified to give:

$$[M] = [M]_o \, e^{-k_p \left(\frac{f k_d [I]}{\langle k_t \rangle}\right)^{1/2} t} \qquad (2.17)$$

2.3 Controlled/living free radical polymerization

The polymers that are produced by conventional free radical polymerization are mostly homopolymers with broad molar mass distributions, which are almost always above 1.5. This can be expected, because of different termination reactions (combination and disproportionation) that lead to the formation of an unreactive polymer chain (dead polymer chain) with a very wide range of chain lengths. Under these circumstances there is no possibility of chain extension by adding a new monomer and reactivating the polymerization.

The desire to produce polymers that meet certain requirements for applications in our daily life is endless. The modification of certain polymers to improve certain properties, by adding functional groups or by adding a second block of another monomer to form block-copolymers, is a field of continuous interest.

The key to designing and producing different and complex macromolecular architectures is the modification of the actual polymerization system, from a conventional to a controlled/living free radical polymerization system. This can be achieved by reducing or minimizing all types of termination reactions, i.e. since all reactive radicals in essence exterminate each other, and this needs to be done by trapping the active center using a special additive capable of reversibly transforming a growing chain into a dormant state, and allowing for re-initiation of the growing chain, while the rate of initiation must be significantly greater than that of propagation.

The development of new radical polymerization techniques has allowed a revolution of polymer chemistry in the past decade.[44] These techniques produce polymers with predetermined molecular weights, narrow polydispersity, block copolymers and complex architectures, and are considered "living" radical polymerization systems.

There are several methods for achieving "living" characteristics. All of these methods exploit a dynamic equilibration between growing radical chains and the different types of dormant species. At present, techniques that appear to be the most efficient and have received the greatest interest are (ATRP),[45] stable free radical mediated polymerization

techniques which include (NMP),[46] and (RAFT) mediated polymerization.[47,48] A brief description of each of the methods will be introduced, focusing mainly on the RAFT process as it is the technique used in this study.

2.3.1 Nitroxide-mediated polymerization

NMP, one of the more successful living radical polymerization techniques, was pioneered by Moad *et al.*[49] and refined by Georges *et al.*[50] NMP has been widely exploited for the synthesis of homo and block copolymers with narrow molar mass distributions.[46] Monomers that have been successfully polymerized include styrene and acrylates.[4,51-53] The "living" characteristics of NMP are achieved using stable radical compounds such as 2,2,6,6-tetramethylpiperidinyloxy (TEMPO). The principle of this technique involves a radical reaction between the propagating species $P_n^{\bullet}$ and a stable radical X°, for example TEMPO, to form a dormant species P_n-X. The resulting dormant species can then be reversibly cleaved to generate the free radical again. This process is the key step for reducing the overall concentration of the propagating radical chain ends, while minimizing irreversible termination reactions such as combination and disproportionation. All chains should ideally, be initiated only from the desired initiating species. The general mechanism of the NMP process is presented in Scheme 2.9.

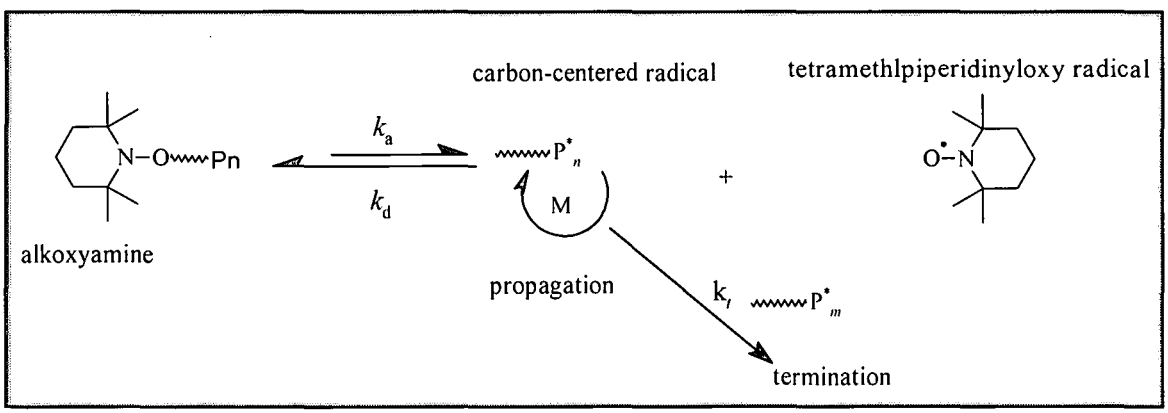

Scheme 2.9: General description of the NMP process.

Although NMP is one of the simplest methods of LFRP, it has some disadvantages. It usually requires high temperature conditions, typically above 100 °C, because the reactions are inherently slow, while the end-capped species (dormant species) is very stable, and will only be unstable at high temperatures. Furthermore, the stability of the

formed dormant alkoxyamine limits the types of monomer that can be used, and many monomers, such as methacrylates.[54,55] have not yet been polymerized.

2.3.2 Atom transfer radical polymerization

ATRP was first reported by Wang and Matyjaszewski[56,57] and Kato *et al.*[58] The ATRP process is based on reversible cleavage of a covalent bond in the dormant species via a redox reaction. The process is catalyzed by transition metal derivatives such as ruthenium, iron, or copper the most commonly used transition metal. Scheme 2.10 represents the general ATRP process.

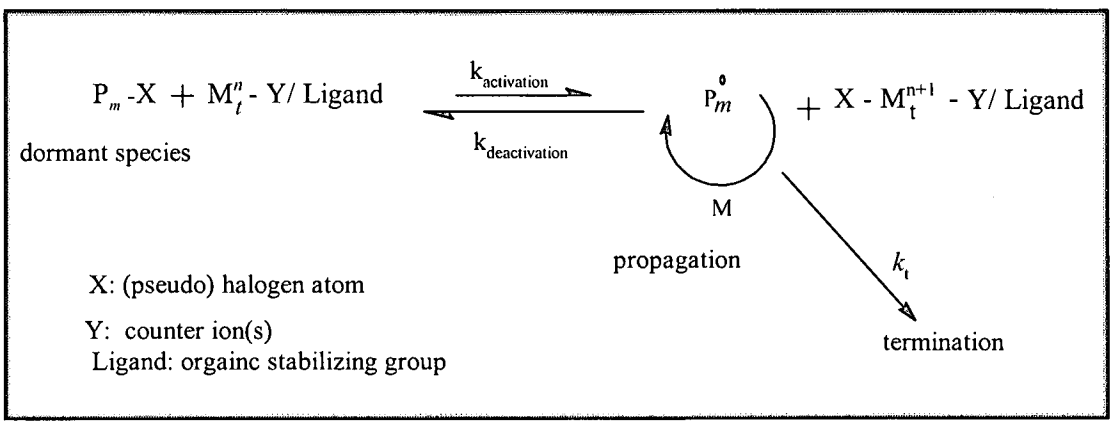

Scheme 2.10: General description of the ATRP process.

This technique is substantially more versatile than NMP, and it has been successfully applied for the polymerization of a wide range of monomers including styrenes, (meth)acrylates, (meth)acrylamides, and acrylonitrile.[45,59] It has, however, shown limitations in the direct polymerization of vinyl acetate and acrylic acids.[55] The advantages of using this process are the convenient reaction conditions, i.e. it can be performed at ambient and low temperatures, and the fact that the initiation step is very fast if suitable reagents are chosen.

The major drawback of the ATRP system is that the polymers produced contain traces of metal ions that often must be removed and possibly recycled, which is typically a complicated process. In addition, to date, the process has not been proven to be sufficiently successful in aqueous media with water soluble monomers, where control is restricted over a limited range of conditions, and low molecular weight polymers are produced. Recently Matyjaszewski and coworkers[60] introduced a new convenient initiation system termed *a*ctivator *g*enerated by *e*lectron *t*ransfer (AGET ATRP) that led to a successfully controlled homo and copolymerization of water soluble monomers such

as oligo(ethylene glycol) monomethyl ether methacrylate with high molecular weights and narrow molecular weight distributions.

2.3.3 Reversible addition-fragmentation chain transfer

The RAFT process is one of the recent entries in the development of living free radical polymerization techniques. The process was developed in Australia by the Commonwealth Scientific and Industrial Research Organization (CSIRO) and was patented by Le *et al.*[47] in 1998. Since then it has been one of the most versatile living polymerization techniques. It is applicable to a wide range of monomers (nearly all monomers that are polymerizable with conventional free radical polymerization can be used) and it is tolerant to various reaction conditions and traces of impurities.[4,48]

The basis of the RAFT process is attributed to the addition-fragmentation transfer reaction in the presence of a suitable thiocarbonyl thio compound (RAFT agent) that has a general structure presented in Figure 2.3.

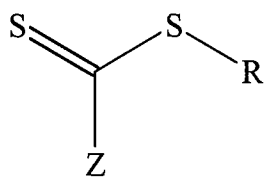

R: leaving group

Z: activating group

S: sulfur

Figure 2.3: The basic structure of a RAFT agent.[61]

Selecting the suitable RAFT agent is usually a challenge, as it should be designed according to the polymerization conditions and the type of monomer that is used. The thiocarbonyl thio compound is presented in different categories depending on the character of the Z group. There are many different types of thiocarbonyl thio compounds reported in literature. these include dithioesters,[4,62-68] dithiocarbamates[4,69-71] (Z = N-functional), trithiocarbonates[71-78] (Z = substituted sulfur), xanthates[4,71] (Z = O-functional), phosphoryl- and (thiophosphoryl)dithioformates[79,80] (Z = phosphorus) and more recently RAFT agents bearing a fluorine Z group (F-RAFT).[81,82] Examples of different Z groups in RAFT agents are illustrated in Figure 2.4.

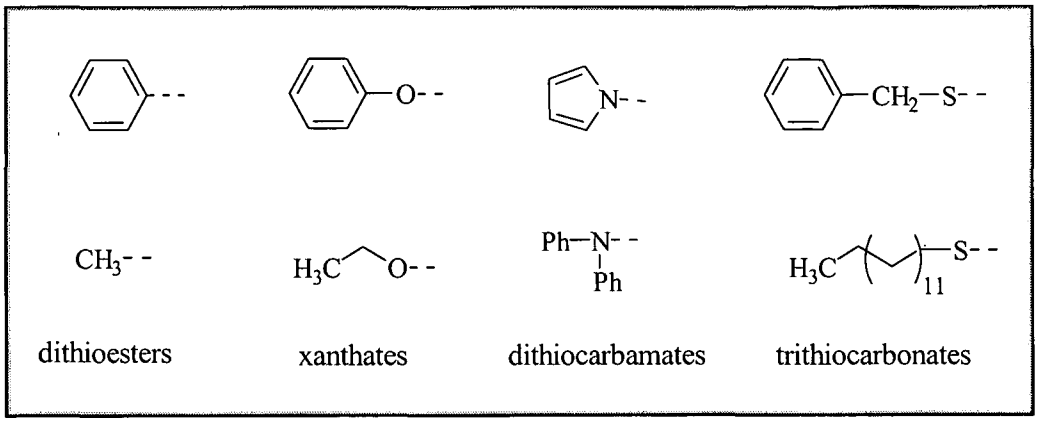

Figure 2.4: Examples of Z groups in RAFT agents.[4]

2.3.3.1 The RAFT mechanism

The elementary reactions of the RAFT process are illustrated in Scheme 2.11.[71] Evidence for the RAFT mechanism has been provided by analytical techniques such as (NMR), UV/visible[48] and electron spin resonance (ESR) spectroscopy.[83-86] The RAFT process involves conducting a polymerization in the presence of a dithioester **1** (RAFT agent) that reacts by reversible addition fragmentation chain transfer. The guiding principle is that the dithioester moiety is transferred between a dormant and an active chain. This behavior lends a "living" characteristic to the polymerization reaction. The Z group should be a suitable activating group for the thiocarbonyl (C=S) double bond to promote radical addition, and R should be a good homolytic leaving group and be reactive enough to reinitiate polymerization.[4,47,48,71,87]

To establish the "living" characteristics in the reaction, both the initial **1** and polymeric **2** RAFT agents should possess reactive (C=S) double bonds (i.e. high k_{add}).[10,88]

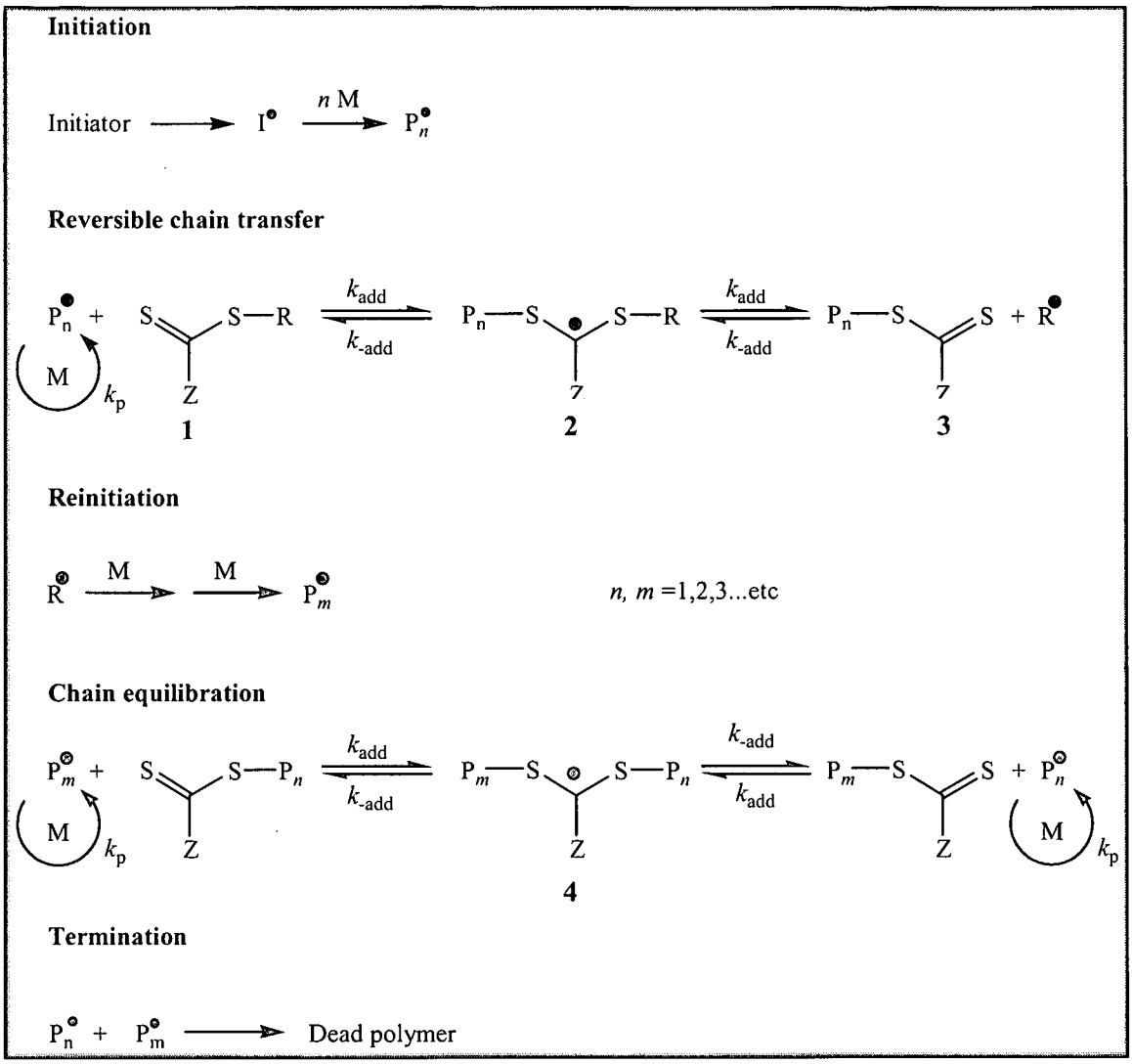

Scheme 2.11: Elementary reactions of the RAFT process.

Once the intermediate radicals **2** and **4** are formed, a rapid fragmentation should take place (i.e. high k_{-add}), which is dependent on the strength of the S-R bond that is influenced by the activity of Z group.[88] In an ideal case, no side reactions take place.

The main equilibrium illustrated in Scheme 2.11 is in essence the core of the RAFT process,[10,89] where the rate coefficients k_{add} and k_{-add} control the position of the equilibrium. k_{add} controls the addition step between the polymeric free radical and the polymeric RAFT agent **3** and leads to the formation of the intermediate **4**. k_{-add} can be referred to as the average inverse lifetime of the polymeric RAFT intermediate radical (which ideally should be short lived).

The RAFT process has been extensively used with different monomers and it is reported that the performance of RAFT agents depends strongly on the R, and Z groups[90] and the

monomer used. Some examples of common radicals formed from the R groups that have been extensively used so far are presented in Figure 2.5.

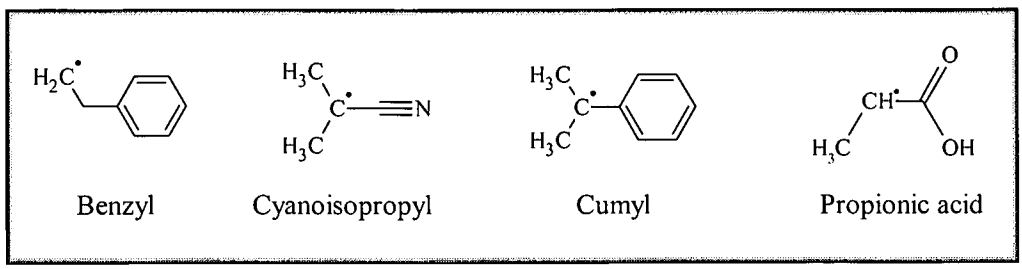

Figure 2.5: Examples of different R groups of RAFT agents.[4]

Recent studies by the CSIRO group and others[71,87,91] investigated the role of the R and Z groups in the polymerization of different monomers such as styrene and methyl methacrylate. It was found that the reactivity of the RAFT agent is enhanced when using phenyl as the activating group, and the transfer coefficient decreases in the series where Z is Ph >SCH_2Ph ~ SMe ~ Me ~ N-pyrrolo>> OC_6F_5 > N-lactam > OC_6H_5 > O (alkyl) >N (alkyl).[71,90]

There are important factors that determine the ability of the adduct **2** depicted in Scheme 2.11 to partition between starting materials and products, which is dependent on the relative leaving dependency of the group R versus the propagating radical. These factors include radical stability, and steric and polar factors.[4,87] The more stable, more electrophilic and more bulky radicals are better leaving groups.[90]

Compounds with good leaving groups such as cumyl and isobutyronitrile produced polymers with considerably narrow polydispersities.

2.3.3.2 Retardation in RAFT mediated polymerization

When RAFT mechanism is considered as shown in Scheme 2.11, ideally, in the addition-fragmentation steps, the transfer of the dithioester moiety between active and dormant chains should be rapid and favor the parallel growth of the polymer chains uniformly. This should occur without influencing the polymerization rate, i.e. to attain control in the RAFT process a practical balance between the (forward and reverse) rates of addition and fragmentation (k_{add} and k_{-add}) together with the rate of initiation, k_i, and propagation, k_p, is vital. However, bimolecular termination of free radicals cannot be avoided, and termination can occur between polymeric free radicals and/or initiator-derived radicals or RAFT agent-derived radicals.

However, with many RAFT agents, various side reactions may potentially complicate the RAFT mechanism, causing rate retardation.[92] A decrease in the polymerization rate is observed using specific RAFT agents and the cause of such retardation effects has been the topic of ongoing debate.[4,93-95]

The argument surrounds the actual kinetic behavior of the two main equilibrium reactions of the macro RAFT adducts **2** and **4**, and whether the intermediate radical is short lived or long-lived, relative to the propagation rate. This in turn results in different consequences of intermediate lifetimes in terms of the actual mechanism; however, both mechanisms may lead to retardation in the polymerization process.

Some research groups have attributed the retardation to the slow fragmentation of the intermediate radicals between starting material and products, which is related to the fragmentation rate coefficient.[94,96-100] Others explained the cause differently, where the retardation effect may be because of various (irreversible or reversible) termination reactions of the intermediate radicals,[85,101-104] for example, the possibility of a cross-termination reaction producing a 3-arm star polymer has been reported.[103,104]

Extensive studies have been carried out in efforts to understand the RAFT mechanism. These have included various experimental,[71,87,88,105] theoretical,[97,106-109] and semiempirical[71,87,110] methods in the presence of common RAFT agents such as cumyl dithiobenzoate (CDB), and cyanoisopropyl dithiobenzoate (CPDB) with different monomers including styrene (St), MMA, methyl acrylate (MA) and butyl acrylate (BA). A pronounced retardation was observed when using high concentrations of RAFT agents such as cumyl dithiobenzoate in the polymerization of styrene.[85,88,92,95,99,111]

Several factors should be kept in mind with respect to the RAFT mechanism. These include the nature of the R and Z substituents and their role in the mechanism, the type of monomer used with regard to the chosen RAFT agent, i.e. the transfer coefficient of the RAFT agent is governed by the type of R and Z group used for any specific monomer.

For example, it has been reported that using an electron withdrawing Z substituent such as a phenyl group can significantly retard the fragmentation rate (high equilibrium constant, $K_{eq} = \frac{k_{add}}{k_{-add}}$) of the intermediate radicals 2 and 4. This has been attributed to the stability of the intermediate radical, as the phenyl ring allows for delocalization of the unpaired electron onto the aromatic ring. Coote and coworkers[97,100,109] have studied the effect of

different R and Z substituents using high-level ab initio molecular orbital calculations[112] that allow for the calculation of the rate and equilibrium constants. In their studies, for example, replacing a phenyl ring by a benzyl substituent significantly inhibits the delocalization effect and hence the retardation effect can be reduced. They concluded that the retardation effect is mainly due to the slow fragmentation of the intermediate radical **4** rather than macro RAFT adduct **2,** based on computational quantum chemistry

Temperature also plays a significant role, since the retardation effect was relieved by increasing the reaction temperature.[4,92,113-115]

Although the origin of rate retardation is understood to some extent, no quantitative proof is available yet. There is still some debate with regards to the actual values of the transfer rate coefficients. Different researchers determined the rate coefficient for CDB and a six order of magnitude difference was recorded.[116] Depending on the kinetic model and the assumptions made, inconsistencies of the measured equilibrium constants can arise. Some of these measurements were based on model simulations of the competing radicals involved in the RAFT process developed by Wang and Zhu,[117] or a correlation of rate and molecular weight data using computational software[95,96,118], and the rate data of the adduct radical concentration measured by ESR spectroscopy.[85]

McLeary *et al.*[114,115,119] have investigated the kinetics of the early stages of polymerization using in situ ^{1}H NMR spectroscopy, in the presence of different RAFT agents such as CDB and CPDB with different monomers such as MA and St, initiated by AIBN. The authors investigated the inhibition effect that has been observed in the early stages of CPDB and CDB mediated polymerizations, which was based on kinetic differences between the period referred to as the initialization period (defined as the period in which the initial RAFT agent is converted to single or higher monomer adducts) and the period thereafter. Often in this initialization period, for a good leaving group, the RAFT agent is mainly converted to its single monomer adduct, forming the intermediate radical **2**, which selectively fragments to give an R-based radical. After all of the initial RAFT agent is consumed the dominant radicals and the resulting kinetics, are different. For example, in the case of CPDB RAFT agent, fragmentation of the intermediate radical formed was selective towards producing isobutyronitrile radicals, which were the significant propagating species available during the initialization period.[83,115] However, when CDB was used, a longer initialization period was observed, and it was suggested that this might be because of the slower addition rate of the cumyl radical to styrene when compared to

the isobutyronitrile radical, and higher average termination rates of the cumyl radicals than for the isobutyronitrile radicals.[114]

Plummer *et al.*[120] have shown that the presence of impurities in the RAFT agent such as CDB can significantly influence the rate of polymerization, resulting in inhibition or retardation. Moad *et al.*[4,88] and Benaglia *et al.*[91] have reviewed all of the possible effects that can cause retardation, including the different termination reaction pathways that the intermediate radicals can undergo.

2.4 Stereo-control in radical polymerization

The development of LFRP techniques such as NMP, ATRP and RAFT has allowed for the synthesis of various homo and copolymers with predetermined molecular weight and narrow molecular weight distribution, controlled functionalities, and complex architectures. However, these techniques do not provide control over chain microstructure in terms of sequence distribution and tacticity.[121]

The numerous studies that concern the tacticity of various vinyl polymers mostly deal with different synthetic routes for achieving stereocontrol of certain polymers, as well as the characterization of such tacticity effects using different analytical techniques, including ^{1}H-NMR and ^{13}C-NMR[122] spectroscopy and differential scanning calorimetry (DSC).[123]

Although stereocontrol has been achieved with certain polymeric systems such as polymethacrylates,[124-132] polyacrylamides,[133,134] and polymethacrylamides,[134,135] it however still provides polymers with uncontrolled molecular weight and broad molecular weight distribution.

Since stereoregularity of polymers is an important feature that affects polymer properties, a new area of interest that has recently attracted polymer chemists, is obtaining stereocontrolled homo and copolymers (controlled microstructure) with controlled macromolecular architectures via living radical polymerization techniques.

In this section, a general introduction to polymer stereosequence isomerism (tacticity) will be given. The focus will be mainly on MMA tacticity and the factors that determine the tacticity of the polymer chain. Mention will be made of some research efforts that have been directed towards achieving stereocontrol via living radical polymerization techniques as reported in the literature.

2.4.1 Polymer tacticity

Polymers have different substructures. The polymerization of a vinyl monomer (mono or di-substituted) involves the addition of each monomer unit to a chiral center. Stereoregularity is the term used to describe the configuration of polymer chains, where configuration is the arrangement of the substituents attached to a chiral center. The addition to double bonds is not completely regiospecific,[136] but most vinyl monomers primarily undergo head-to-tail addition. Different arrangements such as head-to-head and tail-to-tail occur, but in most instances their contribution is minor in the overall polymer structure. The tacticity of a polymer is related to the distribution of the steric configurations along the chain, in other words, the relationship between two adjacent chiral centers. If we consider a vinyl monomer having a general structure shown in Scheme 2.12, the different arrangements of the functional groups X and Y around the chiral center can lead to different stereoregular configurations, and hence the polymer will have tacticity.

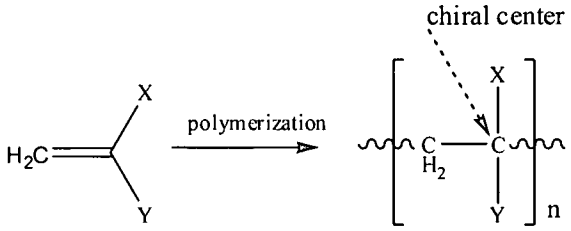

vinyl monomer
X= H, methyl, ethyl...etc
Y= methyl, acetyl, phenyl..etc

Scheme 2.12: General structure of a vinyl monomer with X and Y functional groups.

There are three general chain structures : isotactic, syndiotactic, and atactic chains.[136]

1. In the isotactic chain, the substituents (functional groups) are all on the same side of the polymer chain.

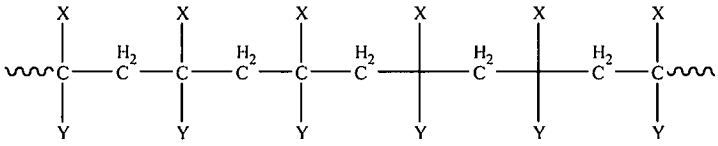

isotactic: chiral centers the same

2. The syndiotactic chain has the substituents alternating in a regular fashion.

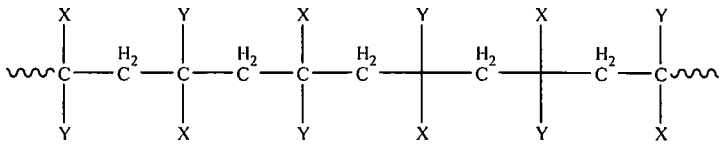

syndiotactic: chiral centers alternate

3. The atactic chain has the substituents randomly distributed along the polymer chain.

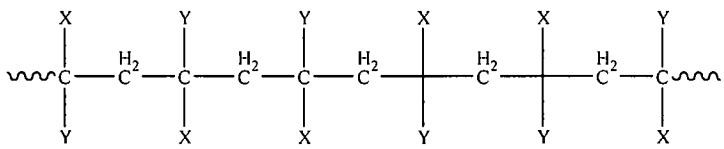

atactic: chiral centers random

Stereoregularity of polymers is determined by the mechanism of polymerization, since the tacticity deals with the relative configurations of substituents, whether they are on the same or opposite side with respect to the substituents on the neighboring unit. However, in most cases there will be a combination of these idealized structures within the polymer, where one type of tacticity or a combination of two or more tacticities are predominant. The tacticity is frequently discussed in terms of meso (*m*) and racemic (*r*) *n*-ads with respect to the configuration of the neighboring monomer units (e.g. a dyad represents two adjacent monomer units); if the chiral centers have the same configuration it is termed a meso (m) dyad, and if the centers have the opposite configuration it is termed a racemic *(r)* dyad. The triad simply represents three adjacent monomer units. Therefore the tacticity is often represented by the amount percentage of dyads, triads, tetrads... *n*-ads. Figure 2.4 illustrates an example of different *n*-ads that can be identified in an *rmmmr* hexad.

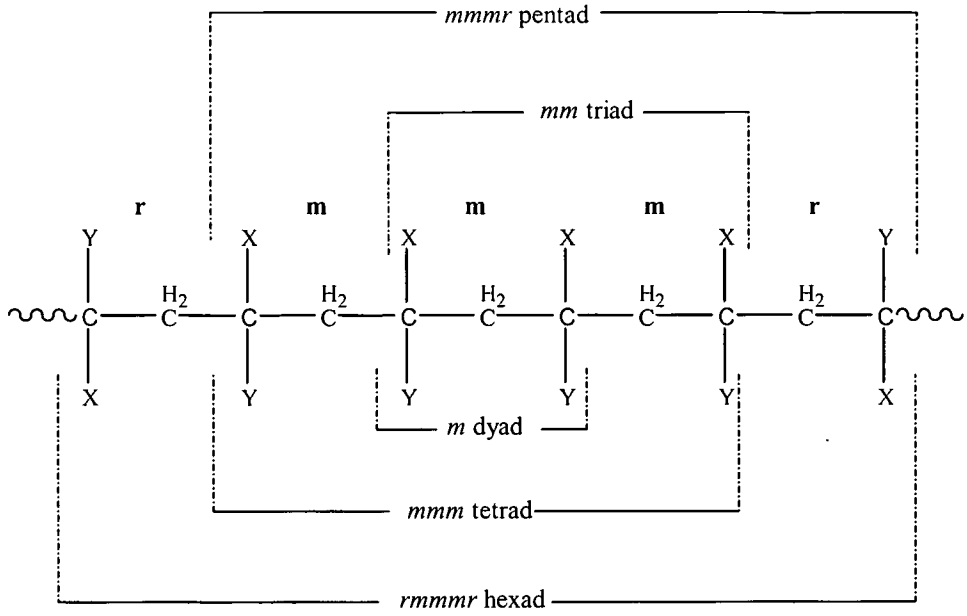

Figure 2.6: Representation of a *rmmmr* hexad tactic chain.

2.4.2 Stereoregulation of vinyl monomers

The stereoregulation of a polymer can be varied by changing the polymerization conditions. Factors such as the type of solvent (polar or non-polar), reaction temperature and the type of catalyst used play significant roles in determining the stereostructure and tacticity.[137] Stereoregular polymerization of vinyl monomers such as MMA has been extensively studied with different catalytic systems and under various reaction conditions. The first stereoregular polymerizations of isotactic and syndiotactic methacrylates were conducted by Fox *et al.*[130] and Miller *et al.*[131] in 1958. They used a variety of lithium, magnesium and aluminium compounds and carried out ionic and free radical polymerization reactions. Since then considerable effort has been made to achieve stereocontrol using alternative catalysts, including organolanthanide metallocenes,[128] metallic sodium, Ziegler-Natta catalysts,[137] horseradish peroxides[132] and Lewis acids.[125] These systems were all found to be effective catalysts for the polymerization of MMA to iso- or syndiotactic polymers.

The desire to enhance certain properties by varying and controlling the tacticity of the polymer produced is a great target, because polymers of various stereochemistry possess different properties. For example, the T_g of methacrylic polymers is known to change as a function of tacticity.[123,138-141] This is mainly because of the different chain packing and crystallizability. A highly syndiotactic PMMA possesses a higher T_g than its isotactic or atactic counterpart. The higher T_g is attributed to higher chain stiffness or stronger

intermolecular interaction between polar vinyl groups because of the different chain packing in the polymer. A high T_g syndiotactic PMMA can be utilized in industrial applications such as in optical fibers and disks.[132] Furthermore, important bulk properties such as tensile strength, melting point and solubility have all been shown to depend on the stereoregularity of the polymer.[142]

Solvents have also been shown to affect the stereoregularity of polymers. It has recently been reported by Okomato *et al.*[124,126,143] that using bulky polar solvents such as fluoroalcohols improved the stereochemistry of vinyl ester and MMA polymerizations. The authors investigated the effect of different solvents on the stereoregularity of these monomers. The primary finding was that using fluoroalcohols including 1,1,1,3,3,3-hexafluoro-2-propanol (HFIP) and perfluoro-*tert*-butyl alcohol (PFTB) as the polymerization medium, improved the syndioselectivity of PMMA. The tacticity of the polymers obtained in different solvents was dependent on the polymerization temperature; at lower temperatures a pronounced increase in the *rr* specificity was observed, e.g. the *rr* content for PMMA was 71% at 20 °C and 78% at –40 °C. The highest rr content was obtained in PFTB, it reached 93%, which is the highest reported value for the free radical polymerization of methacrylates.[124]

2.5 Simultaneous control of molecular weight and tacticity via LFRP

Stereocontrol via LFRP is a relatively new research area; the combination of techniques available that allow stereocontrol to be achieved, together with the LFRP techniques, has attracted polymer scientists to improve polymer properties based on both microstructure and macromolecular design. Research efforts based on the simultaneous control of molecular weight and stereoregularity using LFRP was initially limited to (meth)acrylamide monomers in the presence of certain Lewis acids.

Recently Ray *et al.*[144,145] reported the synthesis of well defined stereoblocks of (atactic-block-isotactic) poly(*N*-isopropylacrylamide) with RAFT-mediated polymerization in the presence of Lewis acids (known to enhance the isotacticity) such as yttrium trifluoromethanesulfonate [$Y(OTf)_3$].[134]

Lutz *et al.*[121], investigated the use of LFRP techniques, including ATRP, RAFT and NMP in the presence of Lewis acids $Y(OTf)_3$ and ytterbium trifluoromethanesulfonate [$Yb(OTf)_3$] for the production of well-defined isotactic poly(*N,N*-dimethylacrylamide)

and stereoblock poly(*N,N*-dimethylacrylamide).[121] They found that the RAFT process was more versatile, as it has very low interference with the Lewis acids. Besides using (meth)acrylamide monomers, LFRP techniques were exploited in the stereocontrolled polymerization of other interesting monomers such as MMA. Miura and coworkers[146,147] reported that the simultaneous control of molecular weight and tacticity of PMMA could be accomplished. A highly syndiotactic PMMA was synthesized[146,147] with a very narrow polydispersity by ATRP in HFIP, using various Cu^{I}/ligand combinations, including ligands such as tris[2-(dimethylamino)ethyl]amine (Me_6TREN), 2,2'-bipyridine (Bpy) and 1,1,4,7,10,10-hexamethyltriethylenetetramine (HMTETA).

Wan *et al.*[148] investigated the stereocontrolled RAFT polymerization of *N*-vinyl pyrrolidone in different solvents including fluoroalcohols in the presence of (*o*-ethylxanthylmethyl)benzene and [1-(*o*-ethylxanthyl)ethyl]benzene as chain transfer agents (CTAs). Their results showed that the higher acidity and bulkiness of the fluoroalcohols led to higher syndiotacticity and there was however, a strong dependence on the solvent to monomer ratio. There have been no such examples for merging the RAFT process with fluoroalcohol mediated stereoselective processes for methacrylates. Since the RAFT process is a convenient polymerization method and compatible with various reaction conditions, it is of interest to expand stereocontrolled polymers mediated via the RAFT process to applicable monomers such as MMA.

In this study therefore the stereocontrolled RAFT mediated polymerization of MMA was investigated in various solvents including HFIP, 2-propanol and toluene at different temperatures. The effect of temperature on the tacticity and the molecular weight distribution of the polymers obtained were also investigated.

2.6 References

1. Saunders, K. J., *Organic Polymer Chemistry: An Introduction to the Organic Chemistry of Adhesives, Fibres, Paints, Plastics and Rubbers,* Chapman and Hall: London, 1973; p 1.

2. Stevens, M. P., *Polymer Chemistry: An Introduction*, Second ed.; Oxford University Press: New York, 1990; pp 3-10.

3. Skupinska, J. *Chem. Rev.* 1991, 91, 613-48.

4. Moad, G.; Rizzardo, E.; Thang, S. H. *Aust. J. Chem.* 2005, 58, 379-410.

5. Klingsberg, A.; Baldwin, T., *Encyclopedia of Polymer Science and Engineering,* Second ed.; Wiley: New York, 1988; Vol. 13; pp 708-797.

6. Sandler, S.; Karo, W., *Polymer Syntheses*, Second ed.; Academic Press: Boston, 1992; Vol. 1; pp 2-35.

7. Hiemenz, P., *Polymer Chemistry: The Basic Concepts*, Dekker: New York, 1984; pp 345-404.

8. Flory, P., *Principles of Polymer Chemistry*, Cornell University Press: New York, 1978; pp 107-146.

9. Walling, C., *Free Radicals in Solution*, Wiley: New York, 1957; pp 67, 74.

10. Moad, G.; Solomon, D. H., *The Chemistry of Free Radical Polymerization*, Second ed.; Elsevier: Amsterdam, 2006; pp 74-75.

11. Seymour, R., *Introduction to Polymer Chemistry*, McGraw-Hill: New York, 1971; pp 136-150.

12. Gowariker, V.; Viswanathan, N.; Sreedhar, J., *Polymer Science*, Wiley Eastern Limited: New Delhi, 1986; pp 105-135.

13. Engel, P. S. *Chem. Rev.* 1980, 80, 99-150.

14. Jaffe, A. B.; Skinner, K. J.; McBride, J. M. *J. Am. Chem. Soc.* 1972, 94, 8510-15.

15. Walling, C., *Free Radicals in Solution*, Wiley: New York, 1957; pp 539-548.

16. Crivello, J. V.; Dietliker, K., *Photoinitiators for Free Radical Cationic and Anionic Photopolymerisation* Second ed.; Bradley, G., Ed. John Wiley: Chichester, West Sussex, 1998; Vol. 3; pp 3-52.

17. Guillet, J., *Polymer Photophysics and Photochemistry: An Introduction to the Study of Photoprocesses in Macromolecules*, Cambridge University Press: Cambridge, 1985.

18. Solomons, T. W. G., *Organic Chemistry*, Fourth ed.; Wiley: New York, 1988; pp 21-35.

19. Morrison, R. T.; Boyd, R. N., *Organic Chemistry* Sixth ed.; Prentice-Hall International Inc.: New Jersey, 1992; pp 597-599.

20. Morrison, R. T.; Boyd, R. N., *Organic Chemistry* Sixth ed.; Prentice-Hall International, Inc.: New Jersey, 1992; pp 991-1024.

21. Crivello, J. V.; Dietliker, K., *Photoinitiators for Free Radical Cationic and Anionic Photopolymerisation,* Second ed.; Bradley, G., Ed. John Wiley: Chichester, West Sussex, 1998; Vol. 3; p 15.

22. Guillet, J., *Polymer Photophysics and Photochemistry: An Introduction to the Study of Photoprocesses in Macromolecules*, Cambridge University Press: Cambridge, 1985; p 8.

23. Crivello, J. V.; Dietliker, K., *Photoinitiators for Free Radical Cationic and Anionic Photopolymerisation,* Second ed.; Bradley, G., Ed. John Wiley: Chichester, West Sussex, 1998; Vol. 3; p 18.

24. Hiemenz, P., *Polymer Chemistry: The Basic Concepts*, Dekker: New York, 1984; pp 350-353.

25. Crivello, J. V.; Dietliker, K., *Photoinitiators for Free Radical Cationic and Anionic Photopolymerisation,* Second ed.; Bradley, G., Ed. John Wiley: Chichester, West Sussex, 1998; Vol. 3; pp 61-81.

26. Kaur, M.; Srivastava, A. K. *J. Macromol. Sci., Polym. Rev.* 2002, C42, 481-512.

27. Decker, C. *Polym. Int.* 1998, 45, 133-141.

28. Allen, N. S. *Photochemistry* 2003, 34, 197-266.

29. Matyjaszewski, K.; Davis, T. P., *Handbook of Radical Polymerization*, Wiley Interscience: Hoboken, 2002; pp 123-124.

30. Halley, P. J.; Mackay, M. E. *Polym. Eng. Sci.* 1996, 36, 593-609.

31. Cokbaglan, L.; Arsu, N.; Yagci, Y.; Jockusch, S.; Turro, N. J. *Macromolecules* 2003, 36, 2649-2653.

32. Aydin, M.; Arsu, N.; Yagci, Y.; Jockusch, S.; Turro, N. J. *Macromolecules* 2005, 38, 4133-4138.

33. Moad, G.; Solomon, D. H., *The Chemistry of Free Radical Polymerization*, Second ed.; Elsevier: Amsterdam, 2006; pp 106-109.

34. Khuong, K. S.; Jones, W. H.; Pryor, W. A.; Houk, K. N. *J. Am. Chem. Soc.* 2005, 127, 1265-1277.

35. Pryor, W. A.; Lasswell, L. D. *Advances in Free-Radical Chemistry (London)* 1975, 5, 27-99.

36. Pryor, W.; Coco, J. *Macromolecules* 1970, 3, 500-508.

37. Flory, P. J. *J. Am. Chem. Soc.* 1937, 59, 241-53.

38. Mayo, F. R. *J. Am. Chem. Soc.* 1968, 90, 1289-95.

39. Hiemenz, P., *Polymer Chemistry: The Basic Concepts*, Dekker: New York, 1984; p 346.

40. Barner-Kowollik, C.; Vana, P.; Davis, T. P., The kinetics of free radical polymerization. In *Handbook of Radical Polymerization*, Matyjaszewski, K.; Davis, T. P., Eds. John Wiley and Sons: Hoboken, 2002; p 197.

41. Barner-Kowollik, C.; Vana, P.; Davis, T. P., The kinetics of free radical polymerization. In *Handbook of Radical Polymerization*, Matyjaszewski, K.; Davis, T. P., Eds. John Wiley and Sons: Hoboken 2002; pp 206-207.

42. Flory, P., *Principles of Polymer Chemistry*, Cornell University Press: New York, 1978; pp 136-148.

43. Moad, G.; Solomon, D. H., *The Chemistry of Free Radical Polymerization*, Second ed.; Elsevier: Amsterdam, 2006; pp 279-283.

44. Moad, G.; Solomon, D. H., *The Chemistry of Free Radical Polymerization*, Second ed.; Elsevier: Amsterdam, 2006; pp 451-564.

45. Matyjaszewski, K.; Xia, J. *Chem. Rev.* 2001, 101, 2921-2990.

46. Hawker, C. J.; Bosman, A. W.; Harth, E. *Chem. Rev.* 2001, 101, 3661-3688.

47. Le, T. P.; Moad, G.; Rizzardo, E.; Thang, S. H. PCT. Int. Appl. 1998, wo98/01478,

48. Chiefari, J.; Chong, Y. K. B.; Ercole, F.; Krstina, J.; Jeffery, J.; Le, T. P. T.; Mayadunne, R. T. A.; Meijs, G. F.; Moad, C. L.; Moad, G.; Rizzardo, E.; Thang, S. H. *Macromolecules* 1998, 31, 5559-5562.

49. Moad, G.; Rizzardo, E.; Solomon, D. H. *Macromolecules* 1982, 15, 909-914.

50. Georges, M. K.; Veregin, R. P. N.; Kazmaier, P. M.; Hamer, G. K. *Macromolecules* 1993, 26, 2987-2988.

51. Chong, B. Y. K.; Ercole, F.; Moad, G.; Rizzardo, E.; Thang, S. H.; Anderson, A. G. *Macromolecules* 1999, 32, 6895-6903.

52. Moad, G.; Rizzardo, E. *Macromolecules* 1995, 28, 8722-8728.

53. Hawker, C. J. *Acc. Chem. Res.* 1997, 30, 373-382.

54. Matyjaszewski, K., *Controlled/Living Radical Polymerization: Progress in ATRP, NMP, and RAFT*, American Chemical Society: Washington, D.C, 2000; pp 20-25.

55. Kricheldorf, H.; Nuyken, O.; Swift, G., Handbook of polymer synthesis, Second ed.; Dekker: 2005; pp 908-910.

56. Wang, J.-S.; Matyjaszewski, K. *J. Am. Chem. Soc.* 1995, 117, 5614-5615.

57. Wang, J.-S.; Matyjaszewski, K. *Macromolecules* 1995, 28, 7901-7910.

58. Kato, M.; Kamigaito, M.; Sawamoto, M.; Higashimura, T. *Macromolecules* 1995, 28, 1721-1723.

59. Kamigaito, M.; Ando, T.; Sawamoto, M. *Chem. Rev.* 2001, 101, 3689-3745.

60. Kwon Oh, J.; Min, K.; Matyjaszewski, K. *Macromolecules* 2006, 39, 3161-3167.

61. Moad, G.; Solomon, D. H., *The Chemistry of Free Radical Polymerization*, Second ed.; Elsevier: Amsterdam, 2006; p 501.

62. Tonge, M. P.; McLeary, J. B.; Vosloo, J. J.; Sanderson, R. D. *Macromol. Symp.* 2003, 193, 289-304.

63. Barner, L.; Quinn, J. F.; Barner-Kowollik, C.; Vana, P.; Davis, T. P. *Eur. Polym. J.* 2003, 39, 449-459.

64. Perrier, S.; Davis, T. P.; Carmichael, A. J.; Haddleton, D. M. *Eur. Polym. J.* 2003, 39, 417-422.

65. Prescott, S. W.; Ballard, M. J.; Rizzardo, E.; Gilbert, R. G. *Macromolecules* 2002, 35, 5417-5425.

66. Severac, R.; Lacroix-Desmazes, P.; Boutevin, B. *Polym. Int.* 2002, 51, 1117-1122.

67. Chong, B. Y. K.; Le, T. P.; Moad, G.; Rizzardo, E.; Thang, S. H. *Macromolecules* 1999, 32, 2071-2074.

68. Shim, S. E.; Lee, H.; Choe, S. *Macromolecules* 2004, 37, (15), 5565-5571.

69. Matyjaszewski, K.; Davis, T. P., *Handbook of Radical Polymerization*, John Wiley and Sons: Hoboken, 2002; pp 661-668.

70. Thang, S. H.; Chong, Y. K. B.; Mayadunne, R. T. A.; Moad, G.; Rizzardo, E. *Tetrahedron Lett.* 1999, 40, 2435-2438.

71. Chiefari, J.; Mayadunne, R. T. A.; Moad, C. L.; Moad, G.; Rizzardo, E.; Postma, A.; Skidmore, M. A.; Thang, S. H. *Macromolecules* 2003, 36, 2273-2282.

72. Smulders, W.; Gilbert, R. G.; Monteiro, M. J. *Macromolecules* 2003, 36, 4309-4318.

73. Degani, I.; Fochi, R.; Gatti, A.; Regondi, V. *Synthesis* 1986, 894-899.

74. Stenzel, M. H.; Davis, T. P. *J. Polym. Sci.: Part A: Polym. Chem.* 2002, 40, 4498-4512.

75. You, Y.-Z.; Chun-Yan, H.; Bai, R.-K.; Pan, C.-Y.; Wang, J. *Macromol. Chem. Phys.* 2002, 203, 477-483.

76. Mayadunne, R. T. A.; Rizzardo, E.; Chiefari, J.; Krstina, J.; Moad, G.; Postma, A.; Thang, S. H. *Macromolecules* 2000, 33, 243-245.

77. You, Y.-Z.; Bai, R.-K.; Pan, Cia-Yuan. *Macromol. Chem. Phys.* 2001, 202, 1980-1985.

78. Lai, J. T.; Filla, D.; Shea, R. *Macromolecules* 2002, 35, 6754-6756.

79. Laus, M.; Papa, R.; Sparnacci, K.; Alberti, A.; Benaglia, M.; Macciantelli, D. *Macromolecules* 2001, 34, 7269-7275.

80. Alberti, A.; Benaglia, M.; Laus, M.; Macciantelli, D.; Sparnacci, K. *Macromolecules* 2003, 36, 736-740.

81. Theis, A.; Stenzel, M. H.; Davis, T. P.; Coote, M. L.; Barner-Kowollik, C. *Aust. J. Chem.* 2005, 58, 437-441.

82. Coote, M. L.; Izgorodina, E. I.; Cavigliasso, G. E.; Roth, M.; Busch, M.; Barner-Kowollik, C. *Macromolecules* 2006, 39, 4585-4591.

83. Tonge, M. P.; Calitz, F. M.; Sanderson, R. D. *Macromol. Chem. Phys.* 2006, 207, 1852-1860.

84. Calitz, F. M.; Tonge, M. P.; Sanderson, R. D. *Macromolecules* 2003, 36, 5-8.

85. Kwak, Y.; Goto, A.; Tsujii, Y.; Murata, Y.; Komatsu, K.; Fukuda, T. *Macromolecules* 2002, 35, 3026-3029.

86. Hawthorne, D. G.; Moad, G.; Rizzardo, E.; Thang, S. H. *Macromolecules* 1999, 32, 5457-5459.

87. Chong, Y. K. B.; Krstina, J.; Le, T. P. T.; Moad, G.; Postma, A.; Rizzardo, E.; Thang, S. H. *Macromolecules* 2003, 36, 2256-2272.

88. Moad, G.; Chiefari, J.; Chong, Y.; Krstina, J.; Mayadunne, R. T.; Postma, A.; Rizzardo, E.; Thang, S. H. *Polym. Int.* 2000, 49, 993-1001.

89. Feldermann, A.: Ah Toy, A.: Hong Phan, Stenzel, M H.: Davis, T P.; Barner-Kowollik, C. *Polymer* 2004, 45, 3997-4007.

90. Moad, G.; Solomon, D. H., *The Chemistry of Free Radical Polymerization*, Second ed.; Elsevier: Amsterdam, 2006; pp 505-514.

91. Benaglia, M.; Rizzardo, E.; Alberti, A.; Guerra, M. *Macromolecules* 2005, 38, 3129-3140.

92. Moad, G.; Solomon, D. H., *The Chemistry of Free Radical Polymerization*, Second ed.; Elsevier: Amsterdam, 2006; pp 517-518.

93. Perrier, S.; Barner-Kowollik, C.; Quinn, J. F.; Vana, P.; Davis, T. P. *Macromolecules* 2002, 35, 8300-8306.

94. Chernikova, E.; Morozov, A.; Leonova, E.; Garina, E.; Golubev, V.; Bui, C.; Charleux, B. *Macromolecules* 2004, 37, 6329-6339.

95. Barner-Kowollik, C.; Quinn, J. F.; Nguyen, T. L. U.; Heuts, J. P. A.; Davis, T. P. *Macromolecules* 2001, 34, 7849-7857.

96. Barner-Kowollik, C.; Quinn, J. F.; Morsley, D. R.; Davis, T. P. *J. Polym. Sci. Part A: Polym. Chem.* 2001, 39, 1353-1365.

97. Coote, M. L.; Radom, L. *J. Am. Chem. Soc.* 2003, 125, 1490-1491.

98. Barner-Kowollik, C.; Coote, M. L.; Davis, T. P.; Radom, L.; Vana, P. *J. Polym. Sci. Part A: Polym. Chem.* 2003, 41, 2828-2832.

99. Monteiro, M. J.; de Brouwer, H. *Macromolecules* 2001, 34, 349-352.

100. Coote, M. L. *Macromolecules* 2004, 37, 5023-5031.

101. Toy, A. A. H.; Vana, P.; Davis, T. P.; Barner-Kowollik, C. *Macromolecules* 2004, 37, 744-751.

102. Venkatesh, R.; Staal, B. B. P.; Klumperman, B.; Monteiro, M. J. *Macromolecules* 2004, 37, 7906-7917.

103. Kwak, Y.; Goto, A.; Fukuda, T. *Macromolecules* 2004, 37, 1219-1225.

104. Kwak, Y.; Goto, A.; Komatsu, K.; Sugiura, Y.; Fukuda, T. *Macromolecules* 2004, 37, 4434-4440.

105. Adamy, M.; Van Herk, A. M.; Destarac, M.; Monteiro, M. J. *Macromolecules* 2003, 36, 2293-2301.

106. Coote, M. L.; Henry, D. J. *Macromolecules* 2005, 38, 5774-5779.

107. Coote, M. L.; Radom, L. *Macromolecules* 2004, 37, 590-596.

108. Feldermann, A.; Coote, M. L.; Stenzel, M. H.; Davis, T. P.; Barner-Kowollik, C. *J. Am. Chem. Soc.* 2004, 126, 15915-15923.

109. Coote, M. L.; Henry, D. J. *Macromolecules* 2005, 38, 1415-1423.

110. Farmer, S. C.; Patten, T. E. *J. Polym. Sci. Part A: Polym. Chem.* 2002, 40, 555-563.

111. Goto, A.; Sato, K.; Tsujii, Y.; Fukuda, T.; Moad, G.; Rizzardo, E.; Thang, S. H. *Macromolecules* 2001, 34, 402-408.

112. Hehre, W.; Radom, L.; Schleyer, P.; Pople, J., *Ab Initio Molecular Orbital Theory* Wiley: New York, 1986.

113. Arita, T.; Buback, M.; Vana, P. *Macromolecules* 2005, 38, 7935-7943.

114. McLeary, J. B.; Calitz, F. M.; McKenzie, J. M.; Tonge, M. P.; Sanderson, R. D.; Klumperman, B. *Macromolecules* 2005, 38, 3151-3161.

115. McLeary, J. B.; Calitz, F. M.; McKenzie, J. M.; Tonge, M. P.; Sanderson, R. D.; Klumperman, B. *Macromolecules* 2004, 37, 2383-2394.

116. Wang, A. R.; Zhu, S.; Kwak, Y.; Goto, A.; Fukuda, T.; Monteiro, M. S. *J. Polym. Sci., Part A: Polym. Chem.* 2003, 41, 2833-2839.

117. Wang, A. R.; Zhu, S. *J. Polym. Sci. Part A: Polym. Chem.* 2003, 41, 1553-1566.

118. Barner-Kowollik, C.; Vana, P.; Quinn, J. F.; Davis, T. P. *J. Polym. Sci., Part A: Polym. Chem.* 2002, 40, 1058-1063.

119. McLeary, J.; McKenzie, J.; Tonge, M.; Sanderson, R.; Klumperman, B. *Chem. Comm.* 2004, 1950-1951.

120. Plummer, R.; Goh, Y.-K.; Whittaker, A. K.; Monteiro, M. J. *Macromolecules* 2005, 38, (12), 5352-5355.

121. Lutz, J.-F.; Neugebauer, D.; Matyjaszewski, K. *J. Am. Chem. Soc.* 2003, 125, 6986-6993.

122. Ferguson, R. C.; Ovenall, D. W. *Macromoleculecs* 1987, 20, 1245-1248.

123. Biros, J.; Larina, T.; Trekoval, J.; Pouchlý, J. *Colloid. Polym. Sci.* 1982, 260, 27-30.

124. Isobe, Y.; Yamada, K.; Nakano, T.; Okamoto, Y. *J. Polym. Sci., Part A: Polym. Chem.* 2000, 38, (Suppl.), 4693-4703.

125. Isobe, Y.; Nakano, T.; Okamoto, Y. *J. Polym. Sci., Part A: Polym. Chem.* 2001, 39, 1463-1471.

126. Isobe, Y.; Yamada, K.; Nakano, T.; Okamoto, Y. *Macromolecules* 1999, 32, 5979-5981.

127. Collins, S.; Ward, D. G.; Suddaby, K. H. *Macromolecules* 1992, 27, 7222-7224.

128. Giardello, M. A.; Yamamoto, Y.; Bard, L.; Marks, T. J. *J. Am. Chem. Soc.* 1995, 117, 3276-3277.

129. Allen, P. E. *Ind. Eng. Chem. Prod. Res. Dev.* 1985, 24, 334-340.

130. Fox, T. G.; Garrett, B. S.; Goode, W. E.; Gratch, S.; Klinciad, J. F. S., A.; Stroupe, J. D. *J. Am. Chem. Soc.* 1958, 80, 1768-1769.

131. Miller, R. G.; Mills, B.; Small, P. A.; Turner-Jones, A.; Wood, D. G. M. *Chem. Ind.* 1958, 1323.

132. Kalra, B.; Gross, R. A. *Biomacromolecules* 2000, 1, 501-505.

133. Isobe, Y.; Fujioka, D.; Habaue, S.; Okamoto, Y. *J. Am. Chem. Soc.* 2001, 123, 7180-7181.

134. Habaue, S.; Isobe, Y.; Okamoto, Y. *Tetrahedron* 2002, 58, 8205-8209.

135. Suito, Y.; Isobe, Y.; Habaue, S.; Okamoto, Y. *J. Polym. Sci.: Part A: Polym. Chem.* 2002, 40, 2496-2500.

136. Moad, G.; Solomon, D. H., *The Chemistry of Free Radical Polymerization*, Second ed.; Elsevier: Amsterdam, 2006; pp 167-177.

137. Klingsberg, A., Baldwin, T., Stereoregular Linear Polymers. In *Encyclopedia of Polymer Science and Engineering*, Mark, H. F.; Bikales, N. M.; Overberger, C. G.; Menge, G., Eds. John Wiley & Sons: New York, 1989; Vol. 15; pp 698-700.

138. Wittmann, J. C.; Kovacs, A. J. *J. Polym. Sci., Polym. Symp.* 1969, 16, 4443-4452.

139. Sauer, B. B.; Kim, Y. H. *Macromolecules* 1997, 30, 3323-3328.

140. Denny, L. R.; Boyer, R. F.; Elias, H. G. *J. Macromol. Sci., Part B: Polym. Phys.* 1986, B25, (3), 227-65.

141. Karasz, F. E.; MacKnight, W. J. *Macromolecules* 1968, 1, 537-540.

142. Porter, N. A.; Allen, T. R.; Breyer, R. A. *J. Am. Ceram. Soc.* 1992, 114, 7676-7683.

143. Yamada, K.; Nakano, T.; Okamoto, Y. *Macromolecules* 1998, 31, 7598-7605.

144. Ray, B.; Isobe, Y.; Morioka, K.; Habaue, S.; Okamoto, Y.; Kamigaito, M.; Sawamoto, M. *Macromolecules* 2003, 36, 543-545.

145. Ray, B.; Isobe, Y.; Matsumoto, A.; Habaue, S.; Okamoto, Y.; Kamigaito, M.; Sawamoto, M. *Macromolecules* 2004, 37, 1702-1710.

146. Miura, Y.; Satoh, T.; Narumi, A.; Nishizawa, O.; Okamoto, Y.; Kakuchi, T. *Macromolecules* 2005, 38, 1041-1043.

147. Miura, Y.; Satoh, T.; Narumi, A.; Nishizawa, O.; Okamoto, Y. *J. Polym. Sci., Part A: Polym. Chem.* 2006, 44, 1436-1446.

148. Wan, D.; Satoh, K.; Kamigaito, M.; Okamoto, Y. *Macromolecules* 2005, 38, 10397-10405.

Chapter 3: The Synthesis and Characterization of RAFT Agents

3.1 Introduction

In the past few years, numerous (RAFT) agents have been synthesized.[1] These compounds are mostly dithioesters (Figure 3.1), which could differ in the type of R and Z groups, with a view to give a wide range of chain transfer agents that could be used in various polymerization systems.[1,2] Substantial efforts have been made to investigate optimum and efficient polymerization conditions with various monomer systems under various reaction conditions. Thus, it is not unusual for some RAFT agents to be efficient with a certain monomer and inefficient with another, because the polymerization systems differ from one another, according to the monomers used.

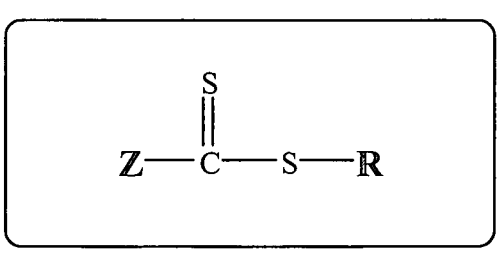

Figure 3.1: General structure of the dithioesters.

In Sections 2.3.3.1 and 2.3.3.2, the importance of a RAFT agent in controlling the polymerization was described and examples of some well known RAFT agents given. Some of the research efforts directed at studying various RAFT agents in terms of the respective roles of the R and Z substituents, with different monomers and reaction conditions, were also discussed. A useful guideline to several Z and R group selections with respect to effective transfer rates for different polymerization systems has been reviewed by Moad *et al.*[2] The results show that the reactivity of the RAFT agent is enhanced when using phenyl as the activating group, and the transfer coefficients

decrease in the series where Z is: Phenyl >SCH_2Ph ~ SMe ~ Me ~ N-pyrrolo>> OC_6F_5 > N-lactam > OC_6H_5 > O (alkyl) >N (alkyl).

The phenyl group as the **Z** substituent appears to contribute to an effective RAFT agent in terms of the transfer constant,[3] but also provides stability to the polymeric intermediate radical and may retard the polymerization rate.[4]

On the other hand, selecting the type of R group is crucial with respect to the reactivity of the monomer used, as it has a dramatic affect on the addition and fragmentation rate coefficients especially in the early reaction stages, according to several RAFT-mediated polymerization studies.[2]

Numerous studies display the challenge of designing suitable RAFT agents to meet the demands for specific polymerization systems, thus, the investigation of new different R and Z groups is always an area of great interest.

It is unlikely that the use of an aromatic system similar to a phenyl ring, such as thiophene, has ever been reported. Thiophene is a five carbon heterocyclic aromatic compound. It has two C-C double bonds and a sulfur atom that lends a lone pair of electron, which becomes sp^2-hybridized and acquires a positive charge, as its electron pair is delocalized around the ring of electrons to establish aromatic character to the ring system (Figure 3.2). Thiophene and benzene are both aromatic organic compounds and are similar in their chemical behavior.[5]

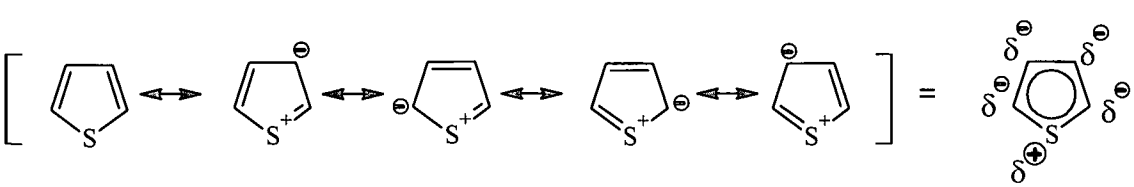

Figure 3.2: Resonance structures of thiophene.

Therefore, from an academic point of view, it was considered to be of interest to study the effect of the thiophene ring as an activation group (Z) in the RAFT agent and to investigate the role of thiophene-based compounds on the polymerization mechanism.

There are several synthetic routes for the synthesis of RAFT agents, including dithioesters, and dithiobenzoate derivatives,[6] reported in the literature. Most of these

synthetic methods are reviewed by Moad *et al.*[2] and also can be found in a book by Solomon and Moad.[1] Among these methods, are the following:

(a) The reaction of a carbodithioate salt with an alkylating agent. This process has been used for preparing benzyl dithiobenzoate.[7]

(b) For RAFT agents requiring tertiary R groups, the radical-induced decomposition of bis(thioacyl) disulfides, in the presence of azo compounds is one of the most widely used methods. Examples such as 2-cyano-4-methylpent-2-yl-4-cyano dithiobenzoate,[4] and 2-cyano-2-propyl dithiobenzoate[8] are prepared by this method.

This chapter describes the synthesis and characterization of six RAFT agents. Three of these are used as model compounds bearing a phenyl ring as the Z-substituent [bis(thiobenzoyl) disulfide, 2-cyano-2-propyl dithiobenzoate and benzyl dithiobenzoate], while the other three are novel compounds with a thiophene ring as the Z-substituent instead of a phenyl group.

All the prepared RAFT agents were characterized using the following analytical techniques:

- Proton (^{1}H-NMR) and carbon (^{13}C-NMR) spectra were obtained using a Varian VXR 300 MHz NMR spectrometer with a 5 mm four-nucleus probe. The samples were run at 25 °C. For the ^{1}H spectra, the frequency was 300 MHz and for the ^{13}C spectra the frequency was 75 MHz.
- Fourier-Transform Infrared Spectroscopy (FT-IR) spectra were recorded on a Perkin Elmer Paragon 1000 FTIR using a photoacoustic cell (PAS).
- Ultraviolet/visible spectrometer. The UV absorption band of the C=S bond in the RAFT agents was recorded, using a Perkin Elmer UV/visible spectrometer Lambda 20. Dichloromethane was used as the solvent for all compounds.

The characterization results for the phenyl-based RAFT agents correspond with those presented in the literature, the spectral results of each analytical tool used are presented in the Appendix (Figures A1-A6). The results of the novel thiophene based RAFT agents, including their spectra, are presented in this chapter.

3.2 Experimental

3.2.1 Materials:

The following reagents were used as received:

Diethyl ether 99.5% (Merck); hexamethylphosphoric triamide (Hexametapol) 99% (Merck); acetonitrile 99.9% (Aldrich); HCl 32% (ACE); ethanol 99.8% (Sigma-Aldrich); bromobenzene 99% (Sigma-Aldrich); carbon disulfide (CS_2) 99.9% (Aldrich); ethyl acetate 99%; pentane 99%; tetrahydrofuran (THF) and iodine 99% (Aldrich); magnesium sulfate anhydrous 98% (Aldrich), dimethyl sulfoxide (DMSO) (99.7%) (Fluka); ammonium chloride (HOLPRO) chemically pure; benzyl bromide≥98% (Fluka); 2-bromo thiophene 98% (Aldrich); potassium cyanide (KCN) 97% (Merck). AIBN (ACROS) was recrystallized from methanol and dried before use.

3.2.2 Preparation of bis(thiobenzoyl) disulfide (BBD)

BBD was prepared according to the procedure of Rizzardo *et al.* [9] Bromobenzene (15.7 g, 0.1 mol) was dissolved in 50 mL dry THF and the solution was placed in a dry dripping funnel connected to a 100 mL three-necked flask. 25% of the solution was added to the flask containing magnesium turnings (2.4 g, 0.1 mol) and a catalytic amount of iodine at room temperature. Gentle heating was required until the solution became colorless, indicating reaction commencement after an initial brown color from the iodine.

The remaining bromobenzene was added slowly over a period of 40 min, keeping the temperature below 40 °C using an ice bath. After the Grignard reagent was formed, carbon disulfide (7.6 g, 0.1 mol) was added dropwise, while keeping the temperature below 40 °C. The color of the reaction mixture changed from greenish-gray to dark brown/red. After complete addition, the reaction mixture was stirred for 30 min at room temperature. The excess Mg was filtered off and the THF was removed under reduced pressure.

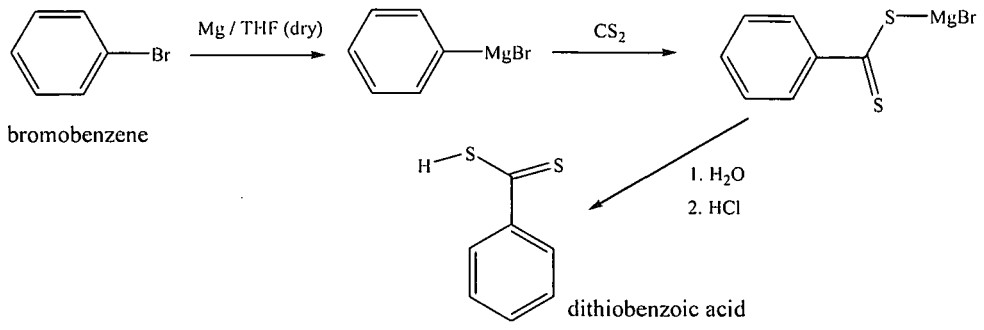

Scheme 3.1: Formation of dithiobenzoic acid.

The Grignard product was then hydrolyzed by adding it to 150 mL cold distilled water. The solution was acidified with 32% HCl until the color of the solution completely changed from dark red to purple at a pH of 1, indicating the formation of dithiobenzoic acid (see Scheme 3.1 for the reaction pathway). The acid layer was then extracted with diethyl ether (3 × 100 mL). The combined organic layers were transferred to a 500 mL flask and the ether was removed by rotary evaporation.

The remaining unstable acid was immediately transferred to a 250 mL round-bottom flask together with 150 mL absolute ethanol and a catalytic amount of iodine. DMSO (14.5 mL, 0.2 mol) was added dropwise at room temperature, while stirring. As the reaction proceeded, pink crystals precipitated (Scheme 3.2). After 2 h, the reaction was stopped and the reaction flask and contents was stored in a refrigerator for 15 h to promote further crystallization. The precipitated crystals were then recrystallized twice from ethanol at 40 °C and dried to give 7.8 g BBD, based on bromobenzene (overall yield 50 %).

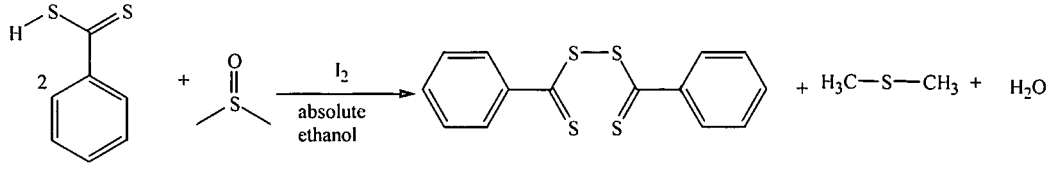

Scheme 3.2: Preparation of bis(thiobenzoyl) disulfide.

Characterization results:

NMR spectroscopy

^{1}H-NMR ($CDCl_3$): δ (ppm) = 7.45 (m, 4H, m-ArH); 7.61 (m, 2H, p-ArH); 8.09 (d, 4H o-ArH,).

^{13}C-NMR ($CDCl_3$): δ (ppm) = 127.81, 128.89, 133.38, 143.95, (C; aromatic: (ArC)); 219.84 (C=S). (Appendix A-1, Figure A1)

FT-IR & UV/vis spectroscopy

FT-IR (cm^{-1}): 3045 (aryl-H stretching); 1693-1442 (C=C aromatic); 1043 (C=S); 636 (C-S stretching). [Appendix A-1, Figure A2 (A)]

UV (C=S): ($n \rightarrow \pi^*$, λ_{max} = 524 nm) c = 0.75 g L^{-1} and ($\pi \rightarrow \pi^*$, λ_{max} = 305 nm) c = 0.017 g L^{-1} (Appendix A-1, Figure A2 (B&C)). ***Note*** that c = the concentration of the sample of which the absorbance data was recorded = (RAFT mass / solvent volume).

3.2.3 Preparation of benzyl dithiobenzoate (BDTB)

BDTB was prepared in the same way as BBD.[7] The Grignard reagent (phenyl magnesium bromide) was prepared from bromobenzene (23.4 mL, 0.1 mol) and magnesium turnings (2.75 g, 0.11 mol) in 50 mL THF, as described in Section 3.2.2. The excess of magnesium was filtered off and carbon disulfide (6 mL, 0.1 mol) slowly added to the solution of the Grignard reagent over a period of 30 min, maintaining the temperature below 40 °C. The reaction mixture was stirred for 30 min at room temperature, followed by the slow addition of benzyl bromide (11.9 mL, 0.1 mol) at room temperature. The mixture was then stirred for an additional 12 h (Scheme 3.3).

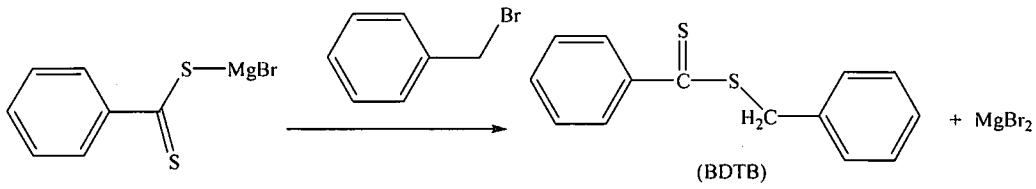

Scheme 3.3: Preparation of BDTB.

THF was removed under vacuum and the residual crude red oil was purified chromatographically through a silica column using hexane:ethyl acetate (9:1) as the eluent. The isolated yield of pure benzyl dithiobenzoate as a red oil was 12.21 g (50%).

Characterization results:

NMR spectroscopy

^{1}H-NMR ($CDCl_3$): δ (ppm) = 4.60 (s, 2H, CH_2-Ph), 7.30-7.54 (m, 8H, ArH), 8.02 (m, 2H, ArH).

^{13}C-NMR ($CDCl_3$): d (ppm) = 41.93 (CH_2); 126, 126.88, 127.69, 128.29, 128.67, 129.24, 132.37, 134.99, 144.65 (ArC phenyl rings), 227.56 (C=S). [Appendix A-2, Figure A3]

FT-IR & UV/vis spectroscopy:

FT-IR (cm^{-1}): 3084 (aromatic C-H stretching); 2966-2918 (methylene C-H stretching); 1501 (C=C aromatic); 1052 (C=S); 479 (C-S stretching). (Appendix A-2, Figure A4 (A))

UV (C=S): ($n \rightarrow \pi^*$, λ_{max} = 507 nm) c = 1.9 g L^{-1}, ($\pi \rightarrow \pi^*$, λ_{max} = 302 nm) c = 0.148 g L^{-1}. [Appendix A-2, Figure A4 (B&C)].

3.2.4 Preparation of 2-cyano-2-propyl dithiobenzoate (CPDB)

Following the procedure of Thang *et al.*[10], a solution of bis(thiobenzoyl) disulfide (3 g, 9.78 mmol) and AIBN (1.6 g, 9.78 mmol) in 100 mL ethyl acetate was stirred for 10 h at 85 °C in a 250 mL round bottom flask. After removing the solvent under reduced pressure, a red oil residue was isolated and subjected to column chromatography with chloroform:hexane (1:1) as the eluent, to yield 3.64 g (84%) of CPDB (Scheme 3.4).

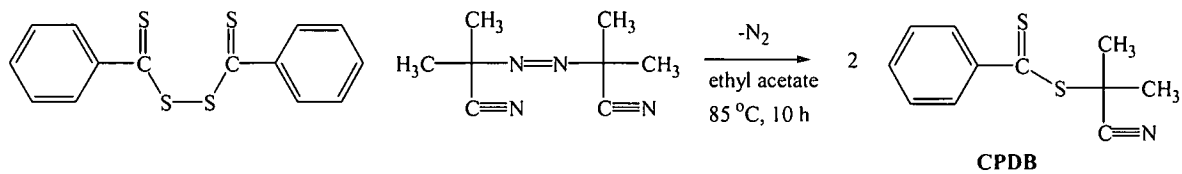

CPDB

Scheme 3.4: Preparation of CPDB.

Characterization results:

NMR spectroscopy

^{1}H-NMR ($CDCl_3$): δ (ppm) = 1.94 (s, 6H,–$(CH_3)_2$);7.39 (t, 2H, *o*-ArH); 7.56 (t, 1H, *p*-ArH); 7.92 (d, 2H, *m*-ArH).

^{13}C-NMR ($CDCl_3$): δ (ppm) = 26.33 ($(CH_3)_2$); 41.62 (C-$(CH_3)_2$); 120 (C = N); 126.59, 28.69, 133, 144.83 (ArC); 223.59 (C=S). (Appendix A-3, Figure A5)

FT-IR & UV/vis spectroscopy

FT-IR (cm^{-1}): 3057 (aromatic C-H stretching); 2979-2929 (methyl C-H stretching); 2231 (CN); 1590 (C=C aromatic); 1365 (-CH_3 deformation), 1048 (C=S); 650 (C-S stretching). [Appendix A-3, Figure A6 (A)]

UV (C=S): ($n \rightarrow \pi^*$, λ_{max} = 514 nm) c = 0.1 g L^{-1}, and ($\pi \rightarrow \pi^*$, λ_{max} = 302 nm) c = 0.2 g L^{-1}. (Appendix A-3, Figure A6 (B&C))

3.2.5 Preparation of bis(2-thienyl thiocarbonyl)disulfide (BTD)

In a similar procedure to that used for preparing BBD, the Grignard reagent thiophene-2-magnesium bromide was prepared from a mixture of 2-bromothiophene (16.3 g, 0.1 mol) and magnesium turnings (5 g, 0.206 mol) in 100 mL of anhydrous THF and a catalytic amount of iodine. 2-Bromothiophene was added dropwise to the magnesium slurry in THF. The reaction was highly exothermic; upon complete addition the solution started to reflux and the color started to change as the reaction proceeded from light yellow/brown to a deeper brown color.

After the exothermic reaction subsided, the mixture was further refluxed[11] for 2 h. The excess magnesium was filtered off, and then CS_2 (7.85 mL, 9.89g, 0.13 mol) and copper (I) bromide (145 mg, 1 mmol) were added at 20 °C. The mixture was warmed to about 30 °C and the color started to change to red. After the exothermic reaction subsided, the reactants were further heated to 50 °C for about 30 min. The mixture was then poured into 200 mL cold distilled water and acidified with concentrated 33% HCl until the pH was below 2. The organic layer was extracted with 4 × 100 mL diethyl ether.

After removing the ether under vacuum, the free thiophene-2-carbodithiocarboxylic acid was immediately transferred to a clean flask and DMSO (0.2 mol, 14.5 mL) was added with a catalytic amount of iodine in 75 mL absolute ethanol. The mixture was stirred for 3 h and then stored in a refrigerator at -20 °C overnight to promote crystallization.

The red/brown solid of the disulfide was filtered off and recrystallized twice from acetonitrile to give dark red crystals. The yield was 2.23 g (7%).

Characterization Results:

NMR spectroscopy

Note: the hydrogen and carbon numbers shown in the results refer to the atom position according to the actual chemical formula of the compound.

^{1}H-NMR ($CDCl_3$): δ (ppm) = 7.21 (t, J = 5.1, 4.0 Hz, 2H, H-4), 7.77 (dd, J = 5.1, 1.1 Hz, 2H, H-3), 8.04 (dd, J = 4.0, 1.1 Hz,2H, H-5).

^{13}C-NMR (CDCl3): δ (ppm) = 205.63 (C=S), 149.98 (C-2), 137.07 (C-4), 129.21/128.71 (C-3/5). (Figure 3.3)

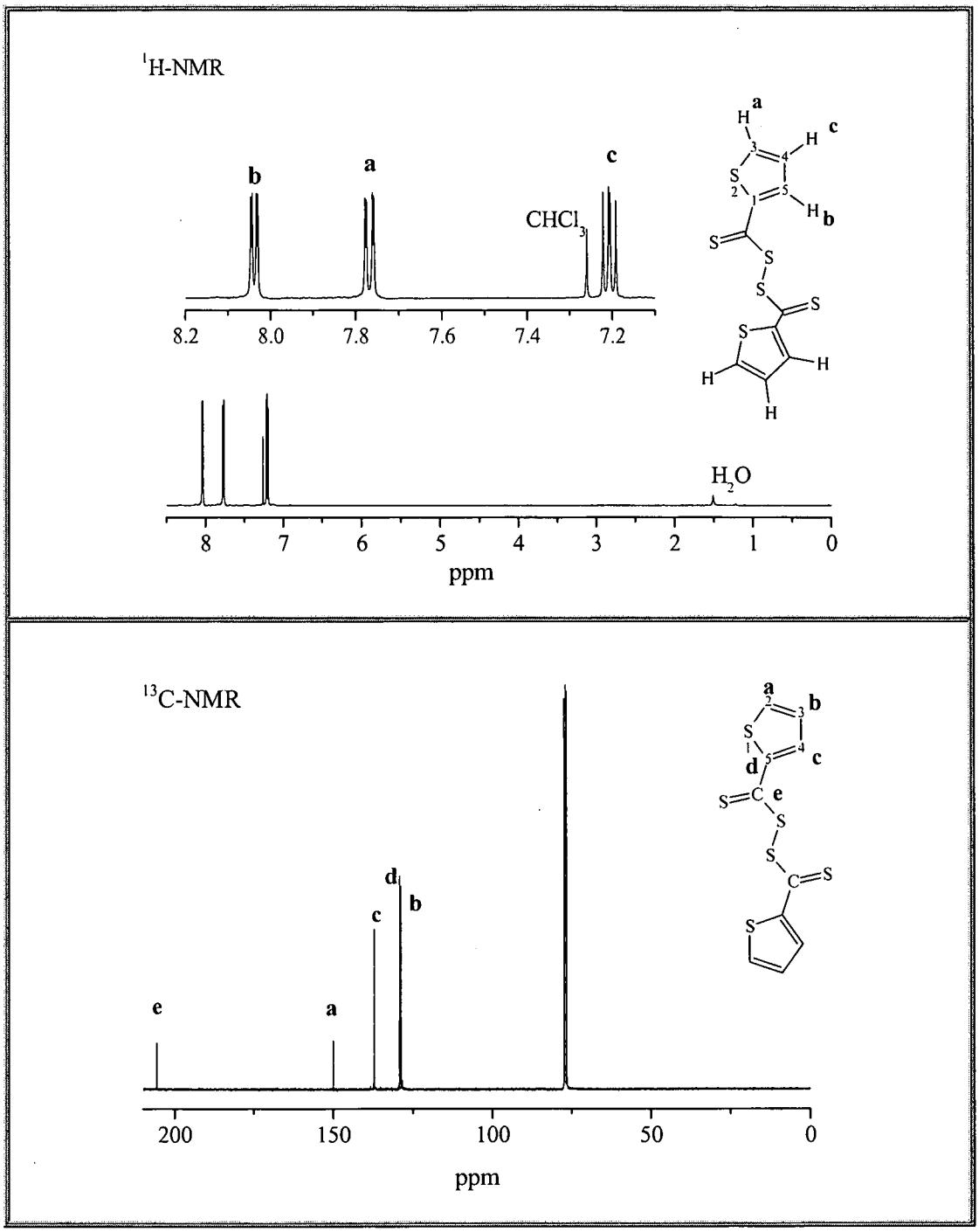

Figure 3.3: ^{1}H-NMR and ^{13}C-NMR spectra of BTD in $CDCl_3$.

FT-IR & UV/vis spectroscopy

FT-IR (cm^{-1}): 3093-2984 (C-H thiophene ring stretch); 548 (thiophene C-S-C stretch); 1042 (C=S); 749 (disulfide C-S). Figure 3.4 (A)

UV (C=S): ($n \rightarrow \pi^*$, λ_{max} = 537 nm) c = 0.2 g L^{-1}, and ($\pi \rightarrow \pi^*$, λ_{max} = 303, 355 nm) c = 0.0167 g L^{-1} [Figure 3.4 (B and C)]

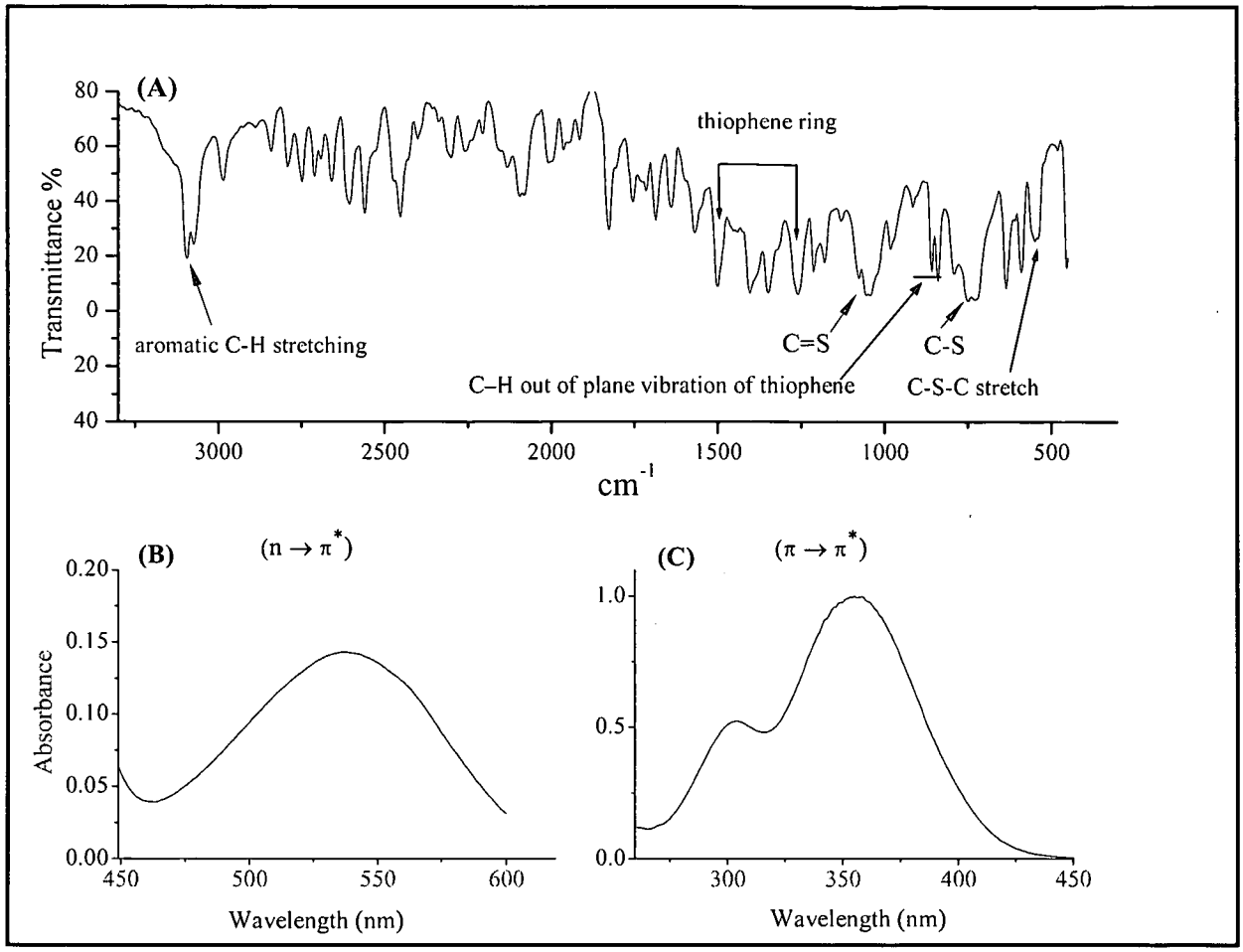

Figure 3.4: (A) FT-IR spectrum of BTD; (B and C) UV (C=S) absorbance spectra of BTD.

3.2.6 Preparation of 1-cyano-1-methylethyl 2-thiophenedithiocarboxylate (CPDT)

Bis(2-thienyl thiocarbonyl)disulfide (1.53 g, 4.8 mmol), AIBN (0.788 g, 4.8 mmol) and 50 mL ethyl acetate were added together in a 100 mL round-bottom flask. The mixture was stirred for 8 h at 85 °C. (Scheme 3.5)

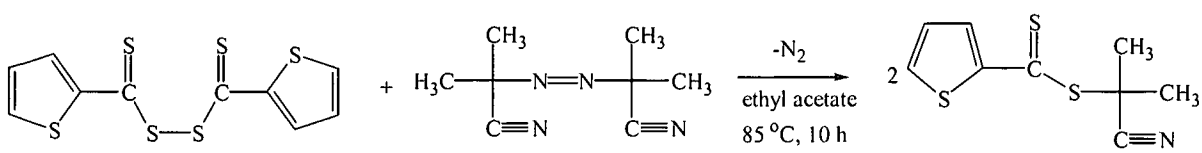

Scheme 3.5: Preparation of CPDT.

The solvent was evaporated and the residue was purified twice by silica-gel chromatography. The initial solvent system was pentane as eluent, and the later, the product was eluted with chloroform:pentane (2:8) to give 1.11 g of a red oil (yield 50%).

Characterizaion results:

NMR spectroscopy

^{1}H-NMR ($CDCl_3$): δ (ppm) = 1.9 [s, 6-H, $(CH_3)_2$]; 7.11 (t, J= 3.9, 5.1 Hz, 1H, H-4); 7.69 (dd, 1H, H-3); 7.76 (dd, 1H, H-5). ^{13}C-NMR ($CCDl_3$): δ (ppm) = 26.73 $(CH_3)_2$); 41.33 (C-$(CH_3)_2$); 120.21 (C=N); 127.13 (C-4); 128.77 (C-3); 135.88 (C-2); 151.49 (C-5); 208.89 (C=S). (Figure 3.5)

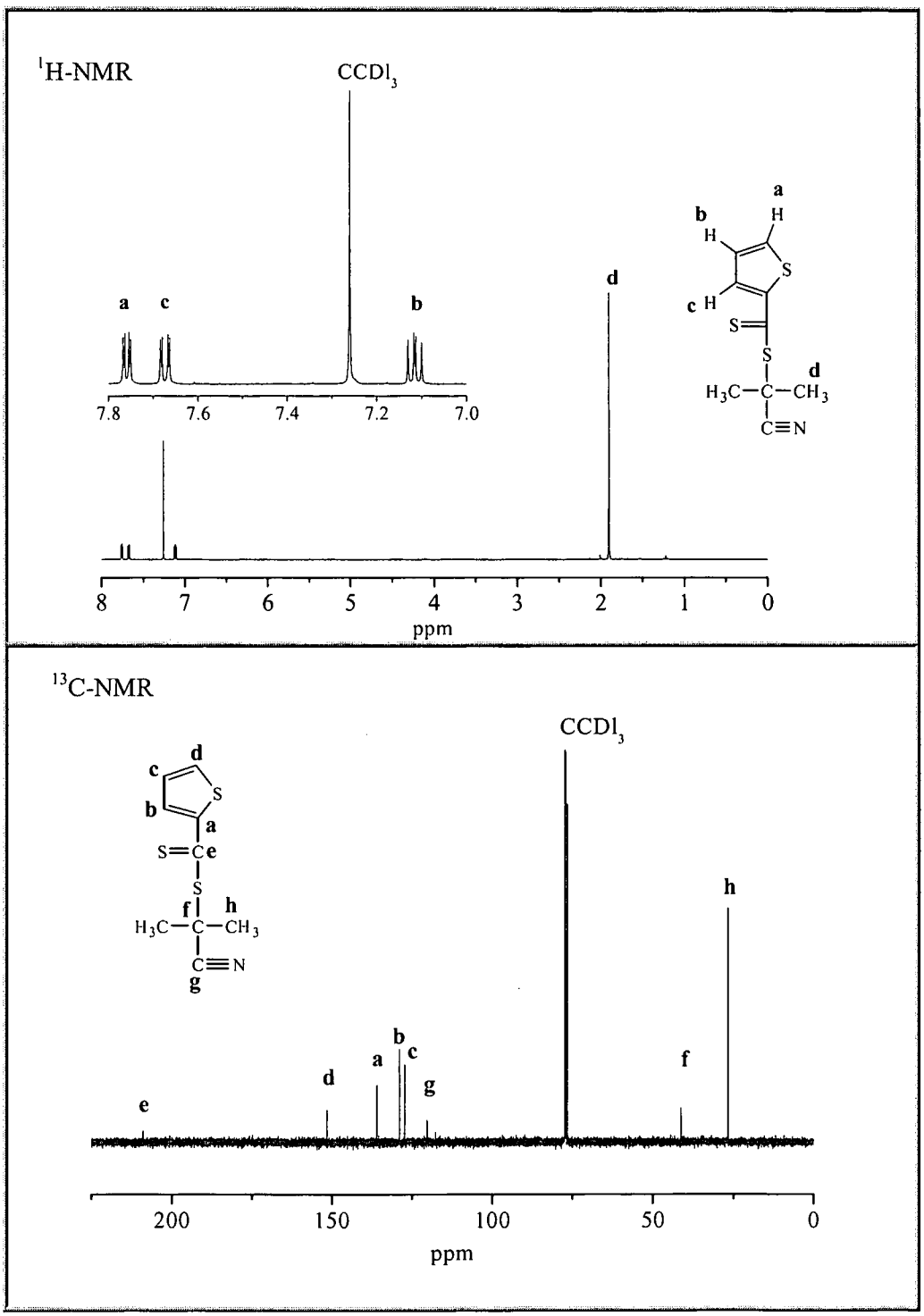

Figure 3.5: ^{1}H-NMR and ^{13}C-NMR spectra of CPDT in $CDCl_3$.

FT-IR & UV/vis spectroscopy

FT-IR (cm^{-1}): 3101 (aromatic ring C-H stretch); 2978 / 2928 (methyl C-H); 1054 (C=S); 639 (C-S); 2231 (*C*≡N); 1501 (C=C). (Figure 3.6 A)

UV (C=S): ($n \rightarrow \pi^*$, λ_{max} = 527 nm) c = 0.22 g L^{-1}, and ($\pi \rightarrow \pi^*$, λ_{max} = 303, 339 nm) c = 0.029 g L^{-1}. (Figure 3.6 B and C)

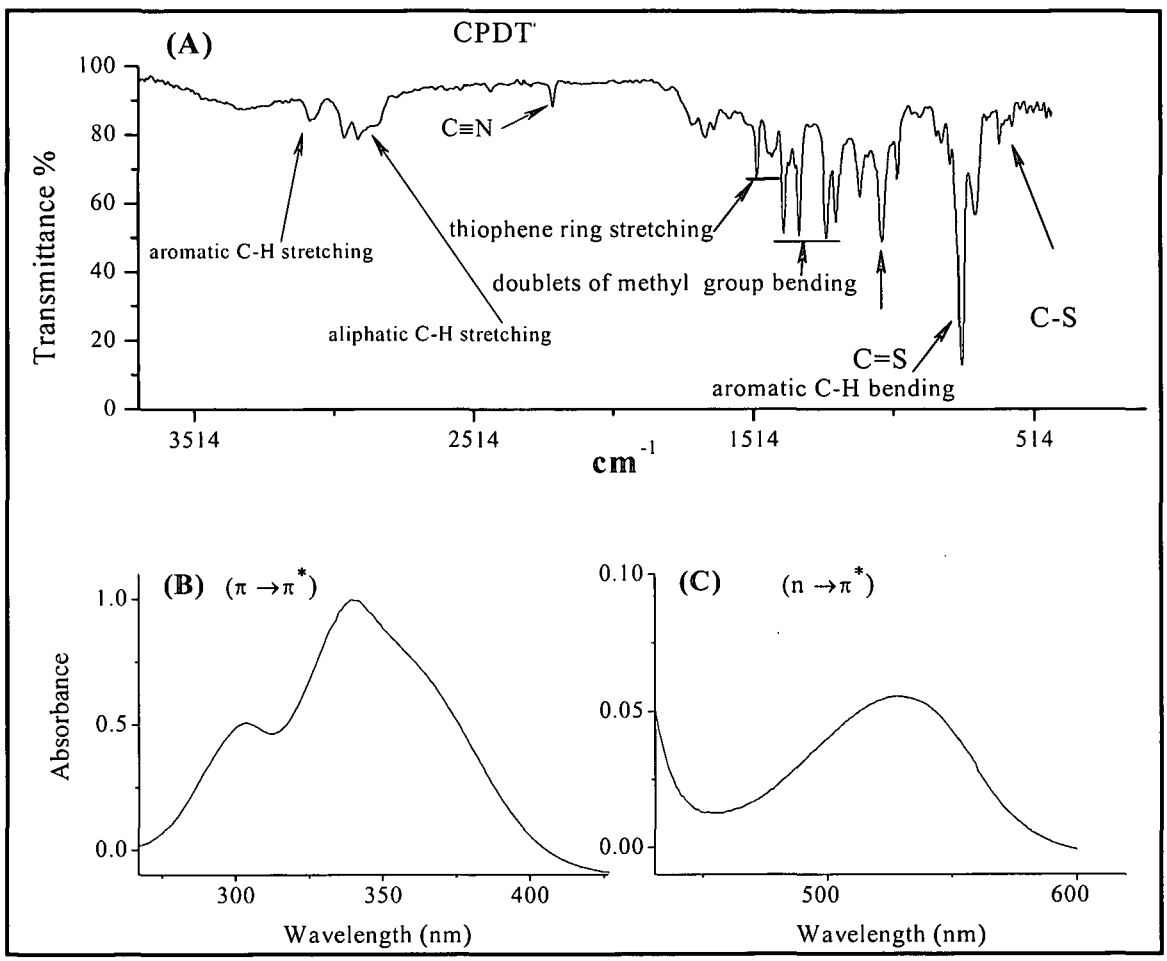

Figure 3.6: (A) FT-IR spectrum of CPDT; (B and C) UV (C=S) absorption spectra of CPDT.

3.2.7 Preparation of benzyl thiophene-2-dithiocarboxylate (BDTT)

A solution of thiophene-2-magnesium bromide was prepared as described in Section 3.2.5. Magnesium (5 g, 0.206 mol) was reacted with 2-bromothiophene (16.3 g, 0.1 mol) in 110 mL dry THF. The Grignard solution was then decanted from the excess Mg. The remaining Mg was then washed with THF and the solvent was added to the main volume.

After the solution was cooled to 20 °C, copper (I) bromide (145 mg, 1 mmol) and excess CS_2 (10.6 g, 0.14 mol) were added. Then the mixture was warmed to 30 °C. After the exothermic reaction subsided, the mixture was heated to 50 °C for an additional 30 min.

Benzyl bromide (11.9 mL, 0.1 mol) and 40 mL hexametapol were added to the solution, which was then stirred for 3 h at 60 °C. (Scheme 3.6)

The crude reaction mixture was added to a beaker containing a solution of 4 g of potassium cyanide and 30 g of ammonium chloride in 200 mL distilled water.[12]

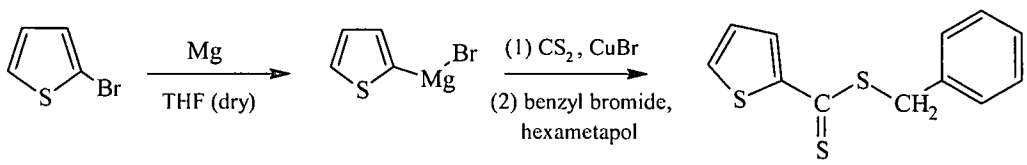

Scheme 3.6: Preparation of BDTT.

After the mixture was vigorously shaken, the two layers were separated. The organic layer was extracted with diethyl ether (4 × 100 mL). The ether layer was then washed with water and dried over magnesium sulfate. The solution was concentrated under reduced pressure to allow crystallization and then stored in a cool place. The light red crystals were recrystallized from acetonitrile and dried to give 8.76 g (35% yield) of benzyl thiophene-2-dithiocarboxylate.

Characterization results

NMR spectroscopy

^{1}H-NMR ($CDCl_3$): δ (ppm) = 4.62 (s, 2H, CH_2-Ph); 7.1 (t, J= 4.9, 3.9 Hz, 1H, H-4); 7.29 (t, J= 7.2 Hz, 1H, p-ArH); 7.34 (t, J= 7.6 Hz, 2H, m-ArH): 7.39 (dd, J= 6.0, 1.0 Hz, 2H, o-ArH); 7.62 (dd, J= 4.9, 1.0 Hz, 1H, H-5), 7.82 (dd, 1H, H-3).

^{13}C-NMR ($CCDl_3$): δ (ppm) = 41.03 (CH_2); 126.83 (C-3); 127.7 (C-4); 134.85 (C-5); 128.44, 128.66, 129.23, 151.21 (ArC); 213.2 (C=S). (Figure 3.7)

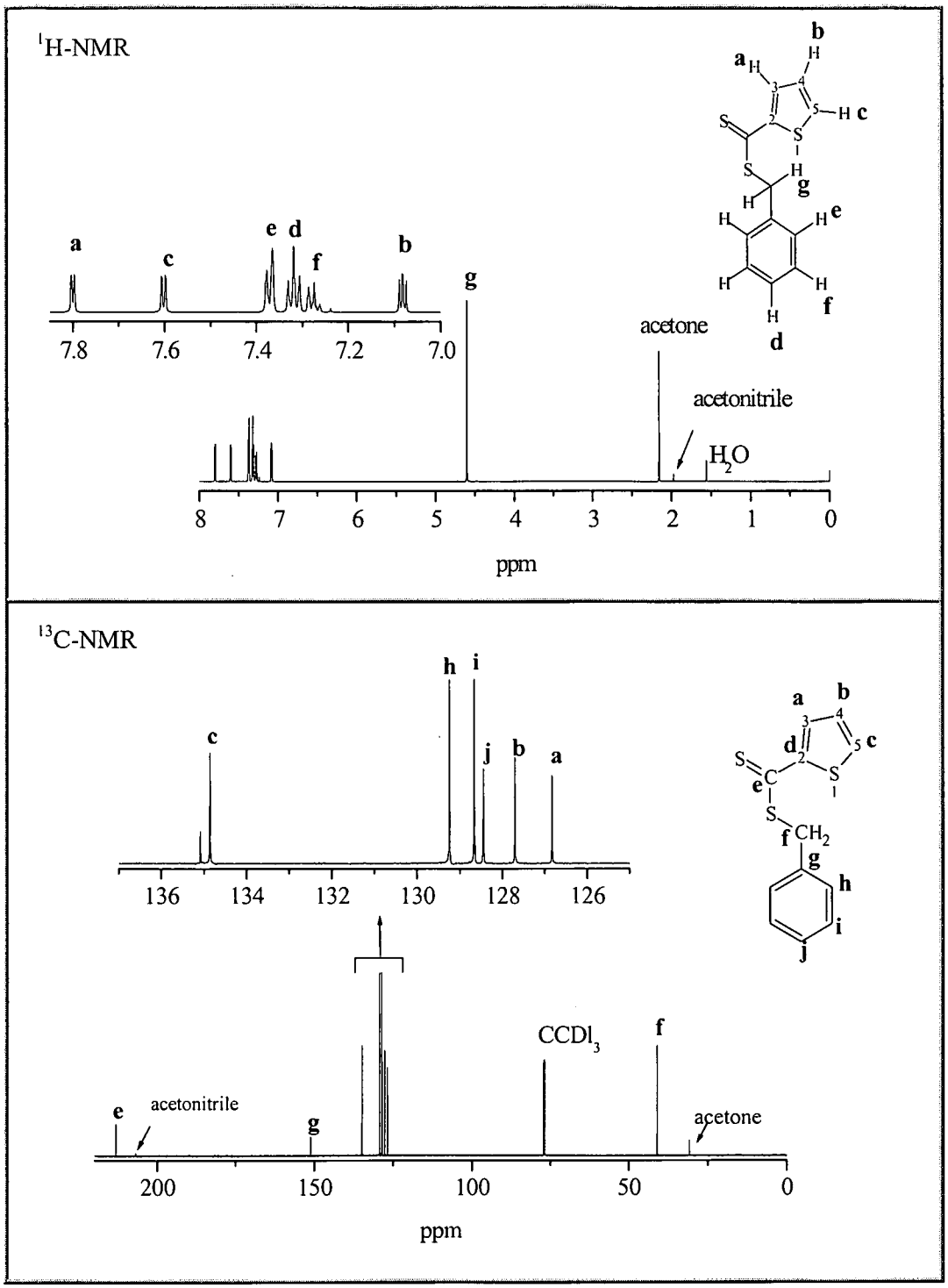

Figure 3.7: ^{1}H-NMR and ^{13}C-NMR spectra of BDTT in $CDCl_3$.

FT-IR & UV/vis spectroscopy

FT-IR (cm^{-1}): 3058 / 3027 (aromatic rings C-H stretching); 2918 (methylene C-H stretch); 1044 (C=S); 648 (C-S); 1494 / 1590 (aromatic C=C stretch); 688/711 (CH_2-S stretch). (Figure 3.8 (A))

UV (C=S): ($n \rightarrow \pi^*$, λ_{max} = 511 nm) c = 0.11 g L^{-1}, and ($\pi \rightarrow \pi^*$, λ_{max}= 299, 346 nm) c = 0.0275 g L^{-1} [Figure 3.8 (B and C)].

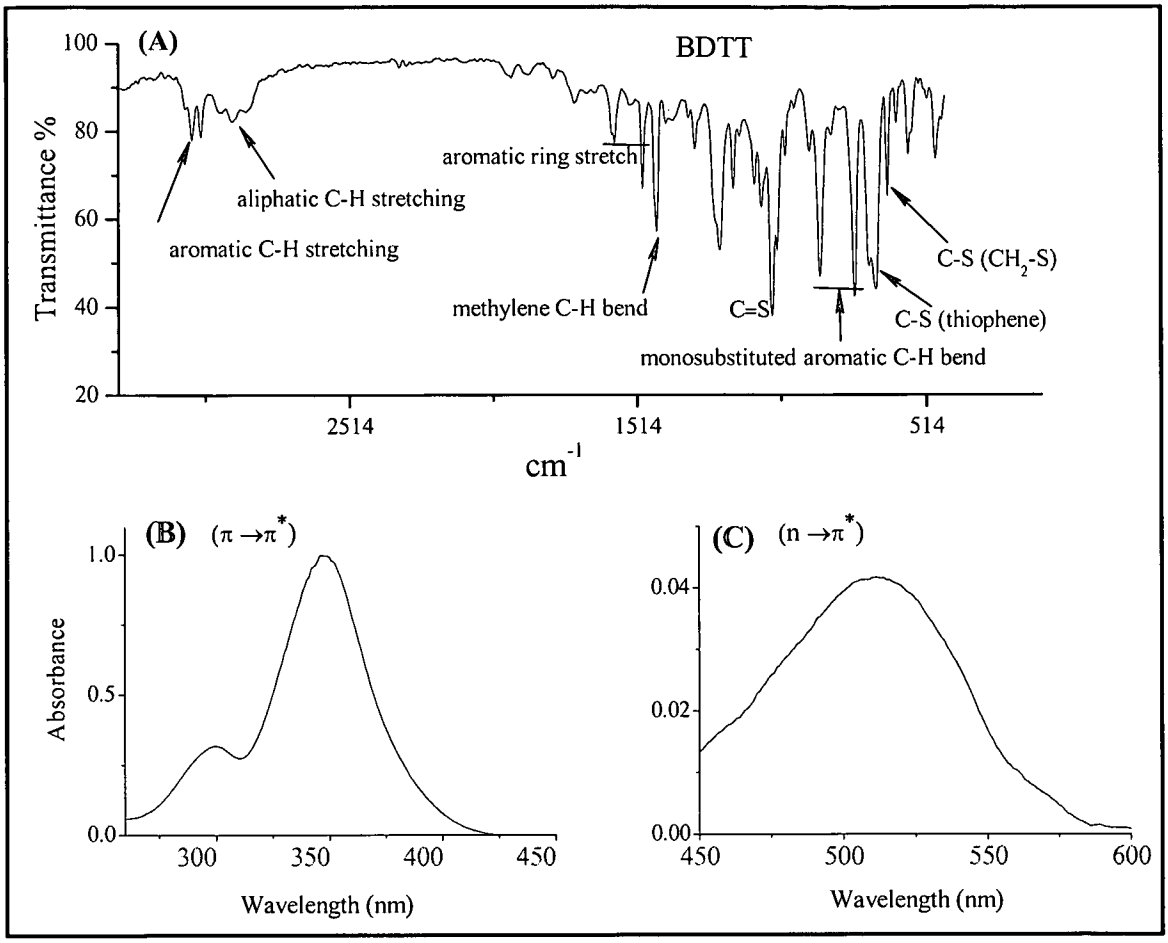

Figure 3.8: (A) FT-IR spectra of BDTT; (B and C) absorption UV spectra of BDTT.

3.3 Discussion of RAFT agent synthesis and characterization

The analytical techniques FT-IR, UV/vis, ^{1}H-NMR and ^{13}C-NMR spectroscopy are powerful tools to identify different functionalities present within each RAFT agent. The characterization results of the compound synthesized were in good agreement with what was previously reported,[7,9,10] for the same compounds that were synthesized here. In terms of the preparation procedure, the phenyl-based RAFT agents were easier to purify, and obtained in medium to high yields when compared to the thiophene-based RAFT agents.

The thiophene-based RAFT agents presented more difficulties with respect to the extraction processes during preparation and the chromatographic purification, especially the compounds BTD and CPDT. The latter, in its oil form, was particularly difficult to

purify. Precautions were taken in the first step of the purification process by passing the crude product extremely slowly through a column to achieve efficient separation of a red product from a thick dark brown layer (first layer) on the column. This was the reason for using a two step chromatographic purification process.

The method used to prepare the thiophene disulfide provided only a low yield. However, recently a synthetic method, developed by Weber[13] provided an alternative way in which to synthesize BTD in a relatively good yield of about 61% via an elimination process rather than the common oxidation method that was used in this work.

The characteristic absorption bands for different chemical bonds such as the thiophene ring, C=S, C-S, C=C aromatic, and other specific bonds for each RAFT agent prepared, were assigned in the infrared spectra of all the RAFT agents according to the tabulated literature[14-17] of each functional group and its absorption band region in the IR spectrum.

An ultraviolet/visible spectrometer is one of the analytical tools which was used in the current study to determine the absorption wavelength (λ_{max}) of the C=S chromophore. The predictable wavelengths of absorption for the ($\pi \rightarrow \pi^*$) transition were in the range 300 – 350 nm for the synthesized RAFT agents.

3.4 Conclusions

The RAFT agents shown in Figure 3.9 were successfully synthesized and characterized.

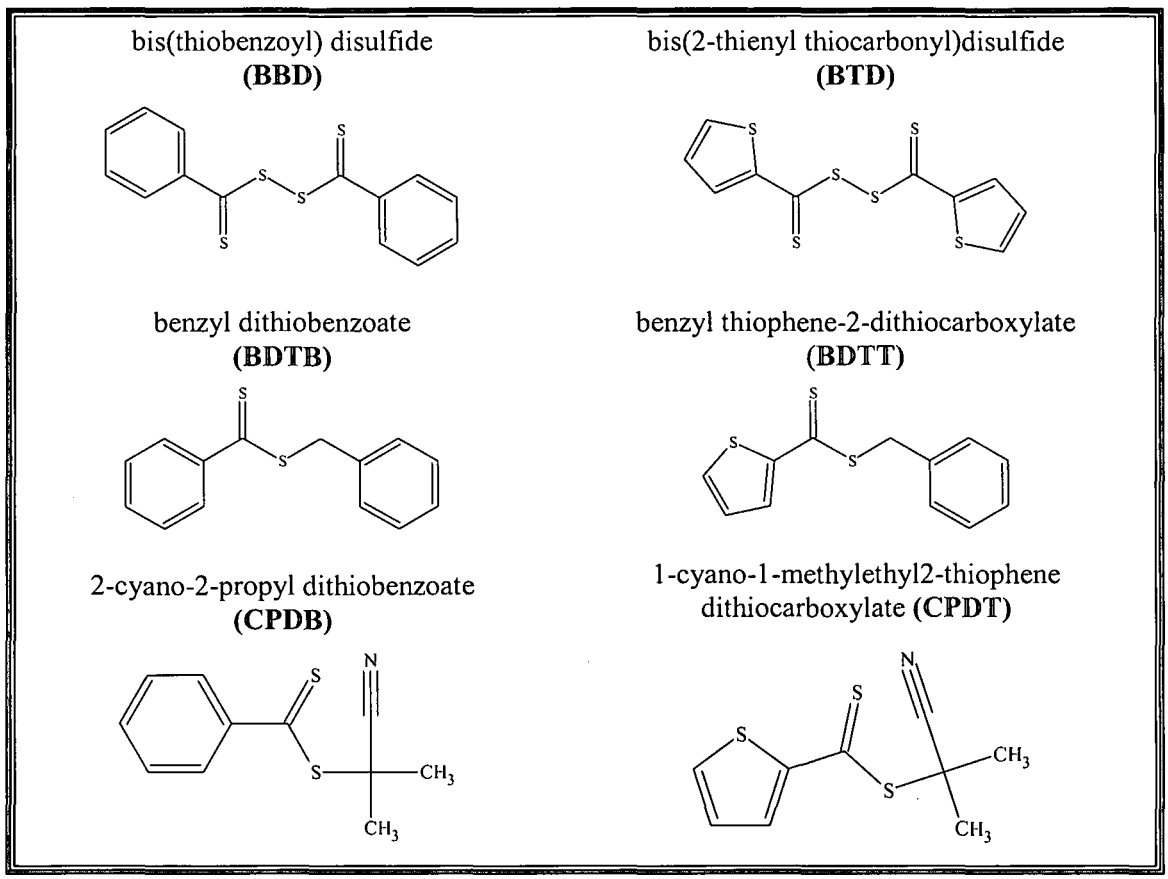

Figure 3. 9: Summery of the synthesized RAFT agents in this study.

All RAFT agents, excluding CPDB and CPDT were prepared on the basis of a Grignard reaction, while the other two were prepared by refluxing the selected disulfide precursor with AIBN in an organic medium. The product yield of BTD was low when using the common oxidation method. Therefore, the alternative elimination method can be utilized in future work for the preparation of the same compound. The purity of the products obtained was high, as estimated from the ^{1}H-NMR spectra. All products were later used in polymerization reactions. (see Section 4.2)

3.5 References

1. Moad, G.; Solomon, D. H., *The Chemistry of Free Radical Polymerization*, Second ed.; Elsevier: Amsterdam, 2006; pp 505-514.

2. Moad, G.; Rizzardo, E.; Thang, S. H. *Aust. J. Chem.* 2005, 58, 379-410.

3. Moad, G.; Chiefari, J.; Chong, Y.; Krstina, J.; Mayadunne, R. T.; Postma, A.; Rizzardo, E.; Thang, S. H. *Polym. Int.* 2000, 49, 993-1001.

4. Benaglia, M.; Rizzardo, E.; Alberti, A.; Guerra, M. *Macromolecules* 2005, 38, 3129-3140.

5. Dyreborg, S.; Arvin, E.; Broholm, K. *Environ. Toxicol. Chem.* 1998, 17, (5), 851-858.

6. Chong, Y. K. B.; Krstina, J.; Le, T. P. T.; Moad, G.; Postma, A.; Rizzardo, E.; Thang, S. H. *Macromolecules* 2003, 36, 2256-2272.

7. Chiefari, J.; Mayadunne, R. T. A.; Moad, C. L.; Moad, G.; Rizzardo, E.; Postma, A.; Skidmore, M. A.; Thang, S. H. *Macromolecules* 2003, 36, 2273-2282.

8. Thang, S. H.; Chong, Y. K. B.; Mayadunne, R. T. A.; Moad, G.; Rizzardo, E. *Tetrahedron Lett.* 1999, 40, 2435-2438.

9. Rizzardo, E.; Thang, S. H.; Moad, G. PCT Int. Appl. 1998, WO 9905099.

10. Thang, S. H.; Chong, Y. K.; Mayadunne, R. T. A.; Moad, G.; Rizzardo, E. *Tetrahedron* 1999, 40, 2435-2438.

11. Ponomarenko, S. A.; Kirchmeyer, S.; Elschner, A.; Alpatova, N. M.; Halik, M.; Klauk, H.; Zschieschang, U.; Schmid, G. *Chem. Mater.* 2006, 18, (2), 579-586.

12. Wakefield, B. J., *Organomagnesium Methods in Organic Synthesis*, Academic Press: London, 1995; pp 147-150.

13. Weber, W. G.; McLeary, J. B.; Sanderson, R. D. *Tetrahedron Lett.* 2006, 47, (27), 4771-4774.

14. Hesse, M.; Meier, H.; Zeeh,, *Spectroscopic Methods in Organic Synthesis* Thieme: Stuttgart, 1997; pp 36-54.

15. Chertkov, Y. B.; Kirsanova, T. I.; Kunina, E. A.; Kalinin, L. L. *Khimiya i Tekhnologiya Topliv i Masel* 1977, 49-52.

16. Katritzky, A. R., *Handbook of Heterocyclic Chemistry*, First ed.; Pergamon: Oxford, 1985; p 67.

17. Coates, J., Interpretation of Infrared Spectra, A Practical Approach. In *Encyclopedia of Analytical Chemistry*, Meyers, R. A., Ed. John Wiley and Sons: Chichester, 2000; pp 10815-10837.

Chapter 4: The Evaluation of Thiophene as an Activating Group in the RAFT-Mediated Polymerization of Styrene

4.1 Introduction

The interesting thermal and physical properties of polystyrene make it one of the most important polymeric materials.[1] Its synthesis is currently, one of the most studied polymerization systems worldwide, and hence there is an abundance of literature available with regards to styrene polymerization under various reaction conditions.

The development of new techniques in polymer chemistry is always of great interest. As mentioned in Chapter 2, there are several LFRP techniques that are either catalyzed by various hybrid organic–inorganic materials or transfer agents that are able to control the polymerization process.[2] The consideration of new materials, e.g. RAFT agents for use in living polymerization systems is of interest, both from academic and industrial point of view.

RAFT-mediated polymerization is one of the most versatile LFRP techniques that is used extensively with a wide range of monomers.[3,4] Since the discovery of the RAFT process numerous RAFT agents have been synthesized, some of which are mentioned in Section 2.3.3.1. It nevertheless, remains a challenge to synthesize new RAFT agents for use in any specific polymerization system. Not only is it important to achieve control over the RAFT polymerization process, it is also critical to focus on the chemical behavior of any RAFT agent that becomes part of the polymeric material. Thus, by incorporating a material containing certain functional groups, such as reactive chromophores, the polymer produced could have interesting physical and chemical characteristics, compared to the virgin polymer.

This chapter describes the RAFT-mediated polymerization of styrene performed in the presence of the RAFT agents, which were introduced in Chapter 3. Styrene was chosen in order to examine the behavior of the new thiophene compounds as RAFT agents and to compare their performances with analogous phenyl-based RAFT agents. Figure 4.1 shows the different RAFT agents that were used in this study.

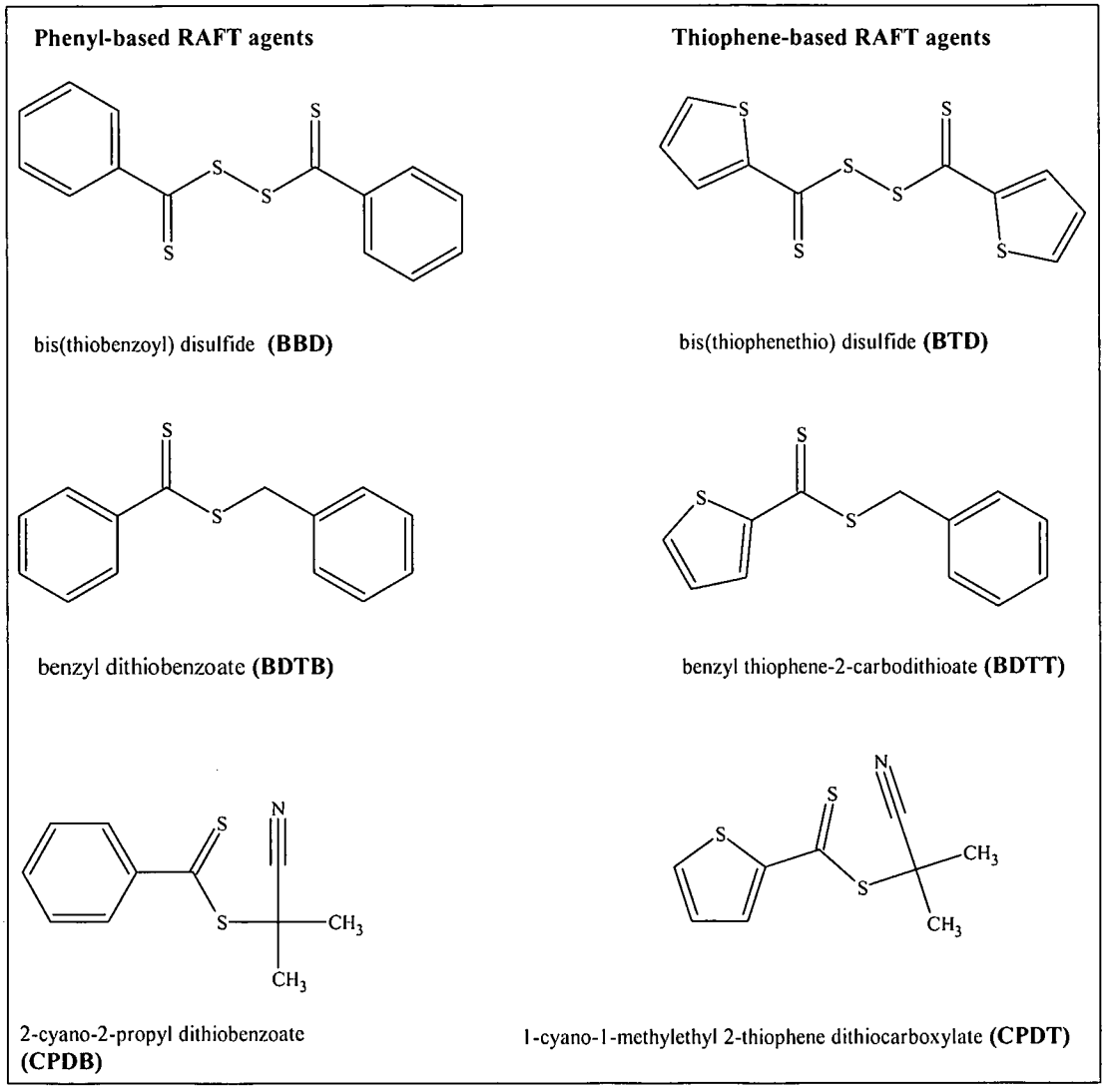

Figure 4.1: RAFT agents prepared and used in this study.

4.2 Experimental: styrene self-initiation polymerization

4.2.1 RAFT-mediated polymerization of St under N_2 flow (unsealed system)

Distilled styrene (0.192 mol, 20g) and 0.00025 mol of the selected RAFT agent were accurately weighed and placed in a 100 mL three-neck round-bottom flask equipped with a condenser. Nitrogen (N_2) gas was purged through the mixture for 10 min before the flask was immersed in a preheated (100 °C) silicone oil bath to start the reaction. The self-initiated polymerization reaction was performed under inert N_2 gas (99.9%) and stirred at 300 rpm using a magnetic stirrer. Samples were taken at different times, left to dry in a fume hood for 3 days and then placed in a vacuum oven at room temperature for 24 hours to dry.

The masses of the reagents used and the reaction conditions are tabulated in Table 4.1

Table 4.1: Formulations used for the RAFT-mediated polymerization of styrene

Reaction	CTA	Mass RAFT agent (g)	Mass Styrene (g)
A	BBD	0.0766	20
B	BTD	0.0796	20
C	BDTB	0.0610	20
D	BDTT	0.0625	20
E	CPDB	0.0553	20
F	CPDT	0.0568	20

* All polymerization reactions were run at constant temperature (100 °C), [RAFT] = 0.0125 mol L^{-1}.

4.2.2 RAFT-mediated polymerization of St in a sealed system

The sealed polymerization experiment was performed in a Schlenk tube. The quantities used were exactly the same as presented in Table 4.1. The tube was deoxygenated by four successive freeze-pump-thaw cycles before starting the polymerization reaction and then sealed with a rubber septum. The reaction was conducted under N_2 and samples were taken at time intervals using a syringe that was purged with N_2 before taking a sample (to prevent oxygen from entering the system during sampling). In order to maintain a sealed system, the following precautions were taken during the sampling exercise. The syringe

while empty was purged with N_2 and then filled with N_2 before piercing the septum, to avoid oxygen traces from entering the syringe before taking the sample. After taking the sample the septum was immediately covered with a thin layer of Parafilm in order to block the tiny hole that was caused by the needle. The reaction was stopped when the polymer solution became very viscous and no further sampling was possible.

4.3 Characterization

The monomer to polymer conversion for all samples was determined gravimetrically. Molecular weights and molecular weight distributions were determined by SEC using the following instrumentation: Waters 117 plus Auto-sampler, Waters 600 E system controller (run by Millennium[32] V 3.05 software) (injection volume 100 µL), Waters 610 fluid unit, two PLgel 5 µm Mixed-C columns and a pre-column (PLgel 50 µm Guard), a Waters 410 differential refractometer and Waters 2487 dual wavelength absorbance at 30 °C. THF (HPLC grade) sparged with IR grade helium was used as eluent at a flow rate of 1 mL min^{-1}. The SEC setup was calibrated against 10 polystyrene standards of narrow polydispersity, ranging from 800 to 2×10^6 g/mol. The refractive index (RI) detector is a concentration sensitive detector that measures the difference in the RIs between the eluent in the reference cell, and the sample plus the eluent in the sample cell (the eluent being THF for all samples).

The UV detector is sensitive to certain chromophores at specific wavelengths, and was used to detect styrene at a wavelength of 254 nm and the dithiocarboxylate moiety at a wavelength of 320 nm.[5,6]

4.4 Results and discussion

4.4.1 Polymerization reaction rates (unsealed system)

From the experimental data of each polymerization system, a semilogarithmic kinetic plot was constructed of $\ln([M]_0/[M]_t)$ versus polymerization time in order to obtain the first-order kinetics for each polymerization system. Figure 4.2 shows a roughly linear relationship of $\ln([M]_0/[M]_t)$ with time for all systems until a moderate polymerization time, indicating a constant propagating radical concentration during that period, after which (at an advanced reaction time), a sudden increase in the rate was observed. This

behavior is often seen in a conventional free radical polymerization due to the Trommsdorff-Norrish "gel" effect.[7,8] This autoacceleration usually takes place at intermediate or high degrees of conversion and is caused by diffusion limitations that primarily hinder the termination process.

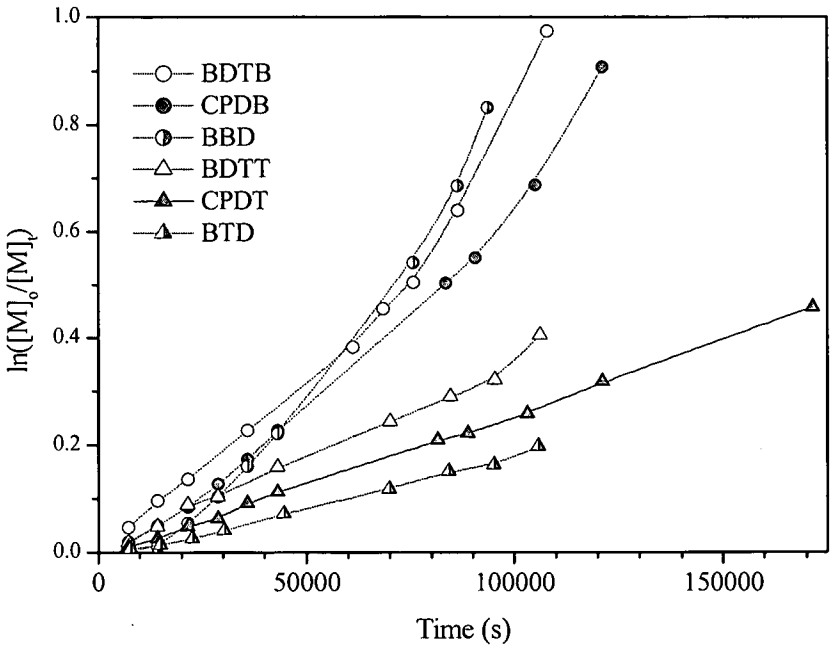

Figure 4.2: Semilogarithmic plots of fractional conversion vs. polymerization time for styrene polymerizations mediated by BDTB, CPDB, BDTT, CPDT, BTD and BBD at 100 °C.

Ideally, in a controlled/living polymerization, the kinetic plot should give a reasonably linear graphs throughout the polymerization reaction if [P$^{\bullet}$] is constant, to show there is a constant number of propagating chains during the polymerization reaction.

In the cases of BDTB, BBD, CPDB and BDTT, the increase in the reaction rates was strong and was thus investigated further. The polymerization reactions were repeated at least once under the same conditions for each RAFT agent used. The repeated experiments gave similar results to the first experiments with a sharp increase in the rate recorded at approximately the same advanced polymerization time as before. To illustrate an example of the repeated experiments, Figure 4.3 shows repeats of styrene polymerization mediated by BBD and BDTT. It can be seen that for both systems, the upward curvature, which usually indicates an increase in the rate, occurs at relatively different times in the duplicate runs, which might be because of monomer loss and/or an increase in the viscosity, leading to decreased termination.

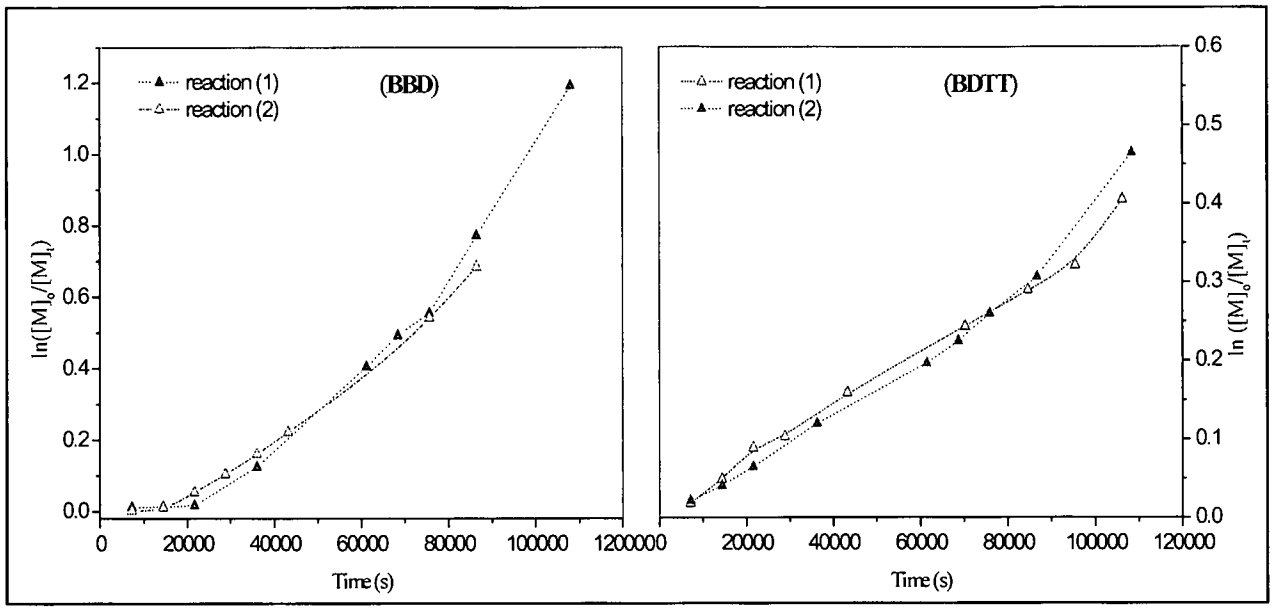

Figure 4.3: Semilogarithmic plots of monomer concentration vs. time for repeat polymerizations of styrene mediated by BBD and BDTT at 100 °C.

It was suggested that the experimental setup that was used might have led to errors in the results due to the fact that the polymerization reactions were performed under N_2 gas flow (although the flow rate was very low, since there is the potential for styrene monomer to escape from the system). If this is the case, then it might explain the gradual increase in the apparent rate where, with decreasing monomer concentration in the system and with progressive polymerization, a rapid increase in the viscosity of the polymer solution may also lead to the Trommsdorff effect reducing long chain termination while simultaneously providing "exaggerated" apparent conversion measurements. The polymerization reactions were therefore repeated in a sealed system, where there was little chance of the monomer escaping from the system.

Apart from the probability of monomer loss from the system, the loss of RAFT agent functionality is also possible, depending on the purity of the N_2 gas. This is because traces of oxygen flowing continuously with the stream can have an effect on the generated radicals in the system. However, using ESR studies, Calitz *et al.*[9] have shown that reactions mediated by dithiobenzoate RAFT agents were not particularly sensitive to oxygen contamination. Thus oxygen traces might not have a significant effect on the intermediate radicals, but are rapidly consumed, which does affect the radical concentration, at least, in the early stages of initiation.

If the RAFT radical adducts are terminated, the system will have less RAFT chain transfer moieties, which are responsible for control of the system. This would result in a rapid propagation rate that would lead to high molecular weights. This was not observed in this case. Although the chance of uncontrolled styrene propagation is still possible as the source of radicals generated from self-initiation is available (see Scheme 4.1); these propagating radicals rapidly become involved in the RAFT process and hence would still be mediated.

4.4.2 Polymerization reaction rates (sealed system)

In order to prove whether the previous experimental setup suffered from monomer leakage, a comparison between a sealed and an unsealed polymerization system had to be performed. BDTB was initially chosen as the RAFT agent, since it showed the most rapid increase in the reaction rate in the previous experimental setup.

The first-order kinetic plot for the sealed polymerization procedure is shown in Figure 4.4. The polymerization rate gave a linear (straight line) relationship, indicating a constant propagating radical concentration during the polymerization reaction. It is observed that the rate of polymerization in the sealed system was slower than in the case of the N_2 flow setup (it was almost half the rate), which is consistent with the premise that monomer escapes the system in the latter case.

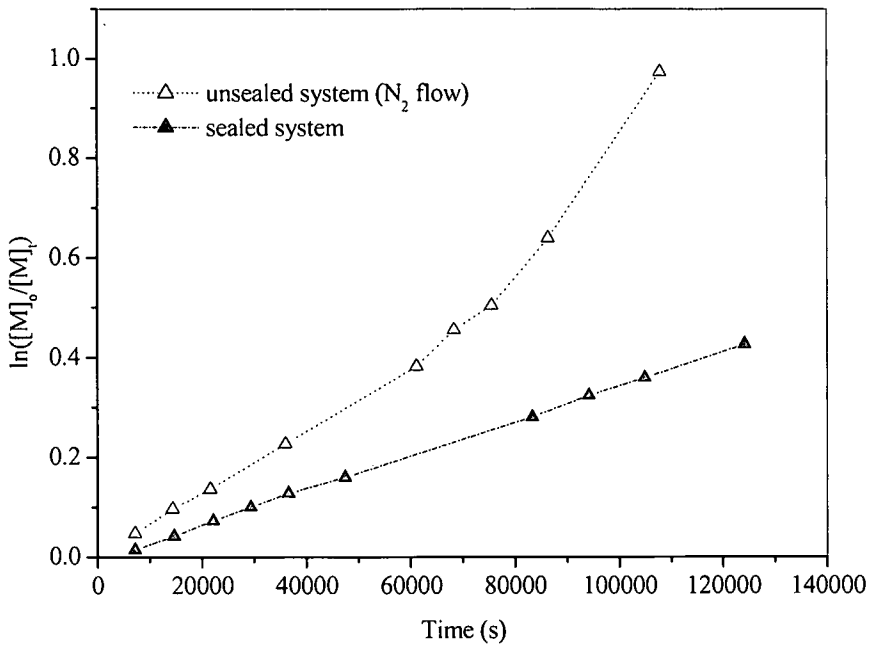

Figure 4.4: Semilogarithmic plot of monomer consumption vs. polymerization time: a comparison between a sealed and unsealed system of styrene polymerization mediated by BDTB as the RAFT agent at 100 °C.

Thus, it was shown that no acceleration took place in the sealed polymerization system. It was postulated that for the other RAFT agent systems besides BDTB, a linear reaction rate would also have been achieved if a sealed polymerization system was used. Therefore, to accomplish an accurate comparison between the performances of each RAFT-mediated polymerization reaction, all reactions were repeated in a sealed system as described in Section 4.2.1. Figure 4.5 shows the first-order kinetic plot of all the repeated sealed polymerization reactions.

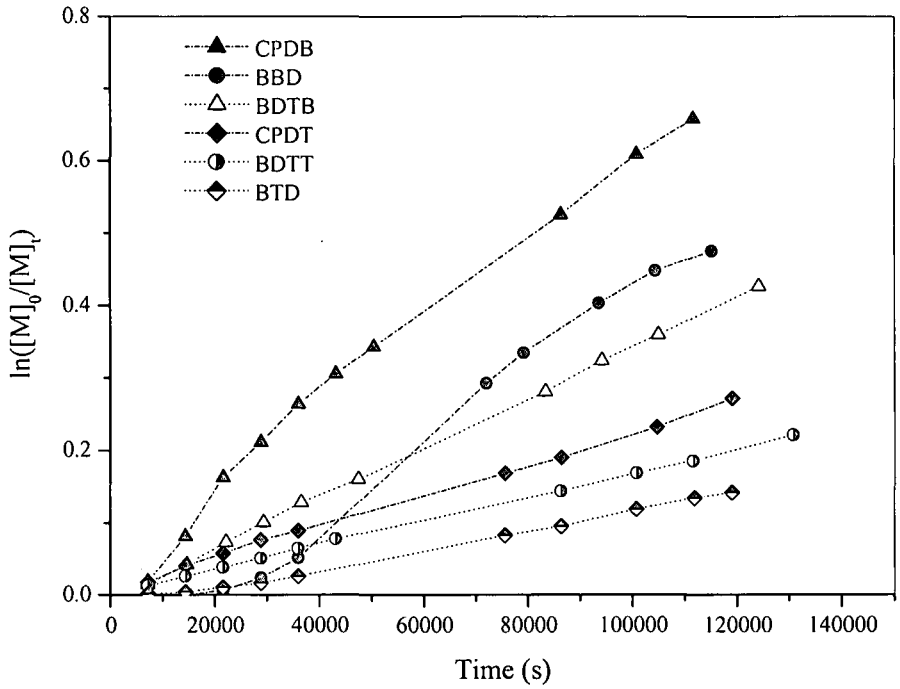

Figure 4.5: Semilogarithmic plots of fractional conversion vs. polymerization time for styrene polymerizations mediated by BDTB, CPDB, BDTT, CPDT, BTD and BBD at 100 °C in a sealed system.

Figure 4.5 shows that no sudden increase in the rate as was the case with N_2 flow reactions. Near linear relationships were noticed for all systems, indicating a constant propagating radical concentration during the course of the polymerization, except for the disulfide reactions, where an inhibition period of approximately 6 hours was recorded. When comparing between the phenyl and thiophene-based polymerization reactions and using the relative rate values in Figure 4.5, it is seen that the polymerization systems mediated by thiophene-based RAFT agents have lower reaction rates. The slower reaction rate (retardation) can be attributed to the nature of the thiophene ring as a Z group; thiophene possesses a higher electron density relative to the phenyl ring,[10] and this will have a significant effect on the intermediate radical stability (as discussed in Section 2.3.3.2). Thus, the thiophene ring, with its relatively high resonance energy, can provide stability to the intermediate radical and hence increase the RAFT equilibrium constant K_{eq}, thereby leading to an increase in the intermediate radical concentration and, as a result, increase the degree of rate retardation.

4.4.2.1 Disulfide polymerization systems

In order to understand the effect of the different Z groups for both BBD and BTD, the polymerization mechanism was investigated. As shown in Figure 4.6, both suffer from an apparent inhibition period. The disulfides, however, are not directly active RAFT agents, but precursors that produce active RAFT agents in situ, in the presence of a radical species. Thus the polymerization mechanism is initially different from that of the other dithiocarbonates.

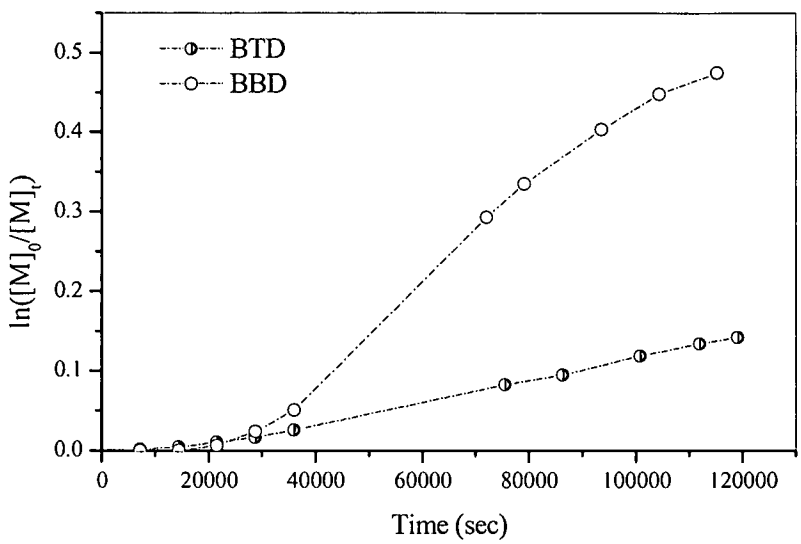

Figure 4.6: Semilogarithmic plot of monomer consumption vs. polymerization time for styrene polymerizations mediated by BBD and BTD at 100 °C.

Ideally, a disulfide molecule should be transformed to produce two active transfer agents (two molecules), capable of controlling the polymerization process, which is in this case styrene polymerization. However, practically this is an oversimplification, since radicals are very reactive species and the possibility of transfer, termination and side reactions cannot be avoided.

Scheme 4.1 illustrates the proposed mechanism of styrene polymerization in the presence of the disulfide BBD. Starting from the formation of the initiating species according to Mayo's mechanism (see Figures 2.7 and 2.8 in Section 2.4), the styryl radical has the possibility of attacking a disulfide precursor dithiocarbonate bond to produce the intermediate radical A (step 1), or propagating with a styrene monomer in a conventional free radical polymerization fashion as indicated in step 2.

Once the intermediate radical A is formed, it may fragment upon the S-S bond cleavage to form an active RAFT agent B and a RCSS$^{\bullet}$ sulfur-centered radical (C). If there is no cleavage of the S-S bond, the adduct A could be transformed to the intermediate radical A'.

The radical adduct C could be implicated in several radical reactions as follows:

- It could react with either a propagating radical or a styrene radical and produce a new active transfer (RAFT) agent D.
- The combination of two RCSS$^{\bullet}$ radicals is a possible step (8), and it can be suppressed if the radical is stabilized electronically, or by steric effects.
- reacting with a styrene monomer is a possibility for initiating a polymer chain (F) and propagating as indicated in step (4).
- The possibility of a decarboxylation step[11] (5) cannot be excluded; the occurrence of this process will lead to the formation of a new radical species (a phenyl radical) and carbon disulfide. The presence of this radical can also affect the mechanism, since it is capable of reacting in different pathways including: attacking styrene monomer and initiating a growing polymer chain [step (9)], or reacting with any radical adduct nearby, such as (C), and producing a dormant (RAFT agent) compound (E) [step (6)]. This will also occur if it terminates a growing chain [step (7)]. The propagating radicals from step (9) can later react with an active RAFT agent such as B or D, and the polymerization proceeds thereafter in a controlled manner.

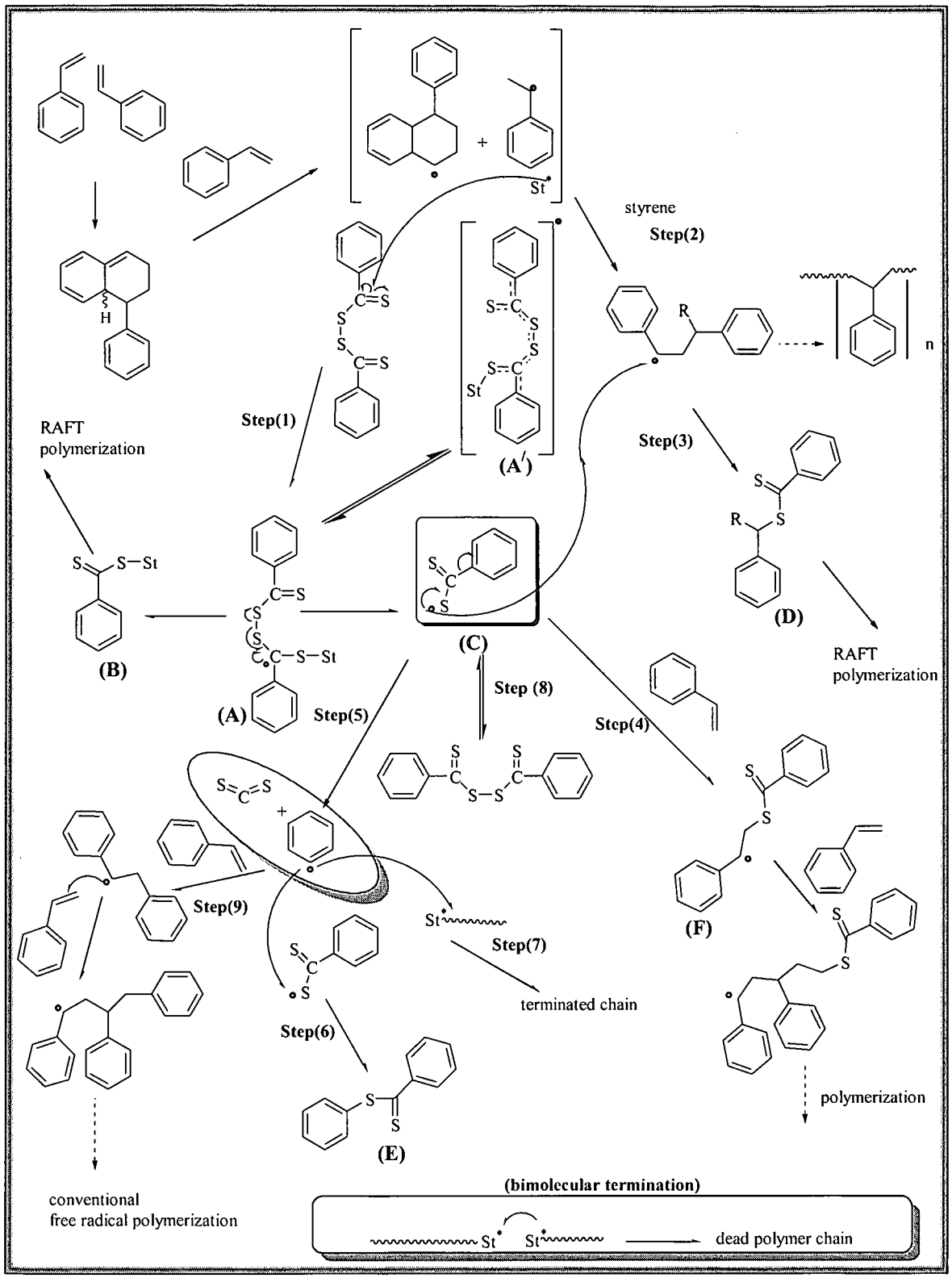

Scheme 4.1: Proposed mechanism of styrene self-initiated polymerization in the presence of BBD.

It must be noted that all the radical reactions indicated in Scheme 4.1 are possible, but the radical-radical reactions probably occur at diffusion controlled rates, i.e. depending on the reactivity and stability of the radical species, the radical reactions could occur at different

rates and be selective towards the more susceptible and reactive chemical species present in the reaction.

In conclusion, the proposed mechanism can help us to understand the cause of apparent inhibition periods with regard to the disulfides. It is believed that the inhibition period, before any polymerization takes place, can be a result of strong selectivity of reactions of the radicals present at that time. It is therefore likely that the radical reactions that consume the initial disulfide are predominant at the early stages of the polymerization reaction. This depends on the rate determining reactions to consume the initial disulfide, and the lifetime of the formed intermediate radical adducts (A and A′). Once the active RAFT agents are produced, and if a source of radicals is still present, the polymerization, thereafter takes place as in a conventional RAFT polymerization process.

However, the proposed mechanism alone is not sufficient; to support the above discussion. It is vital to analyze the SEC results, to investigate the polymerization behavior (whether it is controlled/living) by monitoring the molecular weight and the molecular weight distributions as a function of monomer to polymer conversion and time. A detailed discussion on the "livingness" of all the polymerization processes, based on SEC results, will be presented in the following section.

4.4.3 Molecular weight distributions of PSt as determined by SEC

Evolution of the full molecular weight distributions for styrene polymerization in the presence of the respective RAFT agents are depicted in Figure 4.7.

Figure 4.7 shows that bimodal distributions arise in the case of BBD and BDTB-mediated polymerization systems, while the other polymerization systems show less bimodal distribution, but seen only as a small high molecular weight (M) shoulder, especially as the conversion increased. These shoulders appear approximately at twice the chain length of the peak molecular weight, and so could be attributed to the termination of the propagating chains by combination.[12]

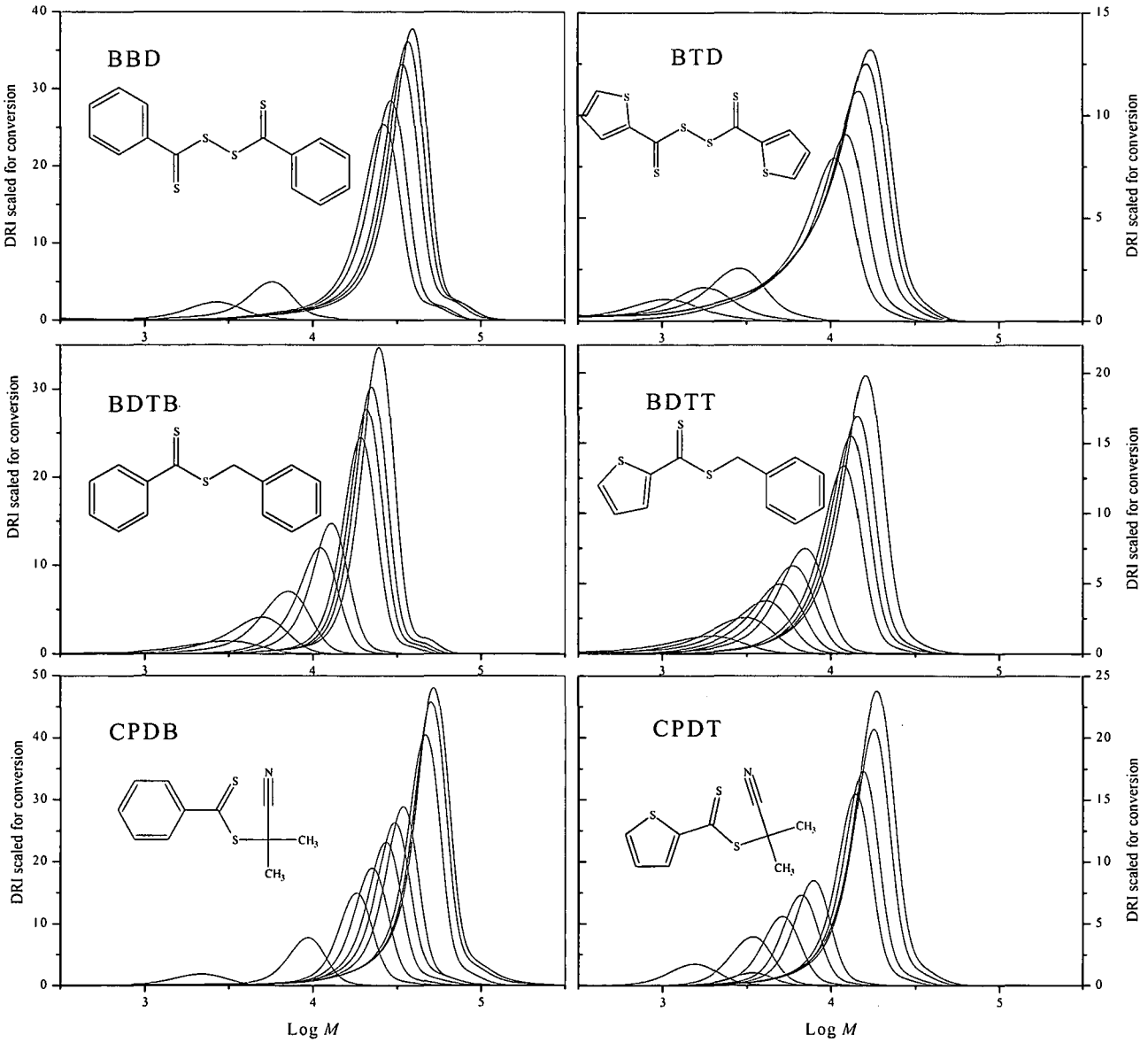

Figure 4.7: Evolution of molecular weight distributions (scaled for conversion) for styrene polymerizations in the presence of RAFT agents BBD, BTD, BDTB, BDTT, CPDB and CPDT.

Another less significant process that has been suggested as contributing to the formation of these shoulders, is the reaction of the polymeric intermediate radical with a propagating radical by combination.[13]

On the other hand, analyzing the response of the dual UV absorbance detector provides valuable information, since the wavelengths are set at 254 nm for detecting styrene and 320 nm for detecting the RAFT moiety. This allows monitoring the distribution of thiocarbonyl thio functionality throughout the molecular weight distribution curve. It should be noted that both the UV and RI signals were normalized. However, to make the signals comparable, and before normalization, the UV signal was multiplied by a factor of

signals comparable, and before normalization, the UV signal was multiplied by a factor of M (molecular weight) when processing the data from the SEC results, i.e. since the RI detector is concentration based, the intensity of the signal will be sensitive to the molecular weight of the polymer chains. In contrast, the UV detector is sensitive only to a single chromophore (in this case the dithiocarbonate moiety) per polymer chain at a wavelength of 320 nm, if present.

4.4.3.1 Comparison between the disulfide mediated systems

When examining the disulfide mediated systems BBD and BTD in Figure 4.7, a shoulder is prominent from low conversion samples all through to higher conversion samples, which was not the case in the other mediated systems, as the shoulder became apparent only at advanced conversions in the higher molecular weight region.

Thus to obtain a better understanding of the performance of each system, the UV/RI overlays were plotted for each polymerization system. Figure 4.8 shows the UV/RI overlays of selected polystyrene samples mediated by BBD and BTD; starting from low to higher conversion samples. Looking at the UV signals in Figure 4.8, and starting from the low conversion samples, a strong UV signal a wavelength of 254 nm appears prior to the main molecular weight peak (as indicated in the figure) and overlays with a hump of the RI signal that is indicative of short chain styrene oligomers present, which could indicate early stage terminations or late initiated polymer chains. It is also apparent that there is hardly any sign of a UV response a wavelength of 320 nm, which indicates the absence of the RAFT functionality in these oligomers.

However, at a slight increase in the conversion, a prominent shoulder appears in the high molecular weight region of the main peak. The UV signal at 254 nm matches very closely to the RI signal, and the UV signal at 320 nm which shows a moderate intensity at the shoulder, appears to be higher than the RI/UV signal at 254 nm as expected for two RAFT moieties per chain. This is very interesting as it might point toward a significant reaction pathway occurring in the course of the polymerization reaction.

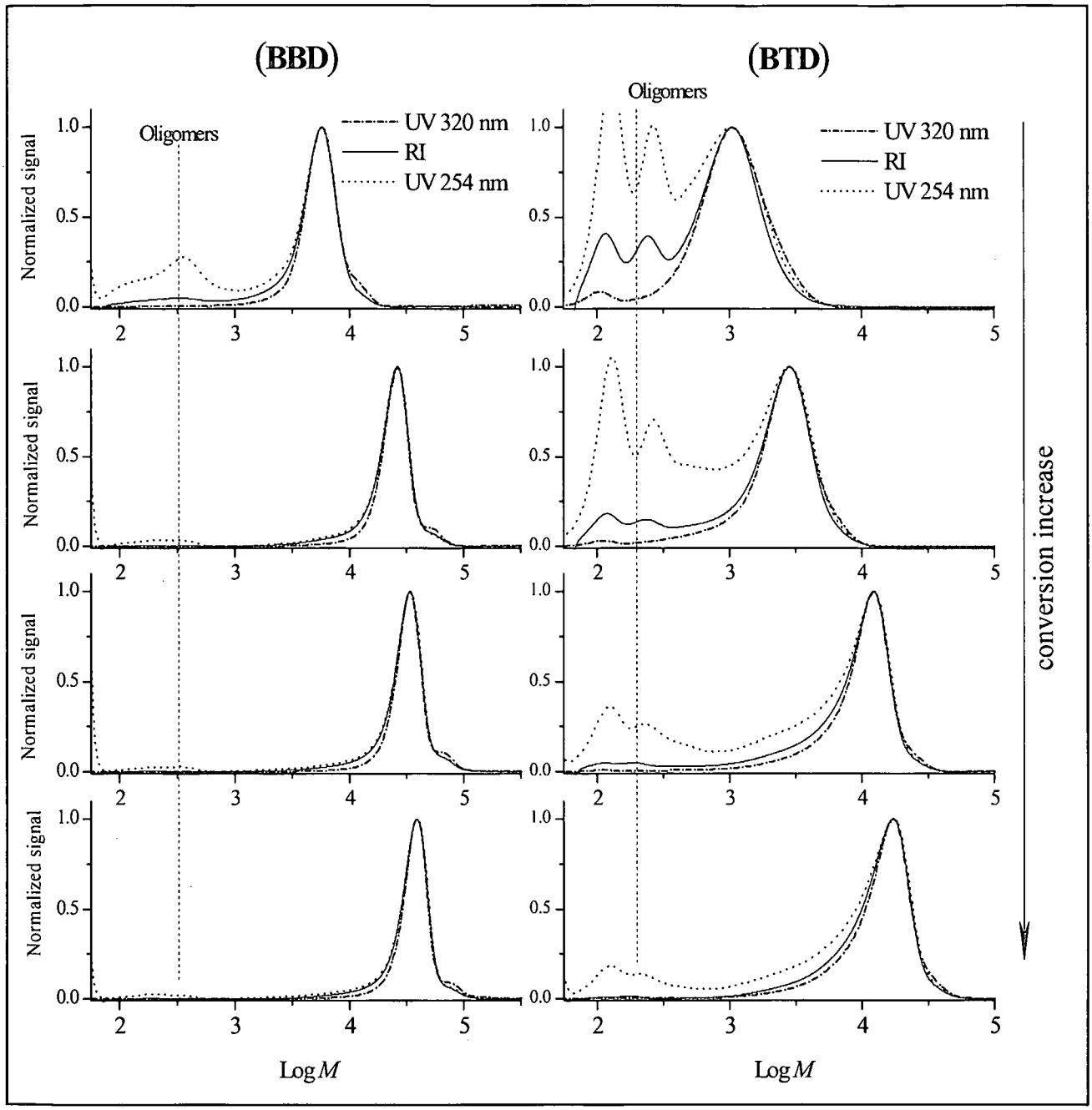

Figure 4.8: UV/RI overlays of polystyrene samples mediated by BBD and BTD at 100 °C.

Referring to the proposed mechanism in Scheme 4.1; if the reaction step (4) which yields product (F) occurs to a reasonable extent, it could provide a mechanism for the production of a living polymer with twice the molecular weight. i.e. when product (F) finds its way to couple with another compound ending with a RAFT functionality, it provides an appreciable chance of a mediated chain growing from both sides (see Scheme 4.2), which could be almost double in length when compared to that of a single mediated chain. On the other hand, it is very important to consider that if product F propagates, then the

polymer chain can grow faster than the mediated ones, if so, then a high M is highly probable. Since the UV signal at 320 nm is strong at that peak it might be that these propagating chains start fairly early in the reaction and very soon couple with another propagating radical of the same kind. This could lead to a difunctional chain end that can grow from either sides, early in the reaction.

To recap, it is seen that the UV signals at 320 nm in the high M shoulders, have high intensity relative to the RI and UV signals at 254 nm. This indicates a high concentration of the dithiocarbonate moiety present in those high molecular weight chains. Since they appear at approximately twice the molecular weight of that of the main peak at each stage of the reaction (i.e. it grows consistently), it is postulated that some polymer chains are mediated from both sides, yielding double the chain length of that of a single mediated chain. Thus the results correlate with the proposed reaction mechanism and it seems that the pathway of reaction step (4) in Scheme 4.2 occurs to a reasonable extent and may have contributed to the final molecular weight distribution curves.

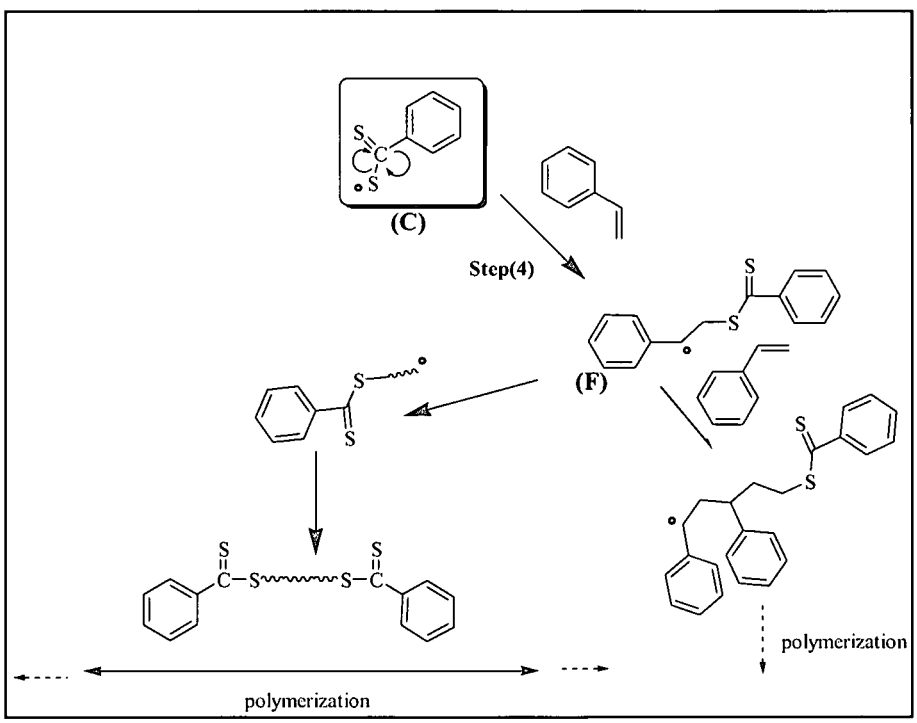

Scheme 4.2: A possible reaction leading to a two-way mediated chain growth.

The BTD-mediated system also showed similar results, although lower conversions were achieved, relative to the BBD-mediated system. It is however expected that the mechanism in the presence of the thiophene disulfide will be similar to that of BBD. The

UV/RI overlays in Figure 4.8 show a stronger UV signal at 320 nm than the RI/ UVsignal at 254 nm observed at the shoulders, but it is not as apparent as in the BBD system.

The thiophene disulfide reaction was much slower than its analogous BBD reaction due to the nature of the thiophene ring, which might have provided more stable intermediate radicals that retard the propagation rate and increases the possibility of side and termination reactions. However, the possibility of mediated chain growth from two sides, as mentioned in the case of BBD-mediated system, is also likely to occur, especially if it does for BBD, since a strong UV signal at 320 nm is present in the high *M* shoulder.

Furthermore, if we look at the RI signal for the BTD in the Figure 4.8, a significant tailing towards the lower molecular weight region is apparent with a strong UV signal at 254 nm overlaid in the same region. It can also be seen that there is barely any sign at 320 nm of a UV, therefore, these RI/UV signals at 254 nm indicate the presence of uncontrolled short chain oligomers that are either terminated, or late initiated, which is likely to occur in this case, because of the fact that the tailing remains significant even at higher conversion samples as indicated in the Figure.

The RI/UV overlays of the dithio-mediated systems (non-disulfides) showed relatively different results. Although a slight shoulder in the RI signal was apparent in some of the systems, such as BDTB, CPDB, and CPDT, it however only became prominent at advanced conversion in the high molecular weight regions. As examples, Figure 4.9 and 4.10 present the RI/UV overlays of the CPDT and BDTB-mediated systems respectively.

The RI/UV overlays of both systems (Figures 4.9 and 4.10) match fairly closely throughout the molecular weight distribution curve. The slightly high *M* shoulder became prominent at higher conversions and all signals overlaid reasonably well. In addition, when looking at the molecular weight at the shoulder compared to the main peak, it measures to almost double the chain length. However, the main difference was that the UV intensity at 320 nm for these shoulders, appear to be as strong as the RI signal, which is likely to indicate the presence of a RAFT group, as the UV signal at 320 nm is closely matched with the RI and the UV signal at 254 nm.

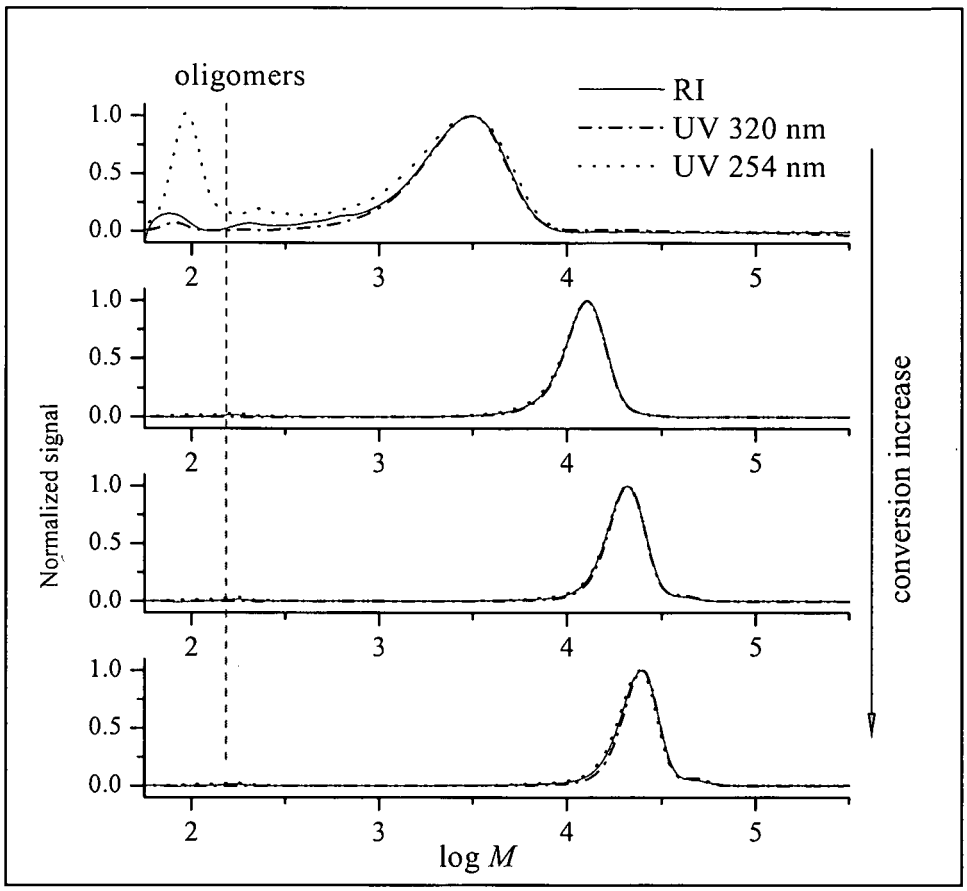

Figure 4.9: UV/RI overlays of polystyrene samples mediated by BDTB at 100 °C.

The RI/UV overlays of both systems (Figures 4.9 and 4.10) match fairly closely throughout the molecular weight distribution curve. The slightly high *M* shoulder became prominent at higher conversions and all signals overlaid reasonably well. In addition, when looking at the molecular weight at the shoulder, compared to the main peak, it measures to almost double the chain length. However, the main difference was that the UV intensity at 320 nm for these shoulders appear to be as strong as the RI signal, which is likely to indicate the presence of a RAFT group, as the UV signal at 320 nm is closely matched with the RI and the UV signal at 254 nm.

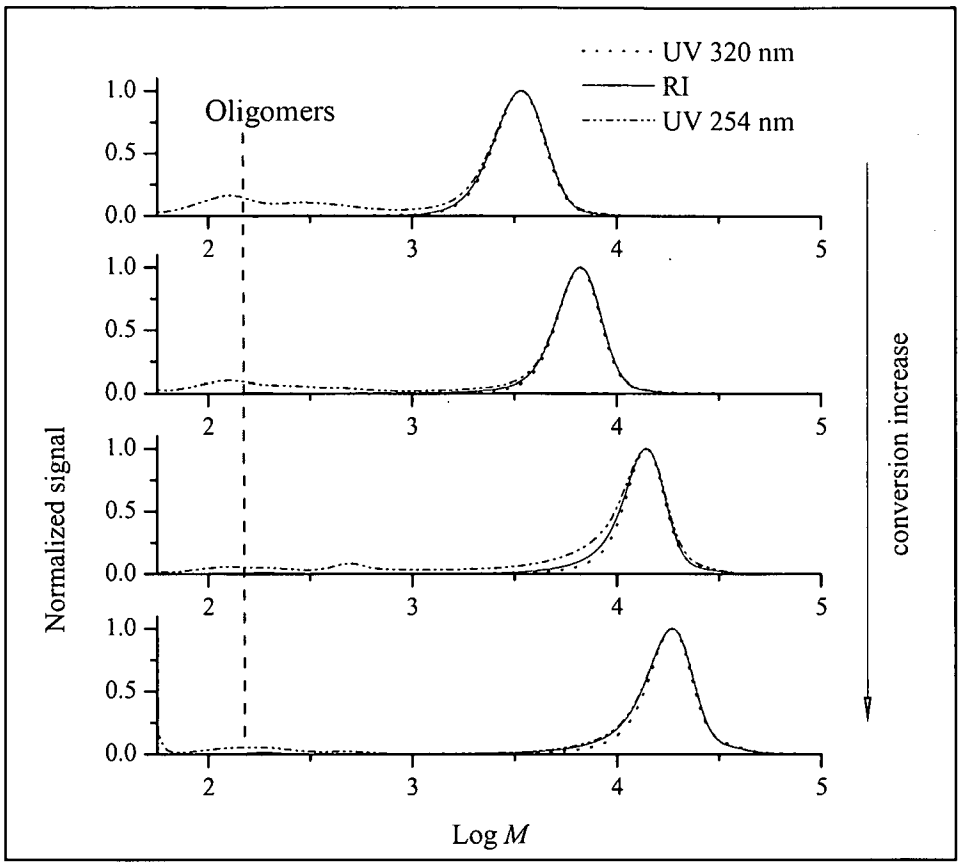

Figure 4.10: UV/RI overlays of polystyrene samples mediated by CPDT at 100 °C.

The SEC curves however also show clear tailing towards the lower molecular weight region. This could be indicative of the cumulative production of terminated polystyrene oligomers during the polymerization process, as well as the continuous initiation (generation of radicals thermally from styrene) throughout the reaction.[14] Hence, a large amount of terminated products are present during the polymerization reaction, leaving a tail of shorter chains, which gradually increases the polydispersity of the final material.

The tailing is however more pronounced in the thiophene-based polymerization systems (BTD, BDTT and CPDT) as shown in Figure 4.7, especially for the BTD-mediated polymerization system. This could be due to broadening because of less control, more cross termination, or other factors. The thiophene-based reactions, give slower reaction rates, so that more termination reactions occur per unit conversion. Due to the nature of thermal initiation from styrene, in the thiophene-based reactions there are more initiation events per unit conversion throughout the course of the reaction. Thus a longer tail could be the result of several factors, including all types of termination reactions.

The BBD-mediated chromatogram also shows quite pronounced tailing, which could be expected in the case of the disulfide, as there is a sequence of radical reactions involved,

starting from the initiated species and throughout the polymerization process. These tailings would seem to indicate that some products are only slowly incorporated into the reaction, or impurities formed from the RAFT agent are reacting with other chains throughout the reaction, through processes such as chain transfer.

The variation in the number average molecular weight ($\bar{M}_n$) of the growing polymeric material, with monomer conversion during the RAFT-mediated styrene polymerizations is shown in Figures 4.11 and 4.12. They examine the "living" behavior of the polymerization mediated by the novel thiophene-based RAFT agents, and compare their performance with the dithiobenzoate RAFT agents. The theoretical number average molecular weights were calculated according to equation 4.1:[14]

$$\bar{M}_n = \frac{X\,[\mathrm{M}]_o\, M_{\mathrm{monomer}}}{[\mathrm{RAFT}]_o} + M_{\mathrm{RAFT}} \qquad (4.1)$$

Here X denotes the fractional monomer conversion, $[\mathrm{M}]_o$ being the initial monomer concentration, $[\mathrm{RAFT}]_o$ being the initial RAFT agent concentration, and M_{monomer} and M_{RAFT} being the molecular weights of the monomer and the RAFT agent respectively.
In living radical polymerization the molecular weight of the resulting polymer increases steadily with reaction time and is approximately linearly related to the monomer conversion.

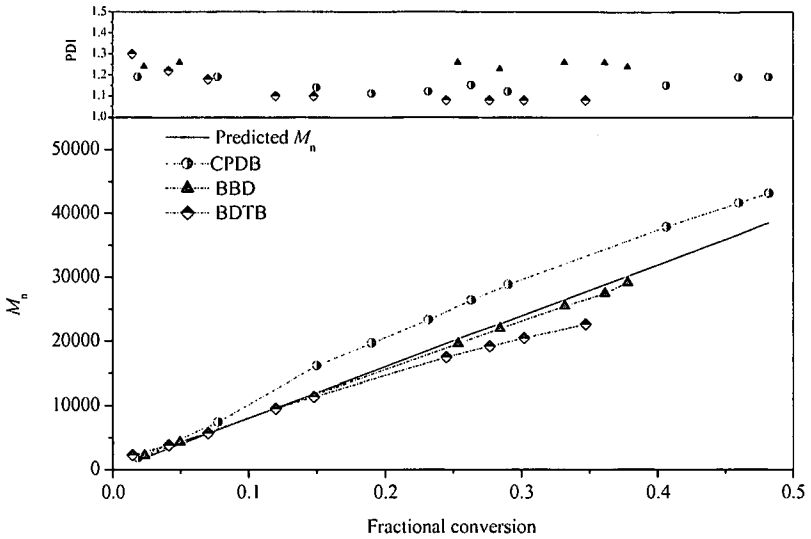

Figure 4.11: Plots of $\bar{M}_n$ and polydispersity as a function of conversion; straight lines represent the theoretically calculated $\bar{M}_n$ for polystyrene samples mediated by CPDB, BBD and BDTB at 100 °C.

Figures 4.11 and 4.12 show the relation ship between the experimentally determined $\bar{M}_n$ values (obtained by SEC) and the polydispersity, versus the fractional conversion of the polymers obtained in each sealed polymerization system. The two straight lines drawn in the graphs represent the theoretically calculated $\bar{M}_n$ values. The calculations were done according to equation 4.1

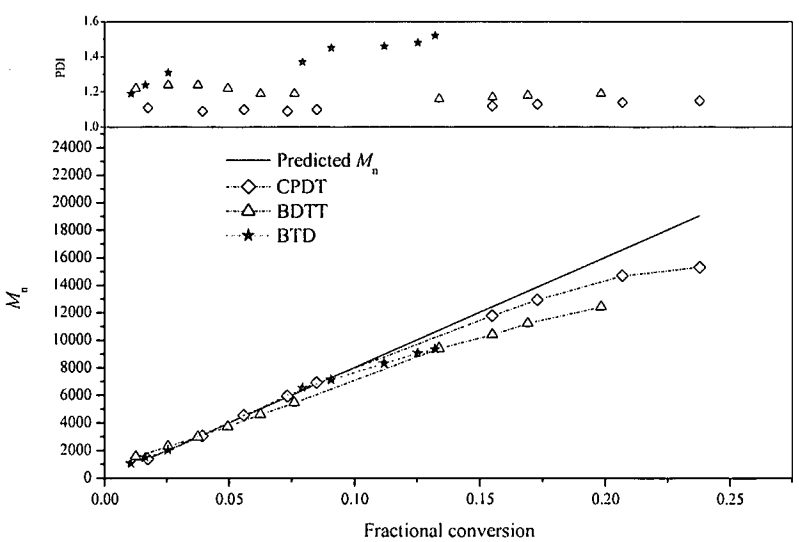

Figure 4.12: Plots of $\bar{M}_n$ and polydispersity as a function of conversion; straight lines represent the theoretically calculated $\bar{M}_n$ for polystyrene samples mediated by CPDT, BDTT and BTD at 100 °C.

Figures 4.11 and 4.12 show that the experimental $\bar{M}_n$ values of all mediated systems increase with monomer to polymer conversion, and in most cases a downwards deviation

from the upper theoretical $\bar{M}_n$ value is observed, except for the CPDB-mediated system where it shows upward deviation from the predicted $\bar{M}_n$. The downward curvature will partly be because of the continuous initiation of new chains with time, which will increase the number of chains but decrease the target $\bar{M}_n$ value, and thus it is expected that the line will deviate downwards from the theoretical one.

Considering firstly the BBD- and BTD-mediated reactions, the relationships between the experimental and the predicted $\bar{M}_n$ values are reasonably close, especially at lower conversions. A slight deviation from the upper theoretical $\bar{M}_n$ values is observed as the conversion increased. This however, does not support the assumption of one disulfide RAFT agent providing two chain transfer agents, because if that is the case, then a stronger downward deviation would have been expected. This should indicate an increase in the number of chains and hence reduce the target $\bar{M}_n$ value.

However, in the case of the BBD- and BTD-mediated reactions, it seems that eventually one RAFT agent per chain is predominant. Also, according to the UV/RI overlays in Figure 4.8, as discussed earlier, a significant reaction presented in Scheme 4.2 occurs to a reasonable extent and which will yield two RAFT moieties per chain. The polymerization behavior might be related to the lifetime of the intermediate radical (A) as a precursor to produce an active transfer (RAFT) agent, and also the fate of the sulfur-centered radical (C) since it plays a significant role in the reaction mechanism. The lifetime and the reaction pathways of the sulfur radical which that will become involved in any of the reactions, is proposed in Scheme 4.1.It can effectively initiate propagation through step (4) and produce (F), which can then, potentially, allow two RAFT agents per chain and/or can be involved in other side reactions.

This speculation corresponds to the relation between the experimental and the theoretical $\bar{M}_n$ values where it shows no significant deviation from the predicted $\bar{M}_n$ line. This indicates that some of the RAFT moieties are lost through side reactions and/or significant amount of chains have two RAFT ends that are growing with time.

The polymers obtained via the BTD-mediated system, have significantly broader molecular weight distributions than the BBD-mediated systems, as shown by the PDI

values. This broadening is as a result of the terminated short chains and the newly initiated chains that become involved, lately, in the RAFT-mediated reaction. Because of the very slow reaction rate, the possibility of radical termination reactions increase and may account for the broadening of the molecular weight distributions.

If we consider the dithiobenzoates and the analogous thiophene-based RAFT agent systems in Figures 4.10 and 4.11, it can be deduced that the molecular weights increased approximately linearly with time in all mediated systems in the early stages of polymerization. However a slight deviation from the predicted $\bar{M}_n$ values was observed. A detailed comparison between dithiobenzoates and the analogous thiophene-based RAFT agents is discussed in the following section.

4.4.3.2 Comparison between dithiobenzoates and the analogous thiophene-based mediated systems

Thiophene Z-group RAFT mediated polymerization systems performed similarly to the phenyl analogues, except that all the thiophene-based reactions suffered from greater rate retardation and produced polymers with relatively broader molecular weight distributions.

The polymerization systems in the presence of BDTT, and its analogous BDTB are compared in Figure 4.13. In the case of BDTT the experimental $\bar{M}_n$ trend showed a slightly stronger deviation from the theoretical data. This could be mainly because of the continuous initiation of new chains with time and this would increase the number of chains. This decreases the target $\bar{M}_n$ value, causing downward curvature. Because of the lower reaction rate of the BDTT-mediated system when compared to BDTB-mediated system the chances of side reactions will also increase. The side reactions such as cross termination reactions and other radical coupling events can be a result of an increase in the overall radical concentration in the system, which arises from continuous self-initiation species from styrene and the stabilized intermediate radicals.

However, the polymers obtained by the BDTT-mediated system showed reasonable control according to the PDI values, which were below 1.3, e.g. at ~20% conversion, the PDI of 1.19 was obtained, when compared to the PDI of 1.08 at ~24% conversion. This indicates that the polymerization was controlled and it demonstrates the potential suitability of the BDTT as an efficient RAFT agent.

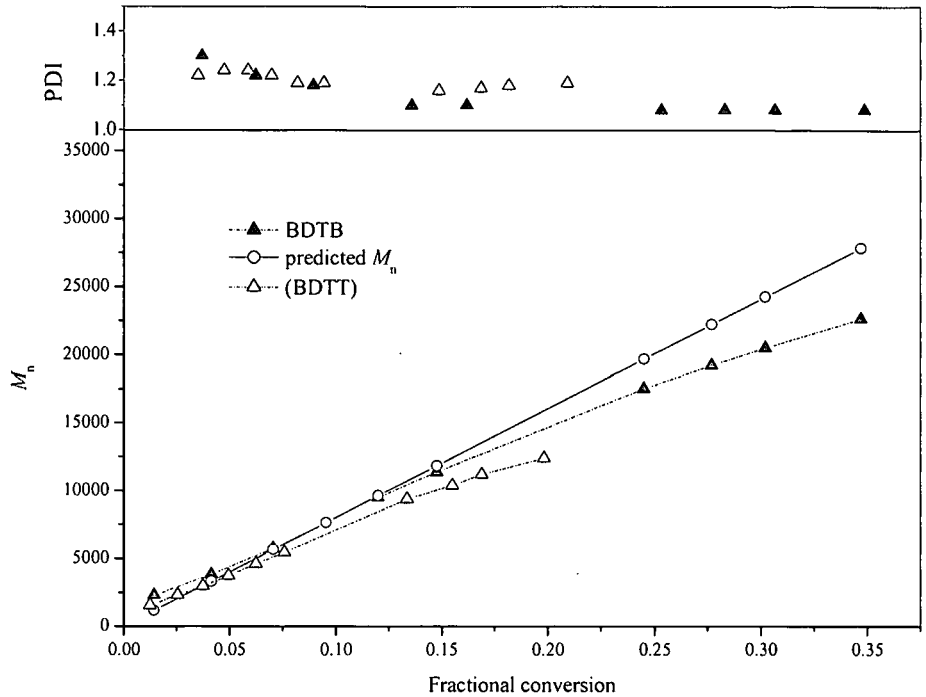

Figure 4.13: Plot of $\bar{M}_n$ and polydispersity as a function of conversion for styrene polymerization mediated by BDTB and BDTT at 100 °C.

The CPDT polymerization system, when compared to the CPDB system showed some differences with respect to the reaction rates and the molecular weight distributions of the polymers obtained. Figure 4.14 shows the relation of $\bar{M}_n$ and polydispersity as a function of conversion for both polymerization systems.

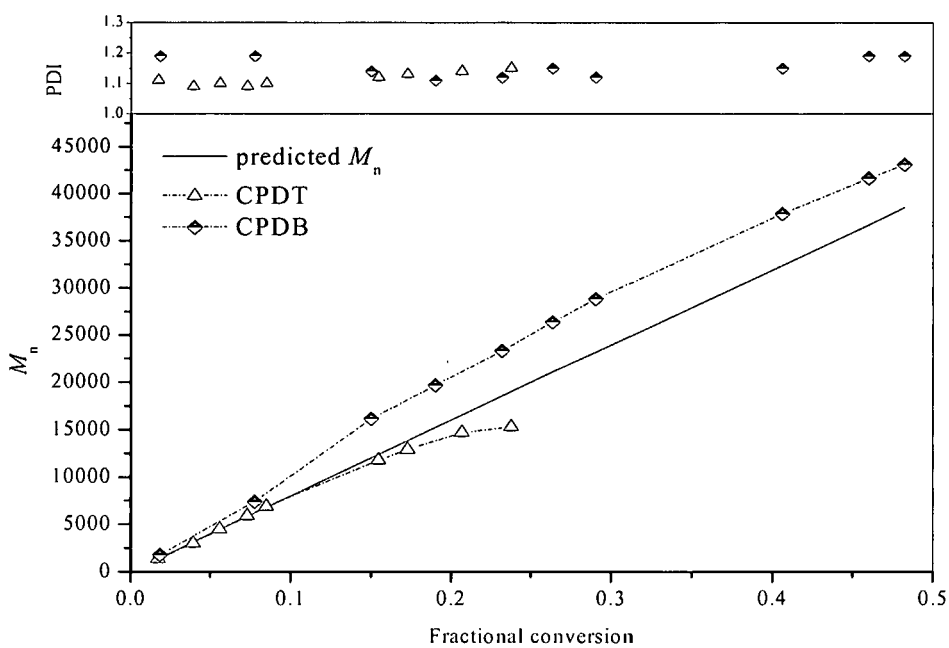

Figure 4.14: Plot of $\bar{M}_n$ and polydispersity as a function of conversion for styrene polymerization mediated by CPDB and CPDT at 100 °C.

When monitoring the molecular weight distributions for both systems over time, similar PDIs were observed in the early stages of polymerization, however a slight increase in the PDI values were recorded with increasing conversion. However, in the case of CPDB-mediated system, a positive deviation (upward) was observed. This could be the result of losing some RAFT moieties in the system, and hence less available active chain transfer agents to mediate the reaction. The loss of RAFT moieties can be due to impurities in the system, or termination reactions that trap the active dithiocarbonate moieties into a permanently dormant and unreactive species. The purity of the RAFT agent also plays a significant role; it could lead to inaccurate estimates of the amount of RAFT agent in the reaction, which will lead to incorrect calculations when using equation 4.1 for the predicted $\bar{M}_n$ values.

On the other hand, the relationship between the measured and the predicted $\bar{M}_n$ values match fairly closely in the case of CPDT-mediated system, especially at lower conversions. It can be seen that the curve starts to deviate downwards at about 25% conversion and the PDIs show only a slight increasing trend with monomer to polymer conversion.

The broadness of the molecular weight distributions is attributed to the following:
If the reaction rates of each polymerization system are compared (see Figure 4.15), it can be seen that the CPDT polymerization reaction showed a much slower rate compared to the CPDB-mediated reaction. The rate retardation of the former is attributed to the potential side reactions present during the polymerization reaction. This could have resulted from the stability of the intermediate radical, leading to a slow fragmentation (high K_{eq}) and/or cross-termination reactions. Slow fragmentation should then mean that the intermediate radicals become more susceptible to undergoing side reactions, since the rate of initiation (thermally from styrene) is still relatively high, and thus the rate of termination per unit conversion is expected to be high. These termination reactions, such as coupling with radical species,[3] cross termination and intermediate-intermediate radical coupling, are all possible, and may significantly affect the polymerization rate. These could be in part, responsible for the retardation in the polymerization reaction, thereby account for the broadening of the molecular weight distribution.

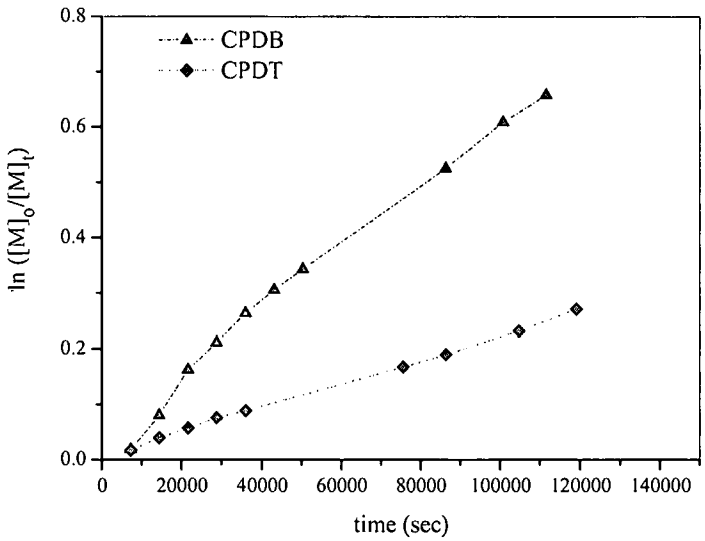

Figure 4.15: Semilogarithmic plot of fractional conversion vs. polymerization time for styrene polymerizations mediated by CPDB and CPDT at 100 °C.

The SEC results of two samples having similar molecular weights obtained from each polymerization reaction (CPDB and CPDT) are shown in Figure 4.16.

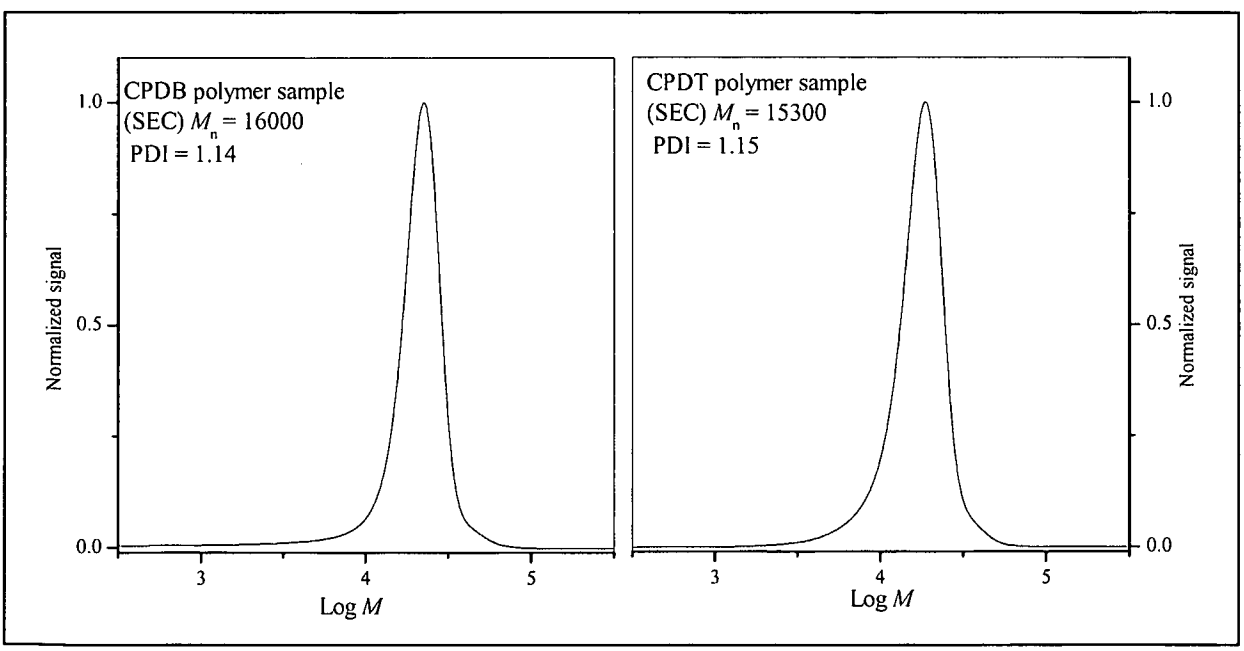

Figure 4.16: Molecular weight distributions of polystyrene prepared via CPDB and CPDT mediated polymerizations at 100 °C.

An apparent difference in the molecular weight distributions of the polymers is recognized in Figure 4.16, especially in the lower molecular weight region, where it can be seen that the low M tailing in the CPDT system was more pronounced when compared

to the CPDB-mediated polymer. Thus, this tailing might be an indication of the presence of a considerable amount of terminated species resulting from various side reactions; mainly from initiation throughout the polymerization reaction (thermally from styrene) and also could be as a result of some chains starting to grow later. However, the main difference between the CPDB and CPDT systems is that the latter suffered from greater rate retardation when compared to the former system, as seen in Figure 4.15. Although the molecular weights are similar there is a significant time gap for each of the presented samples. For example, from the SEC results shown in Figure 4.17, the time at which the samples were taken was 6 h for the CPDB system and 33 h in the case of CPDT system.

Note: It was mentioned in Section 4.4.2 that all polymerization systems were repeated in a sealed system; however, it is of interest to know what could result when working with an unsealed system such as under slow N_2 flow. Therefore, Figure 4.17 below shows the relation of experimental $\bar{M}_n$ values (obtained by SEC) and polydispersity, as a function of the fractional conversion of the polymers obtained in each polymerization system. These results are presented, mainly to illustrate that even if the polymers produced were controlled, the experimental data can give imprecise results and the interpretation of these results might be misleading, especially at temperatures as high as 100 °C. If the plots in Figure 4.17 are compared with Figures 4.11 and 4.12, a significant difference in the relationship between the experimental and the predicted $\bar{M}_n$ values is apparent. It can be seen that $\bar{M}_n$ curves of all polymerization systems display very strong deviations, especially at higher conversions. This is mainly due to monomer evaporation that can lead to a higher apparent conversion than actually the case because of polymerization, and lowers the target $\bar{M}_n$, since there is less monomer available per chain. This correlates strongly for most of the reactions and it is in accordance with the rate acceleration plots shown in Figure 4.2; therefore it is likely to be a significant contributor to the lower $\bar{M}_n$ values from the targeted ones.

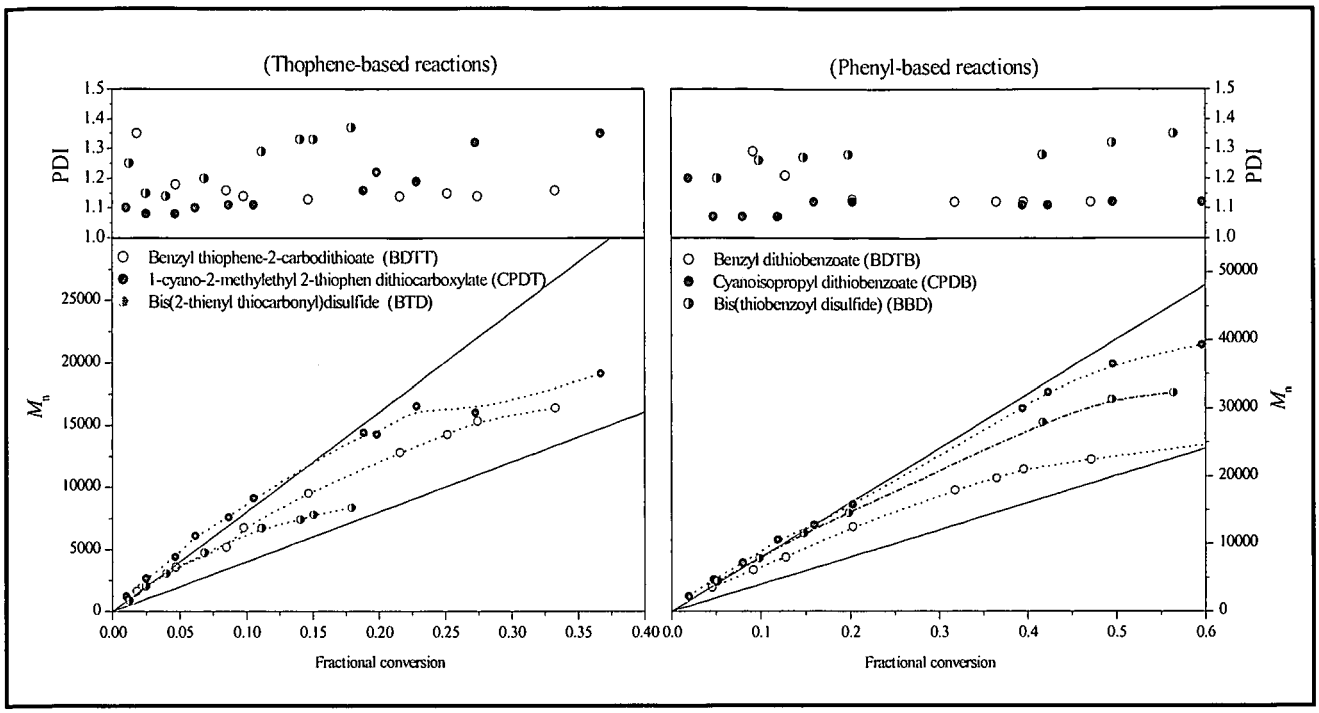

Figure 4.17: Plots of $\bar{M}_n$ and polydispersity as a function of conversion; straight lines represent the theoretically calculated $\bar{M}_n$ (upper line calculations based on one chain transfer agent and the lower line is based on two transfer agents per initial RAFT agent) (conditions: 100 °C, N_2 flow)

4.5 Conclusions

A series of self-initiated polymerizations of styrene with six different RAFT agents was successfully carried out. The polymers obtained from each polymerization system were characterized and analyzed with respect to reaction rates and molecular weight distributions using SEC.

A general comparison between the performances of the thiophene-based RAFT agents and the analogous phenyl-based RAFT agents was accomplished. The finding was that the novel thiophene-based RAFT agents, especially BDTT and CPDT, were potential candidates capable of controlling the polymerization of styrene and thus can be introduced as efficient RAFT agents.

The major difference between the thiophene and the phenyl-based RAFT agents is that the thiophene-based polymerization systems were much slower than the phenyl-based agents, which could have led to a broader molecular weight in general. The nature of the thiophene ring must have influenced the RAFT mechanism, proving better by stronger stabilization of the intermediate radicals, caused by a stronger delocalization in the

electron-rich thiophene ring. Consequently, the rate of termination and side reactions is expected to be higher in these cases, resulting in slightly broader molecular weight distributions when compared to the phenyl-based RAFT agents. However, the polymerization in the presence of the thiophene disulfide BDT was the slowest of all systems, and the poorest in terms of control, as it showed a broader molecular weight distribution in comparison to the analogous BBD system.

In Addition, the disulfide mediated systems revealed interesting results according to the overlays obtained from the SEC results, showing a prominent shoulder throughout the course of the reaction. This behavior was apparent only in the disulfide systems and was attributed to a significant reaction pathway that could have led to these results. It was postulated that a significant amount of chains are mediated by a RAFT agent at each end, which leads to mediated chain growth from both sides.

This is consistent with the consequences of reaction step (4) in the proposed mechanism of Scheme 4.2, which is the main route to achieve a two-side mediated chain growth. Thus, it seems that this reaction occurs to some extent in the process and may contribute to the overall polymerization reaction.

Finally, with regards to the experimental setup, it was shown that the polymerization reaction under N_2 flow can lead to monomer leakage from the system even at very low flow rates, which can affect the actual reaction rates and provide misleading results. Thus, it is advised to work under sealed conditions with minimal chances of monomer or solvent escaping from the system.

4.6 References

1. Moore, E. R.; Skochdopole, R. E.; Birch, A. F.; Gurnee, E. F.; Dibbs, M. G.; Finch, C. R., Styrene Polymers, in *Encyclopedia of Polymer Science and Engineering,* Second ed.; Mark, H. F.; Bikales, N. M.; Overberger, C. G.; Menge, G., Eds. John Wiley and Sons: New York, 1985; Vol. 15; pp 1-6.
2. Moad, G.; Solomon, D. H., *The Chemistry of Free Radical Polymerization*, Second ed.; Elsevier: Amsterdam, 2006; pp 451-564.
3. Moad, G.; Rizzardo, E.; Thang, S. H. *Aust. J. Chem.* 2005, 58, 379-410.
4. Chiefari, J.; Chong, B. Y. K.; Ercole, F.; Krstina, J.; Le, T. P. T.; Mayadunne, R. T. A.; Meijs, G. F.; Moad, C.; Moad, G.; Rizzardo, E.; Thang, S. H. *Macromolecules* 1998, 31, 5559-5562.
5. Russum, J. P.; Jones, C. W.; Schork, F. J. *Macromol. Rapid Comm.* 2004, 25, 1064-1068.
6. Matahwa, H.; McLeary, J. B.; Sanderson, R. D. *J. Polym. Sci. Part A: Polym. Chem.* 2006, 44, 427-442.
7. Trommsdorff, E.; Köhle, H.; Lagally, P. *Makromol. Chem.* 1947, 1, 169-198.
8. Norrish, R. G. W.; Smith, R. R. *Nature* 1942, 150, 336-337.
9. Calitz, F. M.; Tonge, M. P.; Sanderson, R. D. *Macromolecules* 2003, 36, 5-8.
10. Lovestead, T. M.; Berchtold, K. A.; Bowman, C. N. *Macromolecules* 2005, 38, 6374-6381.
11. Moad, G.; Solomon, D. H., *The Chemistry of Free Radical Polymerization*, Second ed.; Elsevier: Amsterdam, 2006; p 466.
12. Moad, G.; Chiefari, J.; Chong, Y.; Krstina, J.; Mayadunne, R. T.; Postma, A.; Rizzardo, E.; Thang, S. H. *Polym. Int.* 2000, 49, 993-1001.
13. Chong, Y. K. B.; Krstina, J.; Le, T. P. T.; Moad, G.; Postma, A.; Rizzardo, E.; Thang, S. H. *Macromolecules* 2003, 36, 2256-2272.
14. Arita, T.; Buback, M.; Vana, P. *Macromolecules* 2005, 38, 7935-7943.

Chapter 5:

Stereo-Controlled (RAFT) Mediated Polymerization of Methyl Methacrylate

Abstract

The preparation of stereoregular polymers is of prime interest in advanced polymer synthesis. The stereo-controlled polymerization of methyl methacrylate mediated by 2-cyano-2-propyl dithiobenzoate was investigated at four different temperatures 60, 30, 4 and –18 °C, and in three different solvents, 2-propanol, toluene and 1,1,1,3,3,3-hexafluoro-2-propanol. The initiator systems were varied according to the temperature used. Higher temperature reactions were initiated thermally, while low temperature reactions were initiated via UV irradiation. The polymers obtained were characterized by ^{1}H-NMR spectroscopy and SEC.

5.1 Experimental

5.1.1 Materials:

The following reagents were used as received: 2-propanol 99% (KIMIX); toluene chemically pure (Saarchem); 1,1,1,3,3,3-hexafluoro-2-propanol (HFIP) = 99% (Fluka) and methanol 99.5% (KIMIX).

MMA was washed with 0.3 M potassium hydroxide solution and distilled before use. AIBN (ACROS) was recrystallized twice from methanol and dried under vacuum.

5.1.2 Thermally initiated polymerizations

MMA (4 mL, 0.0374 mol), CPDB (0.033 g, 0.1513 mmol) and AIBN (8.2 mg, 0.05 mmol) were placed in a Schlenk tube containing 16 mL of the selected solvent (2-propanol, toluene, or HFIP). The tube and its contents were deoxygenated by four successive freeze-pump-thaw cycles and sealed under nitrogen (99.9%). The tube was then immersed in a preheated silicone oil bath at 60 °C. The polymerization was thermally initiated and then carried out for 24 h in each solvent system. The reaction products were precipitated in large excess of methanol, and the polymers obtained were isolated by filtration and then drying in a vacuum oven at 55 °C for 72–96 h.

5.1.3 UV initiated polymerizations

The UV polymerization reactions were initiated using a 450 W mercury vapor lamp (H33CD-400 Sylvania brand). All polymerization reactions were conducted in quartz tubes and sealed with a rubber septum. The reagents used in each polymerization system are listed in Table 5.1. Before starting the reaction, the tubes were deoxygenated by purging the system with dry N_2 gas, as shown in Figure 5.1. The tubes were placed in an ice bath (salt & ice system) at –15 °C and then purged with N_2. The use of an ice bath is essential to prevent monomer and solvent loss during the purging process because of the small quantity of monomer used.

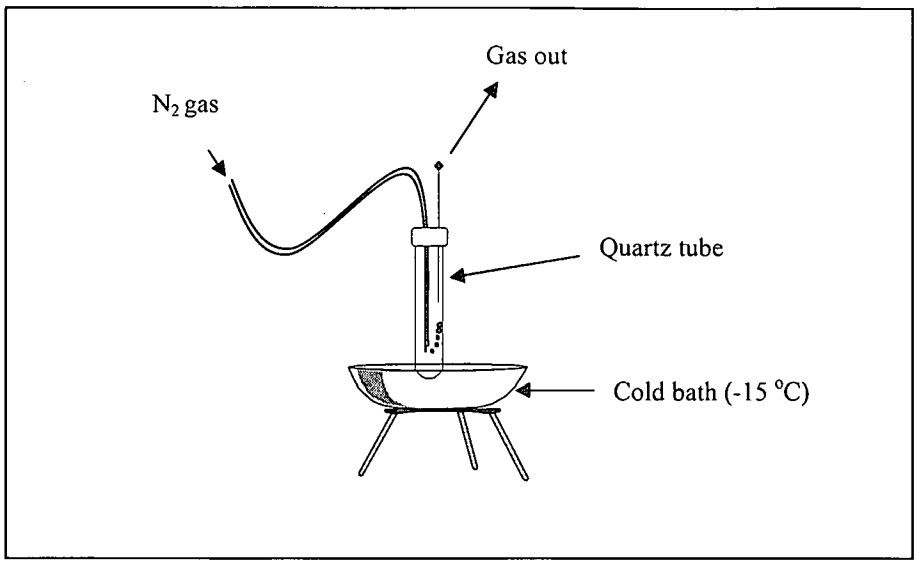

Figure 5.1: Schematic representation of the tube deoxygenation process.

Table 5.1: The reagents and conditions used for the UV-initiated polymerization systems

Temperature (°C)	Reagent	Mass (g)	Moles	Volume (mL)
30	*CPDB*	0.0167	7.55×10^{-5}	-
	AIBN	0.0100	6.0×10^{-5}	-
	MMA	1.8700	18.7×10^{-3}	2
	2-propanol , *toluene, HFIP*	-	-	8
4	*CPDB*	0.0200	9.0×10^{-5}	-
	AIBN	0.0138	8.4×10^{-5}	-
	MMA	1.8720	18.7×10^{-3}	2
	2-propanol , *toluene, HFIP*	-	-	8
−18	*CPDB*	0.0102	4.63×10^{-5}	-
	AIBN	0.0100	6.0×10^{-5}	-
	MMA	0.9360	93.6×10^{-3}	1
	2-propanol , *toluene, HFIP*	-	-	4

5.1.4 Analysis

The ^{1}H-NMR spectra of the prepared PMMAs were recorded on a Varian Unity Inova 400MHz NMR spectrometer with a 5 mm dual broadband PFG probe. All samples were run at 50 °C. The triad tacticity (see Figure 5.2) of the polymers obtained was determined on the basis of the peaks of the α–methyl group in the ^{1}H-NMR spectra. The number average molecular weight ($\bar{M}_n$) and polydispersity index ($\bar{M}_w/\bar{M}_n$) of the polymers obtained were determined by (SEC; Instrument specifications are discussed in Section 4.3).

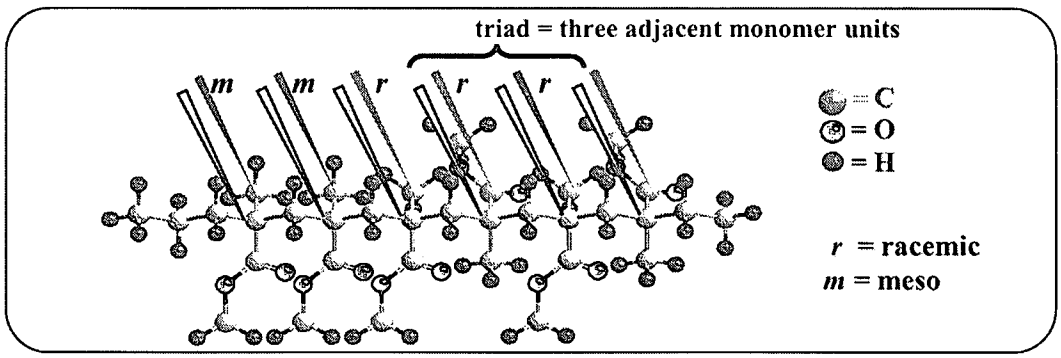

Figure 5.2: Representation of a tactic PMMA chain and the configurations of the substituents (methyl and ester groups).

5.2 Results and discussion

The polymerization of MMA was carried out in 2-propanol, toluene and HFIP at four different temperatures (60, 30, 4, –18 °C) in order to examine the effect of both the solvent and temperature on the tacticity of the synthesized polymers.

Previous studies[1,2] have reported that the polymerization of MMA in fluoroalcohols, including HFIP, resulted in significant enhancement of the syndioselectivity, especially at low temperatures (i.e. increase in the *rr* content). It was proposed[1] that the probable interaction between the polar and bulky fluoroalcohol with the monomer (through hydrogen bonding of the carbonyl group with the OH group of the alcohol) could affect the monomer addition mechanism (see Scheme 5.1). it is believed that the monomer and the growing species become effectively bulkier than the original size because of the hydrogen-bonding of the alcohol.

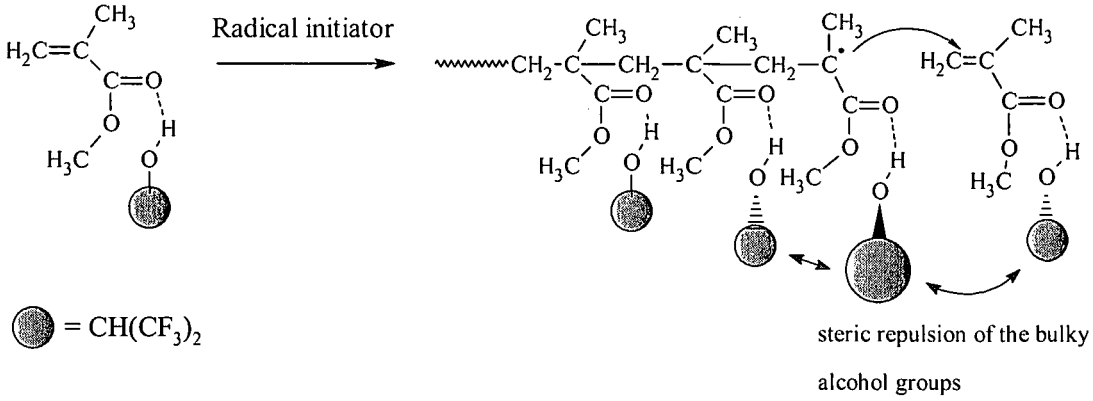

Scheme 5.1: Syndioselective radical polymerization of MMA in HFIP.

Recently Berkessel *et al.*[3] reported that the enhancement of the hydrogen bond donor ability of the HFIP arises from the aggregation of HFIP molecular units rather than just a single molecule. They found that the strength of the H-bond donor ability depends on the conformation along the C-O bond of the monomeric alcohol, where dimerization and trimerization (Figure 5.3) showed a significant effect on the potential to form H-bonds with highly covalent character.[3] This however could affect the addition of the monomer to the growing species, because of the large steric effects in the propagation mechanism. Such clusters of bulky alcohols might create a suitable conformation that could favor syndiotactic monomer addition.[1]

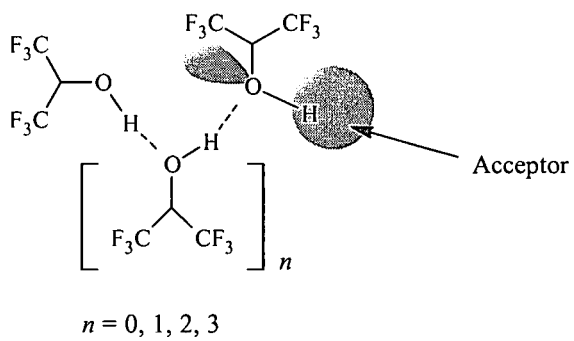

Figure 5.3: Aggregation-induced H-bonding of HFIP according to Berkessel *et al.*[3]

For this study, some of the polymerization conditions selected were similar to those used by Miura *et al.*[4,5]; namely the ratio of solvent to monomer and the type of solvents used.

The aim was to investigate the simultaneous control over the tacticity and molecular weight, and Miura *et al.*[4] had found that utilizing a solvent to monomer ratio of 4:1

yielded optimal results in terms of tacticity and molecular weight control of MMA polymerization in HFIP via an ATRP process.

It has been reported[1,2] that AIBN was used as an initiator (or photoinitiator) in the stereocontrolled polymerization of MMA in different solvents, including HFIP, toluene, and 2-propanol, but only at temperatures above 0 °C. At lower temperatures, an ionic initiation system in the presence of tri-*n*-butylborane [$(n\text{-}Bu)_3B$] was used. In the present study, the initiator used for all RAFT-mediated polymerization reactions was AIBN. The concentration of AIBN was varied according to the polymerization temperature. It was increased as the selected polymerization temperature decreased. The reason for the increase was to provide sufficient radical flux during the reaction, since the initiator efficiency of AIBN is a function of temperature, especially under UV radiation.[6] The efficiency of the initiator may decrease as a result of the loss of radicals through self-reaction within the solvent cage[6,7] (see Sections 2.2.1.1 and 2.2.1.3) and a decrease in the dissociation rate.

Also, it has been shown that the rate of radical generation and efficiency depends mainly on the structure of the initiator.[8] This is attributed to the isomerization process that may occur in the presence of light. It has been proposed by Engel[9] that the main light-induced reaction of dialkyldiazenes (Scheme 5.1) (azo-compounds) is a *trans-cis* isomerization, and the subsequent dissociation to radicals and N_2 is then a thermal reaction of the *cis*-isomer.

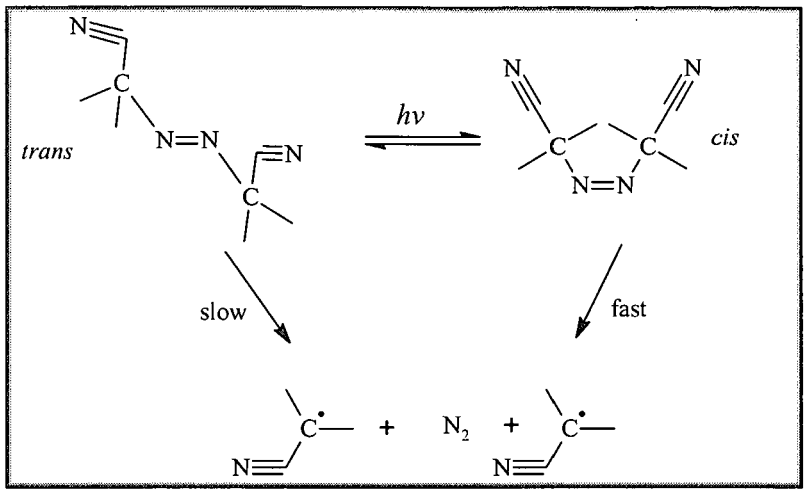

Scheme 5.2: Proposed isomerization and dissociation reactions of AIBN under UV radiation.

Thus, it can be expected that the polymerization reactions performed in this study might suffer from some mechanistic complexity in terms of the initiation process, because of utilizing the full wavelength (λ) range of the UV lamp, which could significantly affect the initiation mechanism. There are several factors that play an appreciable role on the polymerization mechanism, including the type of solvent, polarity and the polymerization temperature.[10-13]

The complexity with regard to the initiation process can be directly linked to the radical sources that can be released either from the initiator AIBN, or from the possible degradation of the RAFT agent through C-S bond cleavage,[14] and the termination or side reactions of radicals that take place.

5.2.1 Characterization results

The polymers obtained were characterized by ^{1}H-NMR and SEC. There was a significant difference in the characteristics of the polymer obtained as a function of the solvent system for the reactions. The reaction conditions used and the results of all polymerization systems are listed in Table 5.2.

Table 5.2: Characterization of products of RAFT-mediated polymerization of MMA carried out under various reaction conditions.

Reaction	T (°C)	Solvent	Time (h)	Conversion (%)	$\bar{M}_n$	$\bar{M}_w/\bar{M}_n$	Tacticity
							mm/mr/rr
1		toluene		16	15	1.13	~2/34/64
2	60	2-propanol	24	17	16	1.18	~2/33/65
3		HFIP		18.5	17	1.12	~2/33/65
4		toluene		17	15	1.45	~2/30/68
5	30	2-propanol	24	21	18	1.38	~2/30/68
6		HFIP		13	13	1.28	~2/29/69
7		toluene		16	14	1.5	~1/30/69
8	4	2-propanol	65	23	27	1.62	~2/31/67
9		HFIP		16.5	24	1.16	~1/26/72
10		toluene		16	18	1.77	~1/26/73
11	−18	2-propanol	65	15	21	1.45	~3/30/67
12		HFIP		16	18	1.32	~1/24/75

The ^{1}H-NMR results showed that the tacticity of the polymers was dependent on the polymerization temperature. Figure 5.4 shows the ^{1}H-NMR spectra overlays, normalized based on the α–methyl group, representing the syndiotactic triads of the polymers obtained in HFIP. The estimated percentage of the *rr* content was determined based on the relative integration values for each of the peaks (*mm*, *rm* and *rr*). Care was required to apply consistently the integration with respect to each peak in terms of the actual area under the peak and the base line.

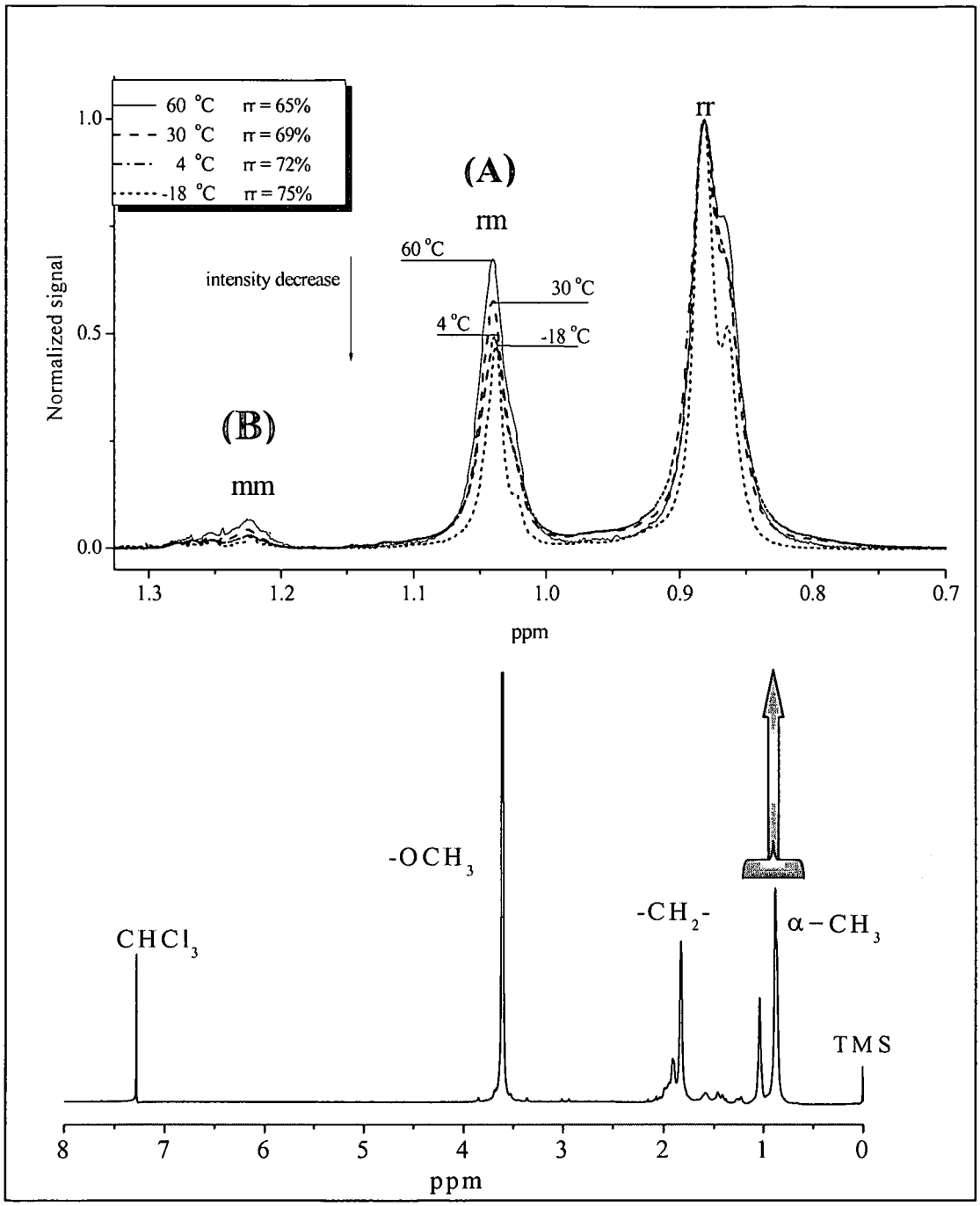

Figure 5.4: ^{1}H-NMR spectrum of PMMA prepared by RAFT-mediated polymerization in HFIP at 4 °C initiated by UV irradiation, and ^{1}H-NMR spectra overlays of PMMA in HFIP at different temperatures. (Conditions: 400 MHz, $CDCl_3$ and 50 °C)

Figure 5.4 shows that as the temperature decreased there was a corresponding decrease in the intensity of the labeled peaks A and B. These peaks correspond to the triads of *rm* and *mm* specificity respectively[1]. This indicates that the *rr* content increases with decreasing the polymerization temperature and was only observed in HFIP and toluene. The estimated *rr* content was the highest in HFIP (*rr* ~75%) at –18 °C. When 2-propanol was used as solvent tacticity peaks A and B did not show a significant decreasing trend with

decreasing temperature. This observation was similar to previously reported results of Isobe *et al.*[1] However, they used conventional radical polymerization which resulted in polymers with broad molecular weight distributions.

Although the primary aim of the study reported in this chapter was to investigate the solvent effects in achieving control over the molecular weight and tacticity via RAFT-mediated polymerization, SEC results showed that molecular weight distributions varied according to the initiation system, polymerization temperature and type of solvent used.

5.2.1.1 Molecular weight distribution of PMMAs as determined by SEC

Figure 5.5 presents the PDI values of the obtained polymers in different solvents versus polymerization temperature. The polymers obtained in HFIP had the lowest PDI values, at all temperatures; they were below 1.4, while in the other solvent systems (2-propanol and toluene), broader distributions were recorded, as PDI values increased at lower polymerization temperatures.

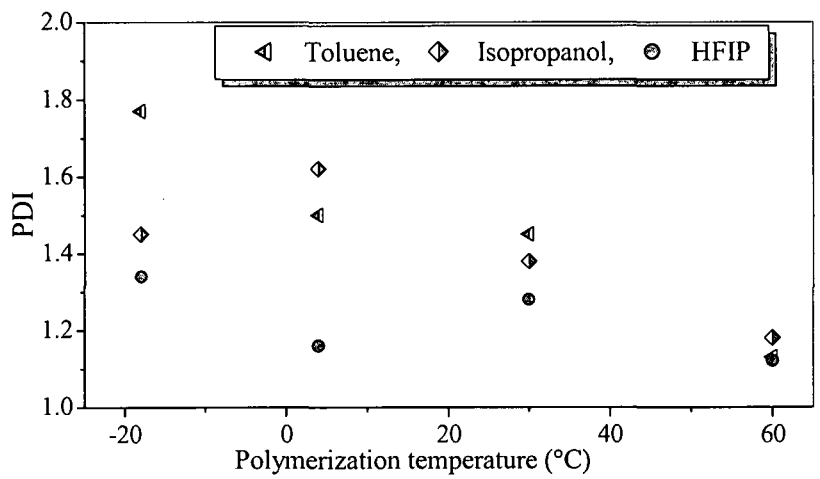

Figure 5.5: Plot of the polydispersities of PMMA obtained in various solvents versus the polymerization temperature.

The relative increase in the polydispersity of the polymers produced is attributed to several factors including radical side reactions, solvent polarity, polymerization temperature and the type of solvent used.

No effect of solvent on tacticity was observed for polymers that were produced at 60 °C, but narrow polydispersities were observed, indicating the fact that the RAFT-mediated polymerization process was operative and functioning efficiently. This finding is considered an improvement on previously reported results by Isobe *et al.*[1] for

conventional MMA polymerization, in terms of better control over the molecular weight distribution. They showed that although the syndioselectivity was significantly enhanced, especially in fluoroalcohols, the polymers obtained had high polydispersities, which increased drastically as the polymerization temperature decreased in all solvent systems, including toluene, 2-propanol and HFIP.

However, in this study the polymerization reactions conducted in all solvents, yielded only low conversions (slower reaction rates) when compared to previous non-living polymerizations.[1] This was expected since the presence of a RAFT agent, such as CPDB in the reaction will retard the polymerization rate through the reversible addition-fragmentation mechanism (described in Section 2.3.3.1).

The low conversions of the PMMA obtained at 60 °C might be attributed to the retardation caused by the stability of the intermediate radicals **4** (Scheme 2.11) in the system, i.e. if the intermediate radicals are well stabilized then the overall intermediate radical concentration increases in the system, promoting the reaction of these radicals with other radicals in the system.[15] Alternatively, the long intermediate radical lifetimes simply reduce the propagating radical concentration (only in the pre-equilibrium state), leading to a retardation of rate.[15-18]

The interaction of each specific solvent with the MMA monomer is possible, as discussed in Section 5.2, however, the interaction of the OH group of the alcohols with the thiocarbonyl group of the RAFT agent is also possible, and should be specifically considered in the case of the HFIP polymerization systems. As HFIP has a significant H-bond donor ability, it might affect the RAFT mechanism, as the radical attack on the C=S group could be hindered due to hydrogen bonding of the alcohol with both MMA monomer and the RAFT agent.

UV-initiated polymerization systems may suffer from inherent complexity in the presence of a RAFT agent. Although UV radiation was implemented in order to accelerate the decomposition of AIBN at lower temperatures; it may also lead to cleavage of the C-S bond of the CPDB RAFT agent.[14]

As the primary aim of the study reported in this chapter was to investigate solvent effects on the tacticity and molecular weight control in the polymerizations, a detailed study of the degradation of the RAFT agents under UV irradiation was not conducted.

The behavior of RAFT reactions initiated by UV irradiation, which in essence rely on the release of the initial radicals through an addition-fragmentation chain transfer process, could be complicated by the differences in the initiating species generated. For example, the UV radiation can create initiating species from the photoinitiator, the RAFT agent and various other constituents in the reaction mixture. However, regardless of whether radicals are generated by the cleavage of the C-S bond of the RAFT agent or by any other bond breaking reaction, it is expected that some radicals will add to the thiocarbonyl group of CPDB, as in a conventional RAFT polymerization.

However, it is also important to consider that different types of radical species can significantly affect the reaction mechanism. Nevertheless, the complications can be reduced if appropriate selection of the RAFT agent and initiator are made, and a specific UV wavelength is applied.[19]

The use of a novel combination of a specific photoinitiator which is active at a relatively long UV wavelength was described by Lu *et al.*[20] They showed that the controlled RAFT mediated polymerization of (MA) at ambient temperature was possible when using trimethylbenzoyl diphenylphosphine oxide (TPO) and initiating with UV radiation at λ = 365 nm. However, although this strategy was fairly successful from the reported results, the RAFT agent still suffered from degradation after a long period of exposure to UV light.

Thus, using UV radiation to generate radicals in a RAFT-mediated polymerization can have a significant effect on the reaction if appropriate conditions and reagents are not chosen. The RAFT process will nonetheless still occur,[14,19] with the radicals still adding to the thiocarbonyl groups of RAFT agents that are not affected by the irradiation.

In order to examine whether the prepared polymer chains have the RAFT end-group moieties, SEC analysis was performed on the polymer products. A UV detector in conjunction with a standard RI detector was used. The RI detector is simply a concentration sensitive detector that measures the difference in the RI between the eluent on the reference side and the sample plus the eluent in the sample side (here the eluent was THF for all samples).

As the UV detector is sensitive to certain chromophores at specific wavelengths, it was used to detect the dithiocarbonate moiety at a wavelength of 320nm.[21,22] If the RAFT group is present in the polymer chain, then a signal will be observed at this wavelength.

5.2.1.2 UV/RI overlays of PMMAs as determined by SEC

Plotting the UV/RI signal overlays provides useful information with respect to the distribution of the dithiocarbonate functionality in the polymer chain and whether it is homogenously or heterogeneously distributed throughout the molecular weight distribution. As an example, the UV/RI trace for the PMMA prepared in HFIP at 60 °C is shown in Figure 5.6. Both UV and RI signals were normalized. However, in order to make the signals comparable, before normalization, the UV signal was multiplied by a factor of *M* (molecular weight) while processing the data from the SEC results, i.e. since the RI detector is concentration based, the intensity of the signal will be sensitive to the molecular weight of the polymer chains. In contrast, the UV detector is sensitive only to a single chromophore (in this case the dithiocarbonate moiety) per polymer chain at 320 nm if present.

The overlaid RI/UV signals in Figure 5.6 match very closely, indicating that most of the chains have a terminal RAFT moiety, and that the thiocarbonyl thio functionality is homogeneously distributed along the molar mass distribution.

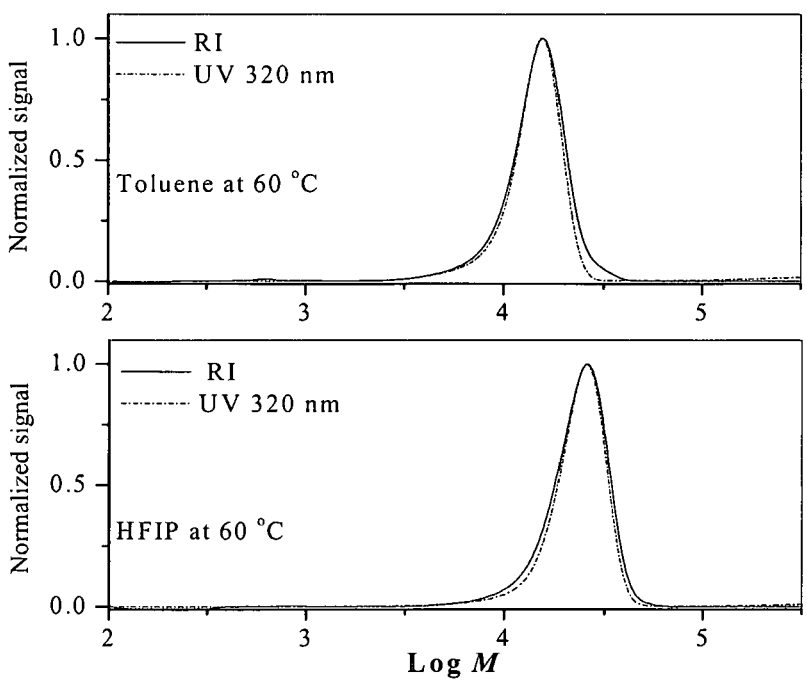

Figure 5.6: RI/UV overlays of SEC traces for PMMA mediated by CPDB at 60 °C after 24 h; [AIBN] = 2.52 mmol L^{-1}, [CPDB] = 7.55 mmol L^{-1}; [MMA]/[HFIP] = 1/4.

Similar results were also observed for PMMA prepared in 2-propanol and toluene at 60 °C. However, the UV/RI traces for the polymers obtained via UV initiation at all temperatures used (30, 4, and –18 °C) showed slightly different responses in terms of the

molecular weight distributions and the homogeneity of the RAFT end group functionality along the polymer chain, and varied according to the solvent used.

Figure 5.7 shows the UV/RI traces for the polymers obtained at 30 °C in different solvents. The UV/RI traces overlay fairly well in the case of HFIP and toluene systems, in contrast to the 2-propanol system, where the UV signal is not overlaid throughout the molecular weight distribution curve. The absence of UV signal in the high molecular weight region implies that this part of the distribution does not possess the terminal RAFT moiety.

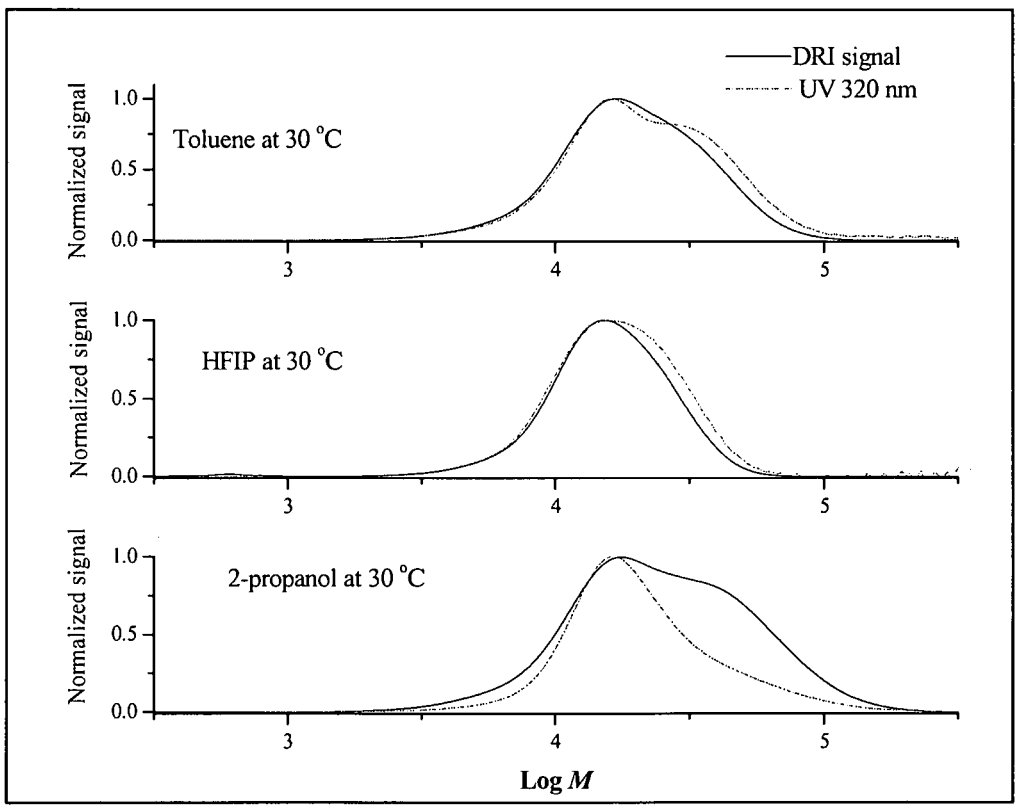

Figure 5.7: RI/UV overlays of SEC traces for PMMA mediated by CPDB at 30 °C after 24 h; [AIBN] = 6.06 mmol L^{-1}, [CPDB] = 7.55 mmol L^{-1}; [MMA]/[solvent] = 1/4.

The following observations possibly contributed to the molar mass distributions that were obtained in the polymerization:

Firstly–the polymerization reaction in 2-propanol became turbid after a conversion of a few percent. The heterogeneity was most likely caused by precipitation of polymer because of the poor solvent properties of 2-propanol at the reaction temperatures ≤ 30 °C. The heterogeneity caused by the solubility problem would have dramatic effects on the polymerization mechanism.

A possible consequence of precipitation is that as the polymerization proceeds so the polymer chains grow, and at a certain molecular weight these chains become insoluble and start to precipitate out of solution. Here there are two possible chain types: either the chain is controlled and possesses the RAFT moiety, or the chain grows in an uncontrolled manner in a heterogeneous dispersion polymerization system. The uncontrolled chains could be the result of chain transfer reactions in the polymerization process, as the hydrogen in the OH group of 2-propanol is liable to chain transfer.[23]

In Figure 5.7, the RI signal clearly shows a bimodal distribution. This indicates the presence of a heterogeneous polymer material. Furthermore, monitoring the UV/RI overlaid signal of the same system indicates that a large amount of polymer chains do not contain the RAFT moiety, especially at the higher molecular weight region where the distinctive shoulder appears. It should also be noticed that the RI and UV signals were arbitrarily normalized, which implies that if there is significant degradation of the RAFT agent, the actual distribution curve of the UV should be lower than it appears.
The above speculation suggests that the shoulder in the high molecular weight region consists largely of uncontrolled PMMA chains that grew faster than the RAFT-mediated systems. Furthermore, the bimodality in the case of the 2-propanol system might be attributed to a phase separation, caused by significant transfer reactions occurring during the polymerization the process.

Secondly–the possible degradation of the dithioester moieties with time should be considered. There is evidence of the loss of the RAFT moieties during polymerization as a result of side reactions, as indicated by the loss of the characteristic color (light red) of the polymer. In the case of the reaction in 2-propanol a white suspension was obtained, while the reactions conducted in both toluene and HFIP provided clear solutions, indicating that a major part of the chromophoric dithioester moiety was destroyed. The loss of dithioester functionality would account for the broadening of the molecular weight distribution. Without RAFT agent in the late stages of the polymerization, the polymerization that occurs will be induced by the presence of monomer and radicals created mainly from the photodecomposition of AIBN, and thus uncontrolled polymerization would proceed, and large molecular weights can be expected.

The loss of the dithioester functionality, however, is not directly indicated from the overlays in Figure 5.7 as it is normalized arbitrarily. When looking more closely at these curves it can be seen that the UV curves sometimes exceed the RI curve which is

rationally not valid in the current case. It is very difficult to assume the presence of more than one RAFT moiety per chain in this type of reaction under UV, but the overlays still provide information of the overall distribution of the RAFT functionality throughout the molecular weight distribution curve.

It is thus more likely that there is a significant amount of RAFT degradation, and initiating complexities occurring in the process due to UV radiation that could have significantly affected the polymerization mechanism.

In comparison to the RI/UV overlays of the obtained polymers and with respect to the solvent and the temperature, the use of HFIP gave the best results in terms of the molecular weight distributions and the homogeneity of the RAFT end group functionality throughout the molecular weight distribution curve. Similar results were observed at all polymerization temperatures when polymerizing in HFIP. See Figures 5.8 and 5.9.

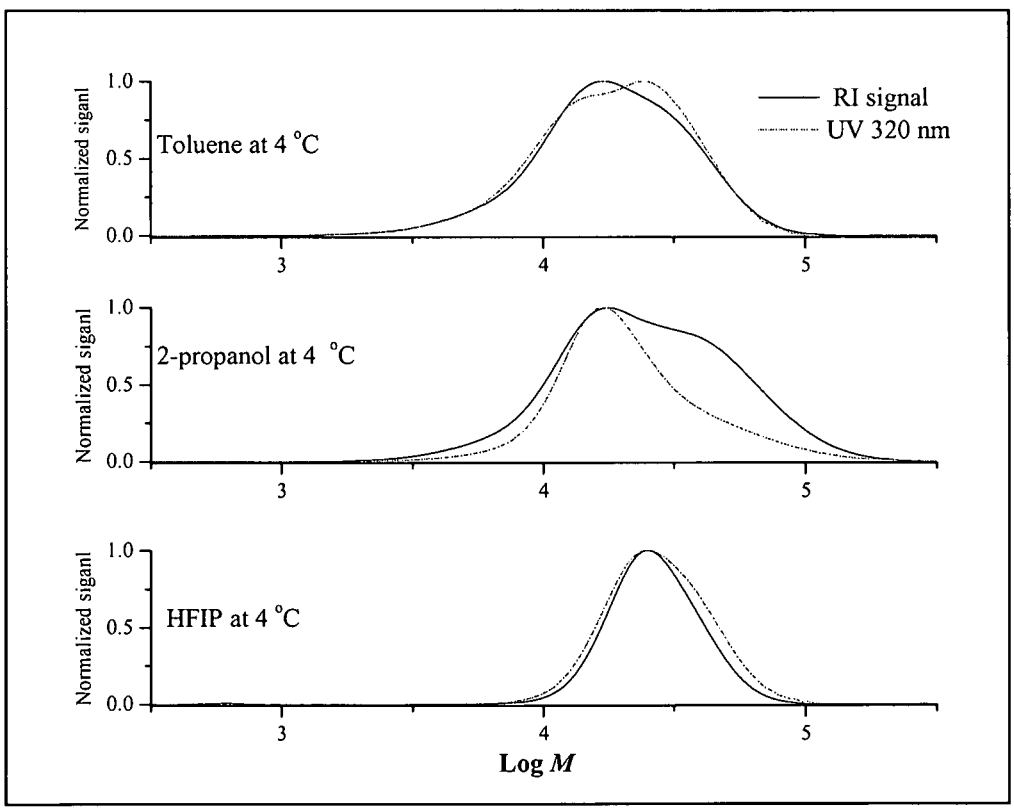

Figure 5.8: RI/UV overlays of SEC traces for PMMA mediated by CPDB at 4 °C after 65 h. [AIBN] = 8.40 mmol L^{-1}, [CPDB] = 9.46 mmol L^{-1}.

Polymers that were obtained in toluene also gave similar results in terms of the homogeneous distribution of the RAFT functionality, but a marked increase in the polydispersity indices was observed. Finally, 2-propanol proved to be a poor solvent for MMA polymerization at low temperatures as it displayed the broadest molecular weight

distributions at all temperatures, compared to toluene and HFIP. Except at –18 °C, the polydispersity value was the highest in toluene. The development of a heterogeneous mixture during the polymerization reaction at temperatures below 60 °C had a major effect on the polymerization system, especially when using UV irradiation as the initiation strategy, which also played a significant role in determining the living character of the obtained polymers, as indicated by the UV/RI overlays.

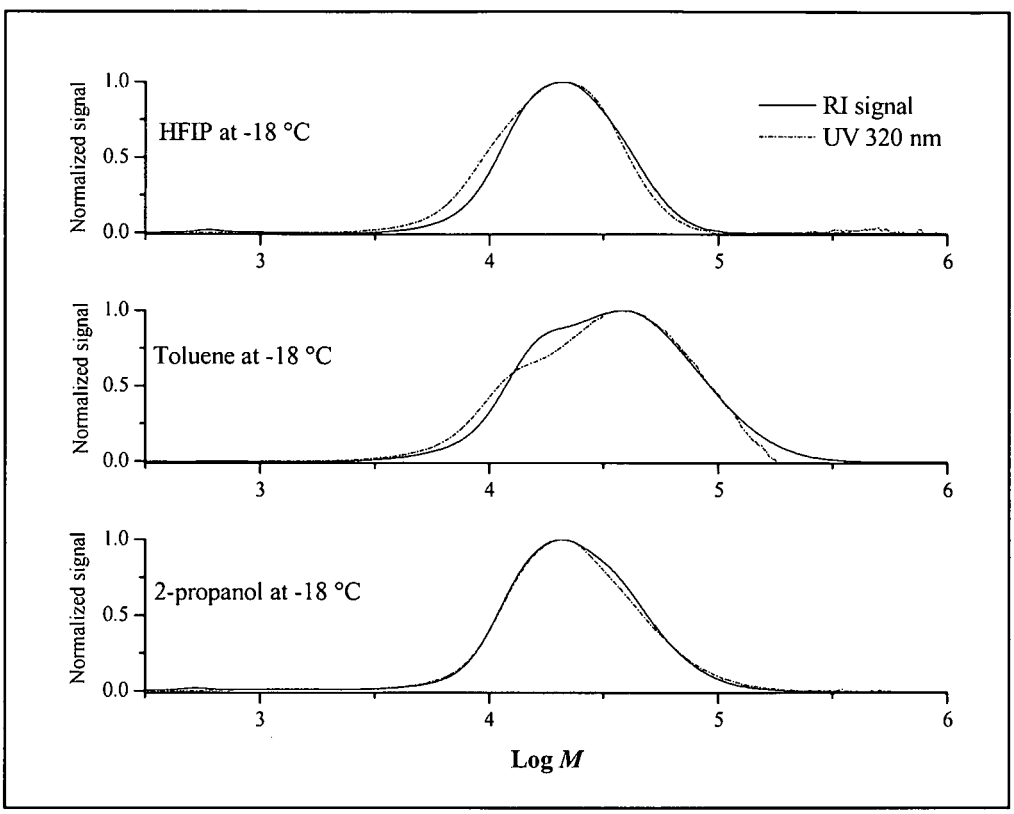

Figure 5.9: RI/UV overlays of SEC traces for PMMA mediated by CPDB at –18 °C after 65 h. [AIBN] = 12.0 mmol L^{-1}, [CPDB] = 9.25 mmol L^{-1}.

In Figure 5.9, a bimodal distribution was observed for the toluene system; and the UV/RI overlays are not homogeneously distributed along the molecular weight distribution curve. The first shoulder at about ~4.2 of the log *M* scale indicates the presence of significant amount of polymer chains not possessing the RAFT moiety. As mentioned earlier, the actual height of the UV signal in this case should be less than that of the RI, and since the UV/RI peak heights match at ~4.6, it thus appears that there is a fraction at lower molecular weight that has less UV signal than RI signal, indicating low concentration of the RAFT moiety in this region. The bimodality of the UV signal might be attributed to terminated chains resulting from the degradation of the RAFT functionality at the chains ends, or uncontrolled PMMA chains that terminated rapidly

before becoming involved in the RAFT-mediated reaction, or more importantly, chain transfer reactions that can terminate a propagating chain and start another chain growth.

However, the stereocontrol achieved over molecular weight and tacticity in HFIP at -18 °C corresponds to the findings of Miura *et al.*[4] They utilized the ATRP technique to achieve stereo-controlled polymerization of MMA in different solvents, including HFIP and toluene. In their results, the PDI value of the PMMA obtained in HFIP was 1.17 and the *rr* triad content was 75% at –20 °C, compared to a PDI of 1.31 and *rr* triad content of 75% achieved via RAFT-mediated polymerization. On the other hand, in comparison, the PMMA obtained via RAFT-mediated polymerization in toluene gave enhanced molecular weight control, e.g. the PDI of the PMMA via ATRP at 30 and –20 °C was 1.83 and 3.25 respectively, while in this study the PDI results at 30 and –18 °C were 1.45 and 1.77, respectively.

Isobe *et al.*[1] have investigated the uncontrolled free radical polymerization of MMA in different solvents, including fluoroalcohols, toluene, methanol and 2-propanol, and their effect on the tacticity of PMMA. They found that the *rr* content of PMMA increased with decreasing polymerization temperature in most of the solvents. However, the fluoroalcohols did show a significant improvement in the syndioselectivity, especially below –40 °C. In addition, the fluoroalcohols gave better yields and high molecular weights, even at temperatures as low as –78 °C, but in all cases the polydispersity increased drastically with decreasing polymerization temperature. An example of the PMMAs obtained[1] in toluene and HFIP are as follows: Toluene at 60°C, *rr* 64% and PDI 1.4; at 20 °C, *rr* 69%, PDI =1.57; at –40 °C, *rr* = 76% and PDI = 2.01 (low yield); HFIP at 60 °C, *rr* 65% and PDI 1.41; at 20 °C, *rr* 71% and PDI 1.45; at –40 °C, *rr* 79% and PDI 1.52.

5.3 Conclusions

Simultaneous control of the molecular weight and stereochemistry of PMMA has been accomplished with a RAFT-mediated polymerization system using CPDB as RAFT agent in HFIP, and AIBN as the initiator at low temperature. The synthesis of well-defined and stereoregulated PMMA via the RAFT process was achieved. HFIP solvent produced the best results in terms of syndioselectivity improvement and molecular weight control. The enhancement of the *rr* content was not very significant when compared to the toluene system, especially at –18 °C where the *rr* content was 75% in HFIP and 73% in toluene,

but better control was achieved in HFIP as the PDI value was 1.32 compared to 1.77 in toluene.

Although the UV-induced polymerization reactions were performed using a full wavelength range of the UV lamp, the results showed that RAFT-mediated polymerization was still operative, but associated with mechanistic complexities because of the initiating radical species generated in the reaction and the degradation of the RAFT agent.

The degradation of RAFT agent is believed to be significant and was feasible in relation to the loss of colour in the polymer solution obtained, as the cumulative UV dose increased with time.

2-propanol was a poor solvent for MMA polymerization and caused precipitation of the polymer formed at low temperature, resulting in poor control of the molecular weight.

5.4 References

1. Isobe, Y.; Yamada, K.; Nakano, T.; Okamoto, Y. *J. Polym. Sci., Part A: Polym. Chem.* 2000, 38, (Suppl.), 4693-4703.

2. Isobe, Y.; Yamada, K.; Nakano, T.; Okamoto, Y. *Macromolecules* 1999, 32, 5979-5981.

3. Berkessel, A.; Adrio, J. A.; Huettenhain, D.; Neudoerfl, J. M. *J. Am. Chem. Soc.* 2006, 128, 8421-8426.

4. Miura, Y.; Satoh, T.; Narumi, A.; Nishizawa, O.; Okamoto, Y.; Kakuchi, T. *Macromolecules* 2005, 38, 1041-1043.

5. Miura, Y.; Satoh, T.; Narumi, A.; Nishizawa, O.; Okamoto, Y. *J. Polym. Sci., Part A: Polym. Chem.* 2006, 44, 1436-1446.

6. Jaffe, A. B.; Skinner, K. J.; McBride, J. M. *J. Am. Chem. Soc.* 1972, 94, 8510-8515.

7. Hammond, G. S.; Wu, C.-H. S.; Trapp, O. D.; Warkentin, J.; Keys, R. T. *J. Am. Chem. Soc.* 1960, 82, 5394-5399.

8. Moad, G.; Solomon, D. H., *The Chemistry of Free Radical Polymerization*, Second ed.; Elsevier: Amsterdam, 2006; p 74.

9. Engel, P. S. *Chem. Rev.* 1980, 80, 99-150.

10. Czerwinski, W. K. *Macromolecules* 1995, 28, 5405-5410.

11. Czerwinski, W. K. *Makromol. Chem.* 1993, 194, 3015-3029.

12. Czerwinski, W. K. *Macromolecules* 1995, 28, 5411-5418.

13. Coote, M. L.; Davis, T. P. Solvent effects on free radical polymerization. In: *Handbook of Solvents*, Wypych, G., Ed. William Andrew Publishing: Norwich, NY, 2001; pp 777-797.

14. Quinn, J. F.; Barner, L.; Barner-Kowollik, C.; Rizzardo, E.; Davis, T. P. *Macromolecules* 2002, 35, 7620-7627.

15. Benaglia, M.; Rizzardo, E.; Alberti, A.; Guerra, M. *Macromolecules* 2005, 38, 3129-3140.

16. Coote, M. L.; Radom, L. *J. Am. Chem. Soc.* 2003, 125, 1490-1491.

17. Feldermann, A.; Coote, M. L.; Stenzel, M. H.; Davis, T. P.; Barner-Kowollik, C. *J. Am. Chem. Soc.* 2004, 126, 15915-15923.

18. Perrier, S.; Barner-Kowollik, C.; Quinn, J. F.; Vana, P.; Davis, T. P. *Macromolecules* 2002, 35, 8300-8306.

19. Lu, L.; Zhang, H.; Yang, N.; Cai, Y. *Macromolecules* 2006, 39, 3770-3776.

20. Lu, L.; Yang, N.; Cai, Y. *Chem. Comm.* 2005, 42, 5287-5288.

21. Russum, J. P.; Jones, C. W.; Schork, F. J. *Macromol. Rapid Comm.* 2004, 25, 1064-1068.

22. Matahwa, H.; McLeary, J. B.; Sanderson, R. D. *J. Polym. Sci. Part A: Polym. Chem.* 2006, 44, 427-442.

23. Pantiru, M.; Iojoiu, C.; Hamaide, T.; Delolme, F. *Polym. Int.* 2004, 53, 506-514.

Chapter 6: Conclusions and Recommendations

General conclusions are now presented according to the sub objectives given in Chapter 1; thus the findings will be presented in two sections, with respect to the two aspects that were investigated.

6.1 Conclusions to part (1) of the study: The evaluation of thiophene as an activating group in the RAFT-mediated polymerization of styrene

1. The synthesis of the following RAFT agents was successfully carried out: three novel RAFT agents bearing a thiophene substituent as the Z group: bis(thiobenzoyl) disulfide (BBD), benzyl dithiobenzoate (BDTB), 2-cyano-2-propyl dithiobenzoate (CPDB), bis(2-thienyl thiocarbonyl)disulfide (BTD), 1-cyano-1-methylethyl 2-thiophenedithiocarboxylate (CPDT), and benzyl thiophene-2-dithiocarboxylate (BDTT). They were characterized by NMR, IR and UV/vis spectroscopy. All RAFT agents except CPDB and CPDT were prepared according to the Grignard reaction method. The other two were prepared by refluxing the selected disulfide precursor with AIBN in an organic medium. The purity of the RAFT agents was high as determined by the respective NMR spectra. They were used as such in subsequent polymerization reactions.
2. The above synthesized RAFT agents were successfully utilized as mediators for the self-initiated polymerization of styrene in bulk at 100 °C. Conversions were determined (gravimetrically) and SEC analyses were carried out.
3. The chain transfer ability of the RAFT agents to induce living characteristics in radical polymerization of styrene was investigated with respect to molar mass control and kinetic behavior. The number average molecular weight ($\bar{M}_n$) of the polystyrene samples was measured by SEC and compared with the predicted molecular weight. In all polymerization systems, the measured molecular weights were similar to the

predicted data in the early stages of the reaction, but with increasing conversion, a deviation from the predicted values was noticed. The deviation was attributed to the continuous initiation of new chains over time, which would increase the number of chains and hence lower the target $\bar{M}_n$ values. The reaction rates of all thiophene-based mediated systems were much slower than the phenyl-based-mediated systems in the order: BTD < BDTT < CPTD < BDTB < BBD < CPDB. The influence of the thiophene ring as the activating group was significant. The retardation was proposed to be as a result of the nature of the thiophene ring and its ability to provide stabilized intermediate radicals, which in turn increases the overall radical concentration in the system, and may increase the chance of termination reactions.

4. The living behavior of the thiophene-based systems was investigated and compared to the analogous phenyl-based systems. It was found that the polymerization systems mediated by the thiophene-based RAFT agents, especially CPDT and BDTT, showed reasonable control over the molecular weight and the resultant polymers had low polydispersities. The thiophene-based RAFT agents can therefore be introduced as new and efficient RAFT agents. The reaction rate of the BBD-mediated system was much faster than its analogous BTD-mediated system. The polymers obtained were also narrower with respect to molecular weight distribution. In addition, monitoring the RI/UV overlays in the SEC results showed evidence of unusual behavior of the BBD-mediated system when compared to the other RAFT-mediated system used. Thus, it was proposed that during the course of the reaction, a two-side mediated chain growth (two RAFT groups per chain) occurred. This was deduced from the RI/UV overlays of the high molecular weight shoulder associated with the main molecular weight distribution peak. The dithio compounds used in the BDTT-and CPDT-mediated systems showed adequate control and displayed the characteristics of a living system. The main difference between the thiophene- and phenyl-based RAFT agents was the reaction rates. In the case of the difference between BDTT and BDTB, control over the molecular weight was comparatively good and narrow molecular weight distributions were achieved with both systems, but a slower reaction rate was observed in the case of BDTT. The polymerizations mediated by CPDB and CPDT showed similar results in terms of molecular weight control, but significant rate retardation was observed for the CPDT-mediated reaction when compared with the CPDB-mediated reaction. However a slight increase in the

polydispersity in both systems was observed as the conversion increased. This was attributed to the possibility of termination reactions that occur in the reaction; including a bimolecular combination, short chain termination, and cross-termination reactions. The termination reactions are believed to be higher in the thiophene-based reactions since they all suffered from greater rate retardation, and, since the rate of initiation (thermally from styrene) is still relatively high, thus, the rate of termination per unit conversion is expected to be high.

6.2 Conclusions to part (2) of the study: Stereo-controlled (RAFT) mediated polymerization of methyl methacrylate

1. A series of MMA polymerizations mediated by CPDB was successfully carried out in three different solvents, namely: toluene, 2-propanol and HFIP, at four different temperatures (60, 30, 4 and –18 °C). The reactions conducted at 60 °C were initiated thermally, while the other reactions at lower temperatures were initiated via UV irradiation. This was the first attempt at the synthesis of well-defined and stereoregulated PMMA via the RAFT process.
2. All the polymers obtained were characterized by the analytical tools ^{1}H-NMR spectroscopy and SEC. The tacticity of the polymers was successfully monitored under different reaction conditions by observing the respective *rr*, *rm*, and *mm* peaks of each spectrum after being normalized on the basis of the α–methyl group representing the syndiotactic triads *rr* in the polymer chain. The $\bar{M}_n$ values and polydispersities for all the polymers prepared were recorded using SEC.
3. ^{1}H-NMR results showed that the *rr* content increased with decreasing polymerization temperature. This was observed in the case of the HFIP and toluene systems. The estimated *rr* content increased from 65% at 60 °C to 75% at –18 °C in HFIP; and from 64% at 60 °C to 73% at –18 °C in toluene. However the 2-propanol system did not show an increasing trend in the *rr* content. Thus, the syndioselectivity at –18 °C was the highest in HFIP. The living/controlled behavior was also investigated, and it was found that the control over molecular weight was achieved with narrow polydispersities. The PDI value, however, increased with decreasing polymerization temperature, especially for the UV-induced polymerization reactions at 4 and –18 °C in 2-propanol and toluene, as solvents. The best stereocontrol results were observed

in the HFIP system, which showed the highest improvement of the syndioselectivity, and attained the lowest PDI value of 1.31. This finding corresponds to previously reported observations for PMMA prepared via ATRP in HFIP (*rr* 75% and PDI 1.17; at –20 °C).

2-propanol proved to be a poor solvent for MMA polymerization, especially at lower temperatures, due to precipitation of the polymer formed during the reaction. The development of a heterogeneous phase during the reaction may have led to the poor control over the molecular weight.

6.3 Recommendations for future work

Interesting mechanistic behavior was observed from the results of the thiophene-mediated systems, including a severe rate retardation of the polymerization reaction, which is likely to be associated with a high intermediate radical concentration. Since the concentration of the RAFT agent plays a significant role in the polymerization reaction, further investigation is advised. The effect of the RAFT agent concentration of the thiophene-based compounds on the reaction mechanism, using electron spin resonance studies for monitoring the radical species in the reaction (most importantly the intermediate radicals) is recommended. Polymerization of other monomers such as meth(acrylates) in the presence of thiophene RAFT agents should also be investigated in order to examine their performances in such systems.

Targeting lower molecular weight chains in the presence of either thiophene-based or dithiobenzoate-based RAFT agents (using a lower monomer to RAFT agent concentration) would lead to a higher fraction of side reactions (especially termination reactions) and a greater number of chains. This would then enable the isolation of products through separation, using HPLC. These products could then be identified and thoroughly characterized by NMR spectroscopy and mass spectrometry. The identification of such products is very important as they could provide quantitative and qualitative information on the amount of each species and how fast each one forms. Hence, a better understanding of the reaction mechanism and the related rate retardation could be obtained.

Using a similar strategy, the mechanism of the disulfide-mediated polymerization can also be investigated by varying different factors, such as the disulfide, monomer and initiator concentrations in the reaction, and identifying the reaction products by NMR and mass spectrometry after isolating the products by HPLC. The interpretation of data provided by

these two techniques should provide greater understanding of the mechanism of RAFT-mediated polymerizations that start from disulfides.

Thiophene functionality is known to be interactive with many metals, hence the presence of the thiophene group at the end of the chain could add interesting properties to the final polymer. Therefore an investigation of the interaction of metal surfaces or metal ions with a thiophene-ended polymer chain may open doors to new possibilities in polymer composites.

It would also be interesting to investigate the ability of the thiophene RAFT moiety to transform to a macro initiator for anionic polymerization by lithiation of the thiophene group. This could lead to the production of block-copolymers, as the thiophene molecule alone has been successfully used in analogous reactions.[1]

6.4 References

1. Martinez-Castro, N.; Lanzendorfer, M. G.; Muller, A. H. E.; Cho, J. C.; Acar, M. H.; Faust, R. *Macromolecules* 2003, 36, 6985-6994.

APPENDIX

Spectroscopic results of phenyl-based RAFT agents

A-1) Bis(thiobenzoyl) disulfide (BBD):

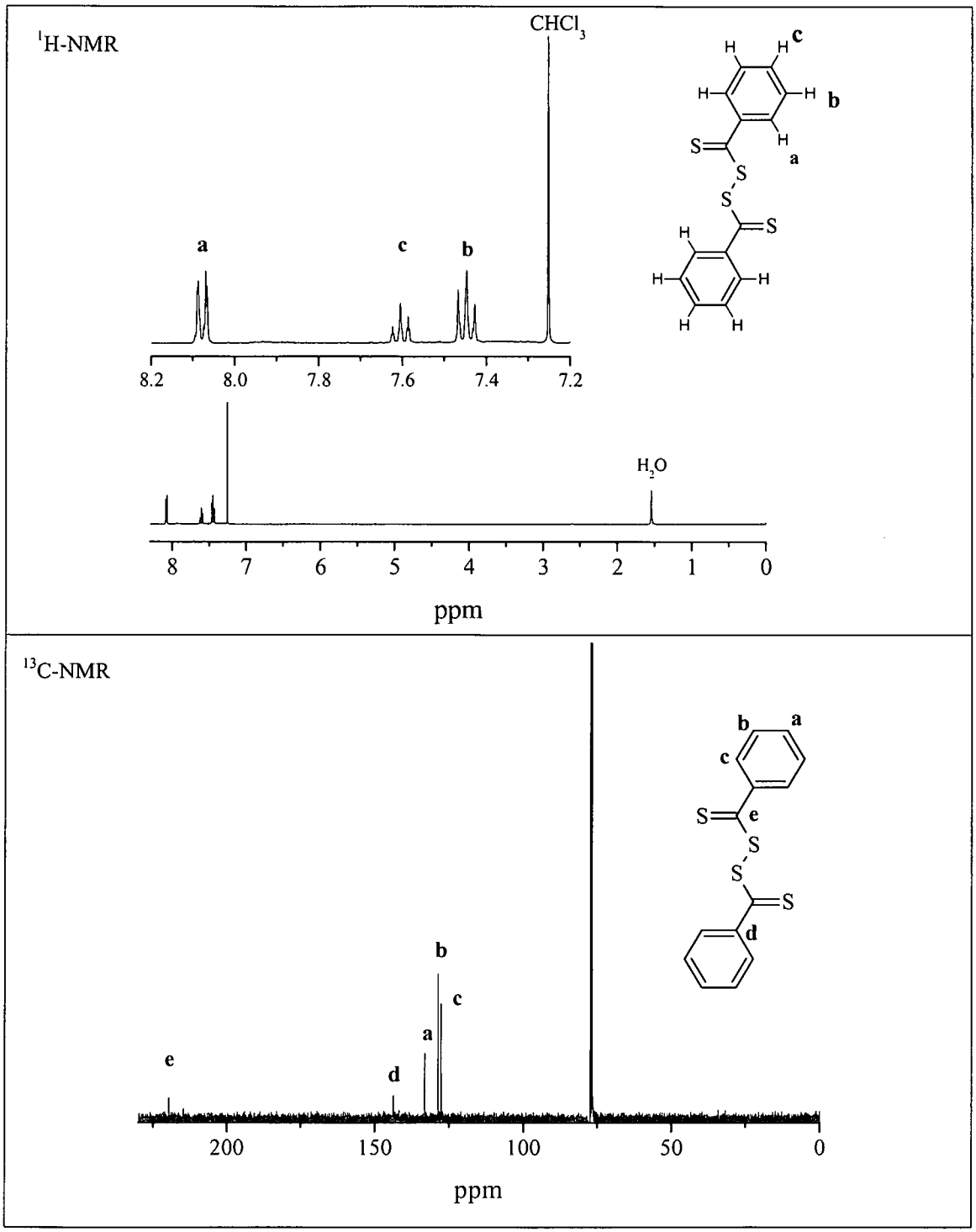

Figure A.1: ^{1}H-NMR and ^{13}C-NMR spectra of bis(thiobenzoyl) disulfide in $CDCl_3$.

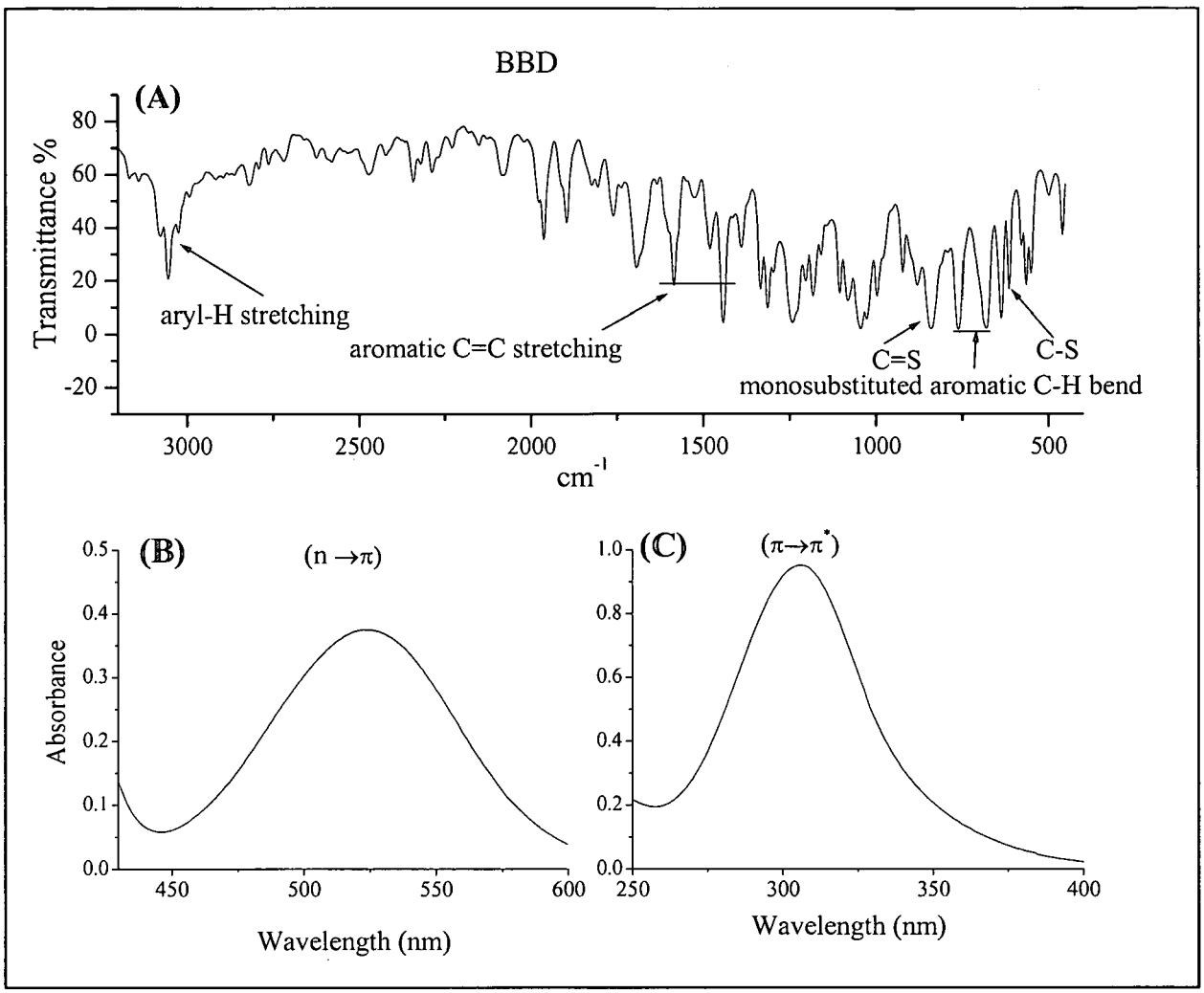

Figure A.2: (A) FT-IR spectrum of CPDT; (B and C) UV (C=S) absorption spectra of BBD.

A-2) Benzyl dithiobenzoate (BDTB):

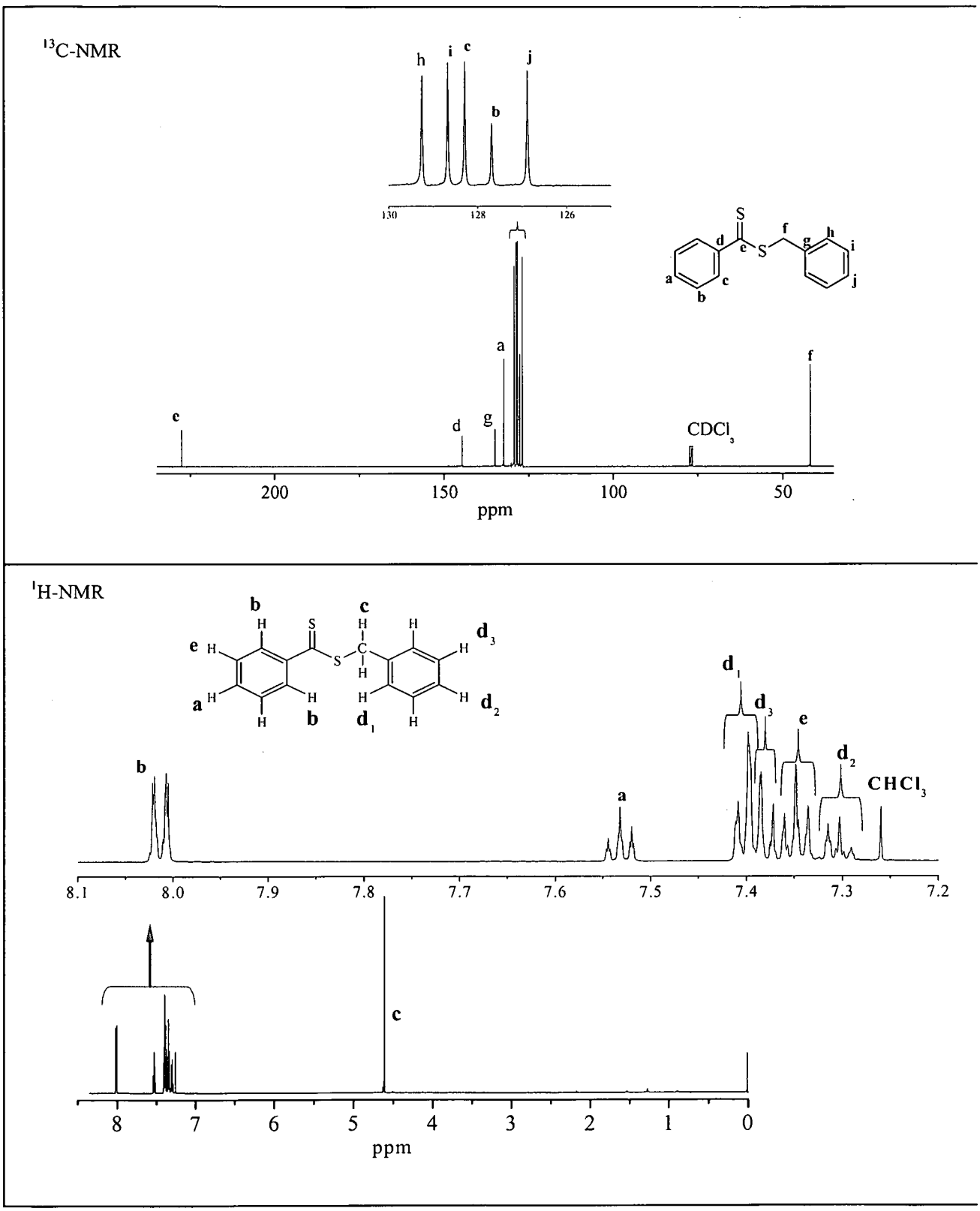

Figure A.3: ^{1}H-NMR and ^{13}C-NMR spectra of BDTB in $CDCl_3$.

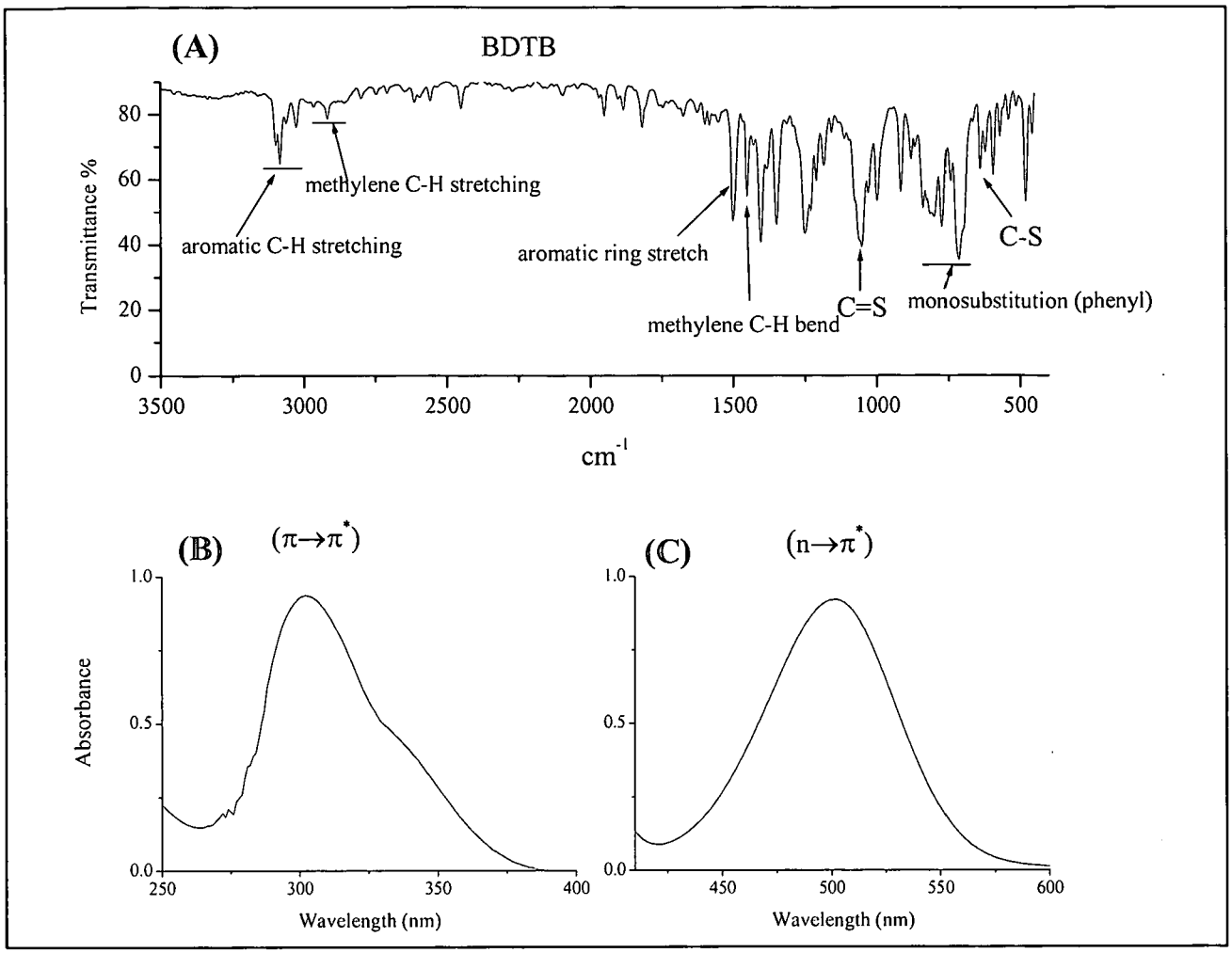

Figure A.4: (A) FT-IR spectrum of CPDT; (B and C) UV (C=S) absorption spectra of BDTB.

A-3) 2-cyano-2-yl dithiobenzoate (CPDB):

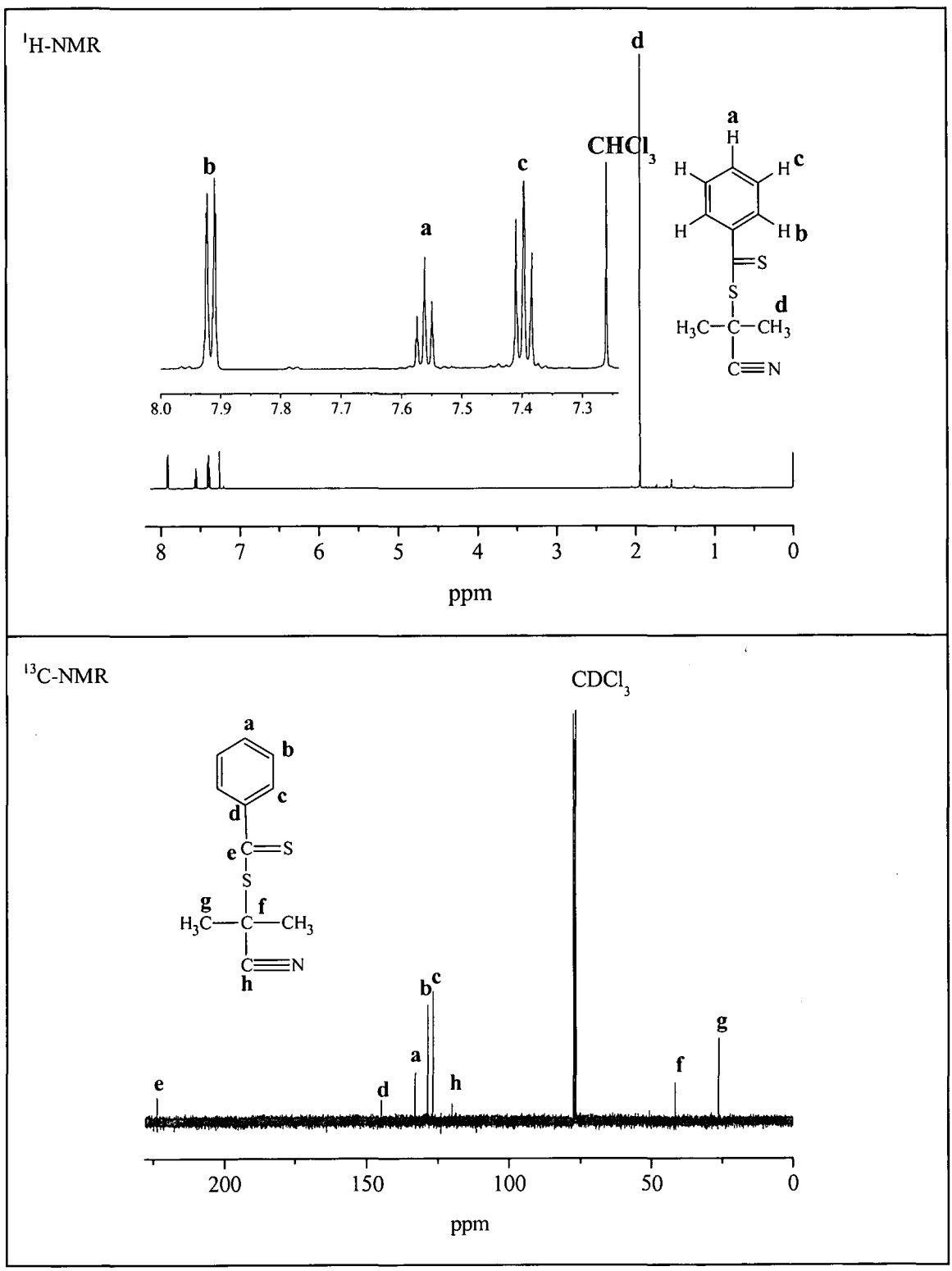

Figure A.5: ^{1}H-NMR and ^{13}C-NMR spectra of CPDB in $CDCl_3$.

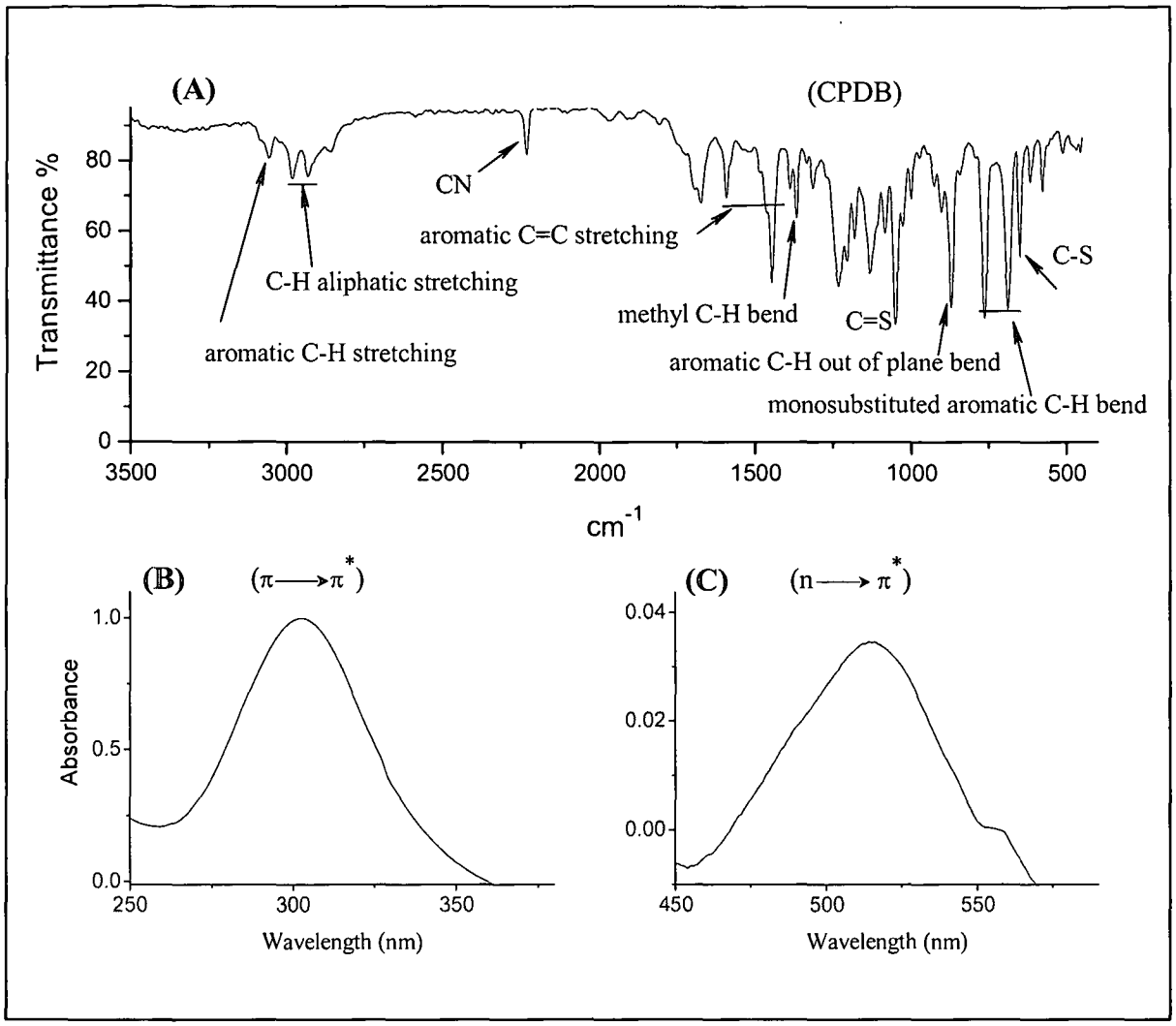

Figure A.6: (A) FT-IR spectrum of CPDT; (B and C) UV (C=S) absorption spectra of CPDB.